

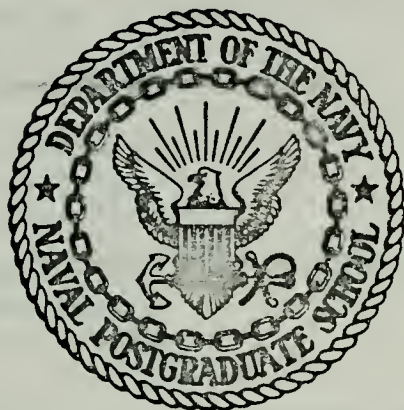
ELECTROEXCITATION OF GIANT RESONANCES
BETWEEN 5 MeV AND 40 MeV
EXCITATION ENERGY IN ^{197}Au

Kenneth Paul Ferlic

DUDLEY KNOX LIBRARY
NAVAL POSTGRADUATE SCHOOL
MONTEREY, CALIFORNIA 93940

NAVAL POSTGRADUATE SCHOOL

Monterey, California



THESIS

ELECTROEXCITATION OF GIANT RESONANCES
BETWEEN 5 MeV and 40 MeV
EXCITATION ENERGY IN ^{197}Au

by

Kenneth Paul Ferlic

and

Ronald Dallas Waddell

June 1974

Thesis Advisors:

F.R. Buskirk

X.K. Maruyama

Approved for public release; distribution unlimited.

T161756

Unclassified

SECURITY CLASSIFICATION OF THIS PAGE (When Data Entered)

REPORT DOCUMENTATION PAGE		READ INSTRUCTIONS BEFORE COMPLETING FORM
1. REPORT NUMBER	2. GOVT ACCESSION NO.	3. RECIPIENT'S CATALOG NUMBER
4. TITLE (and Subtitle) Electroexcitation of Giant Resonances Between 5 MeV and 40 MeV Excitation Energy in ^{197}Au		5. TYPE OF REPORT & PERIOD COVERED Master's Thesis; June 1974
		6. PERFORMING ORG. REPORT NUMBER
7. AUTHOR(s) Kenneth Paul Ferlic and Ronald Dallas Waddell		8. CONTRACT OR GRANT NUMBER(s)
9. PERFORMING ORGANIZATION NAME AND ADDRESS Naval Postgraduate School Monterey, California 93940		10. PROGRAM ELEMENT, PROJECT, TASK AREA & WORK UNIT NUMBERS
11. CONTROLLING OFFICE NAME AND ADDRESS Naval Postgraduate School Monterey, California 93940		12. REPORT DATE June 1974
		13. NUMBER OF PAGES 112
14. MONITORING AGENCY NAME & ADDRESS (if different from Controlling Office) Naval Postgraduate School Monterey, California 93940		15. SECURITY CLASS. (of this report) Unclassified
		15a. DECLASSIFICATION/DOWNGRADING SCHEDULE
16. DISTRIBUTION STATEMENT (of this Report) Approved for public release; distribution unlimited.		
17. DISTRIBUTION STATEMENT (of the abstract entered in Block 20, if different from Report)		
18. SUPPLEMENTARY NOTES		
19. KEY WORDS (Continue on reverse side if necessary and identify by block number) Inelastic electron scattering Nuclear transitions Giant resonances LINAC Multipole transitions Nuclear resonances		
20. ABSTRACT (Continue on reverse side if necessary and identify by block number) Inelastic electron scattering from ^{197}Au between 5 MeV and 40 MeV excitation energy revealed giant multipole resonances. Angular distribution studies with incident 90 MeV electrons show evidence of previously unreported giant monopole states. Reduced matrix elements have been extracted and multipolarity assignments have been made. Seven states have been observed at excitations of 7.3 (undetermined magnetic), 9.2 (E0), 10.8 (E2), 14.0(E1), 18.0 (undetermined), 22.5 (E2), and 33.5 MeV (E0 or E2).		

DD Form 1473 (BACK)
1 Jan 73
S/N 0102-014-6601

Electroexcitation of Giant Resonances
Between 5 MeV and 40 MeV
Excitation Energy in ^{197}Au

by

Kenneth Paul Ferlic
Ensign, United States Navy
B.S., Villanova University, 1973

and

Ronald Dallas Waddell
Lieutenant, United States Navy
B.S., United States Naval Academy, 1967

Submitted in partial fulfillment of the
requirements for the degree

MASTER OF SCIENCE IN PHYSICS

from the

NAVAL POSTGRADUATE SCHOOL
June 1974

ABSTRACT

Inelastic electron scattering from ^{197}Au between 5 MeV and 40 MeV excitation energy revealed giant multipole resonances. Angular distribution studies with incident 90 MeV electrons show evidence of previously unreported giant monopole states. Reduced matrix elements have been extracted and multipolarity assignments have been made. Seven states have been observed at excitations of 7.3 (undetermined magnetic), 9.2 (E0), 10.8 (E2), 14.0 (E1), 18.0 (undetermined), 22.5 (E2), and 33.5 MeV (E0 or E2).

TABLE OF CONTENTS

I.	INTRODUCTION -----	9
II.	THEORY -----	10
	A. ELECTRON SCATTERING -----	10
	B. GIANT RESONANCES -----	11
	C. TRANSITION PROBABILITIES AND SUM RULES -----	17
	D. QUASI-ELASTIC SCATTERING -----	20
III.	DATA ANALYSIS -----	23
	A. DATA REDUCTION -----	23
	B. ERROR ANALYSIS -----	39
IV.	DISCUSSION -----	42
	A. COLLECTIVITY -----	42
	B. MULTIPOLARITY ASSIGNMENTS -----	42
V.	CONCLUSIONS -----	58
APPENDIX A: PROGRAM NAW, SPECTRUM FITTING CODE -----		61
LIST OF REFERENCES -----		109
INITIAL DISTRIBUTION LIST -----		112

LIST OF TABLES

TABLE

I	$A^{-1/3}$ Dependence of ^{197}Au Resonances -----	16
II	Weisskopf Units for ^{197}Au -----	19
III	Sum of EWSR for ^{197}Au -----	19
IV	Experimental Conditions -----	25
V	Observed Resonances -----	25
VI	Scale Factors for Figures 6 - 10 -----	36
VII	Area Ratios and Inelastic Form Factors Squared -----	37
VIII	Fractional Error Contributions -----	41
IX	Ratios of Resonance Strengths to EWSR -----	46
X	Transition Strengths in Weisskopf Units -----	49
XI	Multipolarity Assignments -----	60

LIST OF FIGURES

FIGURE

1	90 MeV, 60° , Spectrum with Background -----	26
2	90 MeV, 75° , Spectrum with Background -----	27
3	90 MeV, 90° , Spectrum with Background -----	28
4	90 MeV, 105° , Spectrum with Background -----	29
5	90 MeV, 120° , Spectrum with Background -----	30
6	90 MeV, 60° , Spectrum with Background Subtracted -	31
7	90 MeV, 75° , Spectrum with Background Subtracted -	32
8	90 MeV, 90° , Spectrum with Background Subtracted -	33
9	90 MeV, 105° , Spectrum with Background Subtracted -	34
10	90 MeV, 120° , Spectrum with Background Subtracted -	35
11	Form Factor Plot, $E_x = 7.3$ MeV -----	51
12	Form Factor Plot, $E_x = 9.2$ MeV -----	52
13	Form Factor Plot, $E_x = 10.8$ MeV -----	53
14	Form Factor Plot, $E_x = 14.0$ MeV -----	54
15	Form Factor Plot, $E_x = 18.0$ MeV -----	55
16	Form Factor Plot, $E_x = 22.5$ MeV -----	56
17	Form Factor Plot, $E_x = 33.5$ MeV -----	57
18	Assumed Elastic Spectrum Shape -----	61

ACKNOWLEDGEMENTS

We would like to express our thanks and appreciation to those who have contributed to the completion of this work. Special recognition must be given to our Thesis Advisors, Professor Xavier K. Maruyama and Professor Fred R. Buskirk, and to Visiting Professor W. Rainer Pitthan. Their encouragement, guidance, and experience were invaluable to the completion of this work.

Thanks are also extended to Professors J. N. Dyer and E. B. Dally for their assistance during the long hours of data acquisition.

To Mr. H. McFarland and Mr. D. Snyder go our thanks for their time, invaluable technical skills, and hard work in keeping the LINAC running.

We are indebted to Professor Y. Torizuka for providing us with current unpublished results of electron scattering experiments conducted at Sendai.

Finally, we would like to thank our wives, Nelda and Marie for their patience and encouragement during the course of our postgraduate studies.

I. INTRODUCTION

Giant resonance investigations of heavy nuclei have been actively pursued at the Naval Postgraduate School electron linear accelerator since 1973. Initial studies by Warshawsky and Webber [Ref. 1] demonstrated the feasibility of measuring inelastic electron spectra in the continuum region of ^{197}Au . They adapted analysis techniques developed at Darmstadt and measured cross sections for several known resonances. Warshawsky and Webber further suggested the existence of previously unreported resonances at about 9 MeV and 23 MeV excitation energy, but their analysis did not conclusively identify the multipolarities.

The work described in this thesis completes the study of ^{197}Au discussed above and extends the excitation energy range to 40 MeV. Seven giant multipole resonances have been observed. Besides the previously reported 7.3, 10.8, and 14.0 states [Refs. 1-4, 18 and 19], the existence of resonances at 9.2 and 22.5 MeV are required to explain the observed electron spectra.

Experimental values of the inelastic scattering form factors were measured at scattering angles of 60° , 75° , 90° , 105° , and 120° with incident electrons of 90 MeV energy. Transition multipolarities have been deduced and reduced transition probabilities have been extracted. Newly identified are resonances at excitation energies of 9.2 MeV (isoscalar E0), 22.5 MeV (isovector E2), and 33.5 MeV (isovector E0 or E2). Previously reported multipolarities for the 10.8 MeV (isoscalar E2) and 14.0 MeV (isovector E1) [Ref. 18] resonances have been confirmed. The analysis contained here is unable to uniquely assign transition multipolarities to the 7.3 MeV (magnetic) and 18.0 MeV structures.

II. THEORY

A. ELECTRON SCATTERING

The Mott cross section for an extremely relativistic electron which scatters elastically from a nucleus of point charge Ze is given by [Ref. 6]

$$\left(\frac{d\sigma}{d\Omega} \right)_{\text{Mott}} = \left(\frac{Ze^2}{2E_i} \right)^2 \frac{\cos^2 \frac{\theta}{2}}{\sin^4 \frac{\theta}{2}} . \quad \text{II-1}$$

The electron is assumed to have spin while the nucleus has neither spin nor magnetic moment. Nuclear charge structure in a nucleus of finite extent modifies the scattering cross section to [Ref. 6]

$$\left(\frac{d\sigma}{d\Omega} \right)_{\text{Measured}} = \left(\frac{d\sigma}{d\Omega} \right)_{\text{Mott}} \left| \int_{\text{nuclear volume}} \rho(\vec{r}) e^{i\vec{q} \cdot \vec{r}} dV \right|^2 . \quad \text{II-2}$$

$\rho(\vec{r})$ is the charge density within the nucleus as a function of \vec{r} , the radius vector from the center of the nucleus, and \vec{q} is the momentum transfer vector. The Born approximation has been assumed. The term describing the nuclear structure is called the square of the form factor,

$$\left| F(q^2) \right|^2 = \frac{\left(\frac{d\sigma}{d\Omega} \right)_{\text{Measured}}}{\left(\frac{d\sigma}{d\Omega} \right)_{\text{Mott}}} . \quad \text{II-3}$$

For inelastic scattering, the cross section may also be written as a modification to the Mott scattering cross section, but the form is more complex, with both transverse and longitudinal contributions which are described elsewhere [Ref. 7]. For inelastic longitudinal scattering the form factor is related to the matrix element of the charge

operator evaluated between initial and final nuclear states. Although transverse components require modification of the simple expression II-2, it is conventional to call the experimental form factor squared the ratio of measured to Mott cross sections as in II-3. This value is compared to theoretical calculations based on particular nuclear models.

For inelastic scattering, the Born approximation may be used to compute the theoretical form factor based on an assumed nuclear transition charge distribution. First attempts at a solution were made by describing the perturbing fields in terms of a multipole expansion, and assuming the incident and scattered electron wave functions to be plane waves. This so called plane wave Born approximation (PWBA) is satisfactory for light nuclei, but becomes less accurate as the number of protons in the nucleus increases. For heavy nuclei, the Coulomb field surrounding the nucleus distorts both the incident and scattered electron wave functions sufficiently that a plane wave solution no longer gives the correct results. Consequently, the plane wave solutions of the PWBA have to be replaced by phase shifted spherical waves. This method, termed the distorted wave Born approximation (DWBA), in practice requires computer computations to extract the form factors [Ref. 8]. Form factors thus calculated are plotted as a function of scattering angle for each desired electric and magnetic transition. Comparison of these plots with experimental results allows for the assignment of transition modes to the observed resonances.

B. GIANT RESONANCES

The term "giant resonance" has been used until recently to describe the giant electric dipole resonance (GDR). This resonance appears as a

well known feature in the nuclear excitation spectra produced by such photonuclear processes as photodisintegration, photon absorption, and inverse reactions such as the (p, γ) reaction. The presence of the GDR is characterized by a giant bump in photonuclear spectra at excitation energies from 10 to 25 MeV. It occurs throughout the periodic table and, according to the Goldhaber-Teller and to the Steinwedel-Jensen model, appears at excitation energies that are proportional to the inverse nuclear radius, $E_x = 80A^{-1/3}$ [Ref. 9].

This conspicuous resonance appears also in inelastic electron scattering spectra. The advantage of electron scattering experiments over the photonuclear processes for exploring the nature of the giant resonances lies in the variable momentum transfer, q . In the case of the photonuclear processes, the momentum transfer is determined uniquely by the excitation energy. The giant resonance in the electron scattering cross section can be measured at different values of q depending on the scattering angle, θ , and the incident electron energy, E_i ; the dependence being given by

$$q^2 = 4E_i E_f \sin^2 \frac{\theta}{2} ,$$

II-4

where E_f is the final electron energy. In addition, at values of q higher than is available from photonuclear work, excitation modes other than $E1$ become observable. Consequently, the term "giant resonance" now refers to all multipole excitation modes which exhibit strongly coherent properties.

Early attempts to explain the giant resonances were based mainly on collective models. The initial Goldhaber-Teller model assumed a rigid displacement of the protons as a whole against the neutrons as a whole, thus producing a large collective dipole moment. The

Generalized Goldhaber-Teller model assumes that nuclear matter consists of four interpenetrating fluids: neutrons with spin up ($n\uparrow$), protons with spin up ($p\uparrow$), neutrons with spin down ($n\downarrow$), and protons with spin down ($p\downarrow$). Any two of these fluids may oscillate 180° out of phase with the other two, giving rise to four possible collective modes. For example, nucleons with spin up could oscillate against nucleons with spin down producing a magnetic resonance [Ref. 5].

The Steinwedel-Jensen model or hydrodynamic model is based on the oscillation of neutron and proton fluids within a rigid nuclear surface. An extension of this model is the dynamic collective model [Ref. 9]. The dynamic collective model replaces the rigid nuclear surface of the Steinwedel-Jensen model by a surface that may vibrate. These surface vibrations, however, are much slower than the internal giant dipole oscillations so that the approximation can be made that the dipole oscillations take place in a deformed nucleus.

A different model of the dipole giant resonances, used mainly for light, closed-shell nuclei, is based on the shell model of the nucleus. This particle-hole (ph) or Brown model arises from the observation by Wilkinson [Ref. 10] that a $1p$ nucleon, promoted into the $2s-1d$ shell, will produce dipole strengths large enough to explain the observed giant resonance cross sections. The shell model description [Ref. 10] gave the strength of the absorption correctly, but the resonance energy was incorrect, and the effect of the particle-hole interaction was noted by Brown [Ref. 11].

It has been shown [Ref. 9] that such a shell model is separable in the relative co-ordinate of all the protons versus all the neutrons; and that, upon absorption of a dipole photon, a particular linear combination of single-particle excitations is produced which corresponds

to a motion of all the protons against all the neutrons; i.e., a Goldhaber-Teller collective vibration. Hence, the shell model and collective models are equivalent in their description of collective states.

Giant resonances, then, may be described as strongly collective modes of excitation in which a considerable number of nucleons take part. In the last several years, much progress has been made in the investigation of these states using models such as those described above. Several modes of excitation other than the GDR have been identified, including the giant electric quadrupole resonance (GQR) and the giant magnetic dipole resonance (GMDR). A short summary of some of these works follow.

Early electron scattering investigation of the giant resonance structure was carried out by Isabelle and Bishop on ^{16}O [Ref. 7]. By studying the angular dependence of cross sections, the giant dipole was observed. These experiments demonstrated the feasibility of systematic studies of the level schemes and transitions in light nuclei.

Yamaguchi et. al. [Ref. 12] have carried out extensive investigations of the fine structure in the giant resonance region of ^{12}C . By making measurements at both backward and forward angles while keeping the momentum transfer constant, they were able to extract the longitudinal and transverse form factors as functions of excitation energy. The resolution of the fine structure in this manner revealed seven peaks associated with the longitudinal form factors and nine with the transverse. The dipole strength is distributed among a number of states to produce this fine structure in the giant resonance region.

An investigation of the isotopic characteristics of the giant dipole resonance has been carried out by Carlos et. al. [Ref. 13]. The giant

dipole resonances for the Neodymium isotopes ^{142}Nd to ^{146}Nd , ^{148}Nd , and ^{150}Nd were studied with a monochromatic photon beam by measuring the partial photonuclear cross sections $\sigma(\gamma, n)$, $\sigma(\gamma, pn)$ and $\sigma(\gamma, 2n)$. As the number of neutrons in the nucleus increased, the dipole resonance began to broaden. For ^{150}Nd , the resonance actually split into two distinct peaks. An interpretation is given by the dynamic collective model in which there is a coupling between dipole oscillations and surface vibrations. The splitting of the resonance in ^{150}Nd characterizes a deformed nucleus, and the experimental cross section was closely reproduced by superposition of two separate Lorentz lines whose centers are separated by four MeV. In the framework of the hydrodynamic model, one can assume for an axially deformed nucleus two modes of excitation at differing energies, equivalent to oscillations in the direction of the two axes.

Pitthan and Walcher [Ref. 14] did (e, e') investigations with Ce, La, and Pr. All three elements show distinct resonances at excitation energies of 9, 12, and 15 MeV. The resonance at 15 MeV was identified as the E1 giant resonance based on correlation of the excitation energy and strength with the GDR seen in photo-neutron experiments. The 12 MeV resonance exhibited longitudinal properties similar to the E1 but did not appear in (γ, n) studies. It was assigned an E2 or E0 excitation mode based on comparison to form factors developed from the hydrodynamic model. The 9 MeV resonance was found to be transverse and most likely an M1 transition.

Later, Lewis and Bertrand [Ref. 15] observed that the (p, p') spectra of ^{27}Al , ^{54}Fe , ^{120}Sn , and ^{209}Bi consistently produced enhancements at excitation energies slightly lower than those of the known giant

dipole resonance. Since the resonance energies of the giant dipole had been previously well measured, they concluded that it was unlikely that the giant dipole excitation was responsible for most of the observed enhancement. This apparent resonance shift was due to the presence of a giant isoscaler-quadrupole vibration located at $E_x = 63 \text{ A}^{-1/3} \text{ MeV}$.

In forward angle (e, e') experiments, Fukuda and Torizuka observed [Ref. 16] similar E1 and E2 resonances in ^{90}Zr . The usual dipole resonance was seen at 16.65 MeV and additional resonances were seen at 14 MeV and 28 MeV. Based on a prediction of the hydrodynamic model that a quadrupole giant resonance should appear at a position 1.6 times the peak energy of the usual giant dipole resonance [Ref. 17], the 28 MeV resonance was assigned an E2 transition. An assignment of either E0 or E2 was made for the 14 MeV peak. Based on similar results for ^{59}Fe , ^{116}Sn , and ^{208}Pb [Ref. 16] these new giant resonances seem to be universal features existing at excitation energies of $65 \text{ A}^{-1/3} \text{ MeV}$ and $130 \text{ A}^{-1/3} \text{ MeV}$ in all nuclei. Table I contains a listing of the $\text{A}^{-1/3}$ dependence of the resonances identified in this work and a list of references where others have seen or predicted corresponding resonances in ^{197}Au and other nuclei.

TABLE I
 $\text{A}^{-1/3}$ Dependence of ^{197}Au Resonances

$E_x (\text{MeV})$	$E_x (\text{A}^{-1/3}-\text{MeV})$	References
9.2	53	t [Refs. 21 & 22] Ce, La, Pr [Ref. 23]
10.8	63	Au [Refs. 3 & 18]
14.0	81	Au [Refs. 3, 18, and 25]
18.0	105	Pb [Refs. 24 & 26]
22.5	130	Au [Ref. 3] Pb [Ref. 24]
33.5	195	t [Ref. 22] Pb [Ref. 26]

t = Theoretical Prediction

C. TRANSITION PROBABILITIES AND SUM RULES

The transverse-electric and magnetic form factors are given by [Ref. 27]

$$\left| F_{E,L}(\vec{q}_I) \right|^2 = \frac{4\pi}{Z^2} \left(\frac{L+1}{L} \right) \left[\frac{q_I^L}{2(L+1)!!} \right]^2 B(E, L, \vec{q}_I, J_i \rightarrow J_f). \quad II-5$$

The continuity equation provides similar relationships for the longitudinal form factor. The coefficients B are the reduced nuclear transition probabilities and, as such, contain all of the nuclear physics of the inelastic scattering problem. The theoretical form factors are calculated by the GBROW computer program as described by Ziegler [Ref. 27].

To determine whether or not the resonances observed are collective phenomena, comparison of experimental to single-particle reduced transition probabilities may be made. For a heavy nucleus, one would expect a strength greater than several times the single-particle value. Furthermore, a giant resonance should exhaust an appreciable fraction of the appropriate sum rule. If an observed resonance greatly exceeds the sum rule under the assumption of a particular transition multipolarity, it is unlikely that the multipolarity assignment is correct.

The single-particle reduced transition strengths are given by the Weisskopf unit [Ref. 28],

$$B(E, L)_{SP} = \frac{e^2 (2L+1)}{4\pi} \left(\frac{3}{L+3} R^L \right)^2 \quad II-6$$

and

$$B(M, L)_{SP} = \frac{e^2 (2L+1) \cdot 10}{\pi} \left(\frac{3}{L+3} \right)^2 R^{2L-2} (0.0111), \quad II-7$$

where $R = 1.2 A^{-1/3} = 6.98$ fm for ^{197}Au . Table II provides values of the single-particle transition strengths for ^{197}Au .

Another, to some extent model-independent, evaluation of the transition strength of EL modes may be achieved by expressing the strength relative to the energy-weighted sum rule (EWSR). Sum rules for magnetic transitions are more dependent on the structure of the nucleus in question and, therefore, no comparisons to these have been made here. States at excitation energies less than 15 MeV appear to be $\Delta T = 0$ except for the EL mode which is $\Delta T = 1$. The sum rule for isoscalar ($\Delta T = 0$) excitation modes with $L > 1$ is given by [Ref. 29]

$$S(EL, \Delta T=0) = \sum_f (E_f - E_i) B(EL, i \rightarrow f) = \frac{Z^2 e^2 L (2L+1)^2 \hbar^2}{8\pi A M} \langle R^{2L-2} \rangle. \quad \text{II-8}$$

The isovector ($\Delta T = 1$) sum rule for $L > 1$ is related to the isoscalar sum rule by

$$S(EL, \Delta T=1) = S(EL, \Delta T=0) \frac{N}{Z}. \quad \text{II-9}$$

The corresponding sum rule for an isoscalar monopole (E0) excitation is [Ref. 30]

$$S(E0) = \sum_f (E_f - E_i) |M_{fi}|^2 = \frac{\hbar^2 Z}{M} \langle R^2 \rangle, \quad \text{II-10}$$

where M_{fi} is the monopole matrix element. The strength of E1 resonances can be expressed relative to the sum rule given by Warburton [Ref. 31]:

$$S(E1) = \frac{e^2 \hbar^2}{2 M_P} \left(\frac{q}{4\pi} \right) \frac{NZ}{A}. \quad \text{II-11}$$

Table III gives values of these sums for ^{197}Au using weighted radii of the ground state charge distribution.

TABLE II
Weisskopf Units for ^{197}Au

L	$\frac{B(EL)}{e^2}^*$	$\frac{B(ML)}{e^2}^*$
1	6.6	.06
2	3.35×10^2	3.1
3	1.63×10^4	1.44×10^2

* Units are fm^{2L}

TABLE III
Sum of EWSR For ^{197}Au

EL	ΔT	Sum	Units
E0	0	9.2×10^4	MeV-fm^4
E1	1	7.04×10^2	$e^2\text{-MeV-fm}^2$
E2	0	7.4×10^4	$e^2\text{-MeV-fm}^4$
	1	1.1×10^5	$e^2\text{-MeV-fm}^4$
E3	0	6.15×10^6	$e^2\text{-MeV-fm}^6$
	1	9.16×10^6	$e^2\text{-MeV-fm}^6$

D. QUASI-ELASTIC SCATTERING

Electrons incident upon a nucleus may scatter elastically with individual nucleons within the nucleus. This process is called quasi-elastic scattering. If sufficient momentum is imparted to the nucleon, it will be knocked out of the nucleus with some kinetic energy. The simultaneous energy loss by the incident electron may result in a measurable quasi-elastic peak. It is of interest to see at which value of E_x this contribution appears on the spectrum of $\frac{d^2\sigma}{d\Omega dE_x}$, to see if it contributes to, and therefore must be subtracted from, the scattered electron spectrum in the region of the giant resonance.

The inelastic electron-nucleus cross section has been calculated in three energy-loss regions with the Fermi gas model for the nucleus [Ref. 32]: the quasi-elastic region; the threshold pion region with its pion electroproduction cross sections; and the region containing the 3-3 resonance of the proton. Pion production begins at 135 MeV and the 3-3 resonance is 298 MeV above the elastic peak, so these regions are not of interest in this work.

In the Fermi gas model, the electron scatters elastically from a single nucleon in the free Fermi sea, with the recoiling nucleon required to scatter out of the Fermi sphere. Because of the Pauli principle, the nucleon cannot scatter into an already occupied state. The final nucleon energy is given by

$$E_{kf} = \left[k^2 + M^2 \right]^{\frac{1}{2}},$$

II-12

where k is the nucleon momentum and M is the nucleon mass. The initial (bound) nucleon energy is

$$\epsilon_{ki} = \frac{k^2}{2M} + U(k^2) = \frac{k^2}{2M^*} + U(0), \quad \text{II-13}$$

where the effective nucleon mass, M^* , is given by [Ref. 33]

$$M^* = \frac{M}{1.4} \quad \text{II-14}$$

and $U(k^2)$ is the effective single-particle potential in nuclear matter. This potential effectively shifts the electron energy loss, ω , to take into account the nuclear binding. Moni treats $U(k^2)$ as a constant, $\bar{\epsilon}$, equivalent to the average nucleon interaction energy. The quasi-elastic peak energy loss will increase with q and approach the effective free nucleon kinetic energy, $q^2 / (2M^*)$, at large values of q .

The magnitude of the above shift for the gold nucleus is of interest. The average nucleon interaction energy, $\bar{\epsilon}$, and the nuclear Fermi momentum, k_F , have been determined for nine elements from ${}^6\text{Li}$ to ${}^{208}\text{Pb}$ [Ref. 34] by a least squares fit of theory to quasi-elastic peak data. In the cross-section formula, an energy-conserving delta function appears, given by

$$\delta\left(\omega + \frac{k^2}{2M} - \bar{\epsilon} - \frac{(\vec{k} + \vec{q})^2}{2M}\right), \quad \text{II-15}$$

which determines ω . The nucleon momentum is approximated by the Fermi momentum and is roughly constant at 260-265 MeV/c for heavy nuclei from nickel through lead. $\bar{\epsilon}_{Au} = 43$ MeV [Ref. 34]. The energy-conserving delta function requires that

$$\omega = \bar{\epsilon} + \frac{kq}{m} + \frac{q^2}{2m} . \quad \text{II-16}$$

For the smallest momentum transfer of these experiments, $\omega = 73$ MeV. The threshold value is $\omega \gtrapprox \bar{\epsilon}_{Au} = 43$ MeV. Thus explicit corrections for the quasi-elastic contribution need not be made for the spectra of this work.

III. DATA ANALYSIS

A. DATA REDUCTION

Five experiments were performed with an incident beam energy of 90 MeV and at scattering angles of 60° , 75° , 90° , 105° , and 120° . The experimental information is given in Table IV. In general the data analysis procedure described by Marshawsky and Webber [Ref. 1] was followed throughout this work. The initial choice of resonance energies was determined from known resonances [Refs. 1, 2, 3, and 4] and by visual inspection. Previously determined resonances occur at 7.3, 9.2, 11.0, and 14.0 MeV. Visual inspection of the background subtracted data revealed wide structures at 18.0, 22.5, and 33.5 MeV.

The fitted inelastic spectra extended from 4 to 40 MeV, except the 120° spectrum which extends only to 51.5 MeV. In some cases the data extends to 50 MeV but no structures were observed at this high excitation energy. Since the 120° data has different boundary conditions for matching the background at high excitation energies, only cross sections for resonances below 20 MeV were extracted at this angle.

Breit-Wigner resonance forms were assumed for each resonance and computer code NAW (see appendix) simultaneously fits the entire inelastic spectrum including the radiation tail and background. The new resonance positions and widths were manually varied while the NAW code varied the peak strengths and background parameters until a best fit was obtained.

The criteria used to determine a reasonable fit were as follows:

1. The data and calculated spectrum should coincide visually.
2. χ^2 per degree of freedom should be less than one. The data is not strictly statistical because the detector momentum interval is larger

than the momentum increment of the spectrometer field and hence correlations exist between energy bins.

3. The difference between the total χ^2 for successive computer iterations was $\Delta\chi^2 \approx 0.5$. Typically there were 300 degrees of freedom and a change of 0.5 in the total chi squared resulted in 1.7×10^{-3} per degree of freedom.

4. All observed resonances should consistently fit each of the five spectra. Table V lists the positions and widths of the resonances required.

Figures 1 - 5 present the experimental data corrected for spectrometer dispersion effects with the fitted total background and the individual resonances drawn. Figures 6 - 10 present these spectra with the total background subtracted, revealing the resonance structures of Table V.

The areas under the inelastic resonances were calculated from the Breit-Wigner resonance shapes and the ratio of each inelastic resonance area to the area under the elastic peak was calculated (A_i/A_e). The inelastic form factors squared are obtained by multiplying A_i/A_e by the square of the elastic scattering form factors (F_{el}^2). Table VII presents the experimental ratios of the inelastic to elastic areas and the square of the inelastic form factors. The elastic form factors were calculated using the program of Rawitscher and Fischer [Ref. 35]. The charge distribution parameters were $c = 6.38$ fm and $t = 2.32$ fm.

TABLE IV
Experimental Conditions

Angle	Target Thickness	Incident Energy	F_{el}^2
60	.048 g/cm ²	90.32 MeV	.1185
75	.096 g/cm ²	90.24 MeV	.0444
90	.096 g/cm ²	90.21 MeV	.0298
105	.144 g/cm ²	89.98 MeV	.0217
120	.240 g/cm ²	89.60 MeV	.0132

TABLE V
Observed Resonances

Excitation Energy MeV	Widths MeV
7.3 \pm 0.3	2.8 \pm 0.4
9.1 \pm 0.4	2.3 \pm 1.0
10.9 \pm 0.4	2.8 \pm 0.4
14.0 \pm 0.4	4.4 \pm 0.4
18.0 \pm 0.6	5.1 \pm 0.6
22.5 \pm 0.6	7.2 \pm 0.6
33.5 \pm 1.4	10.5 \pm 2.5

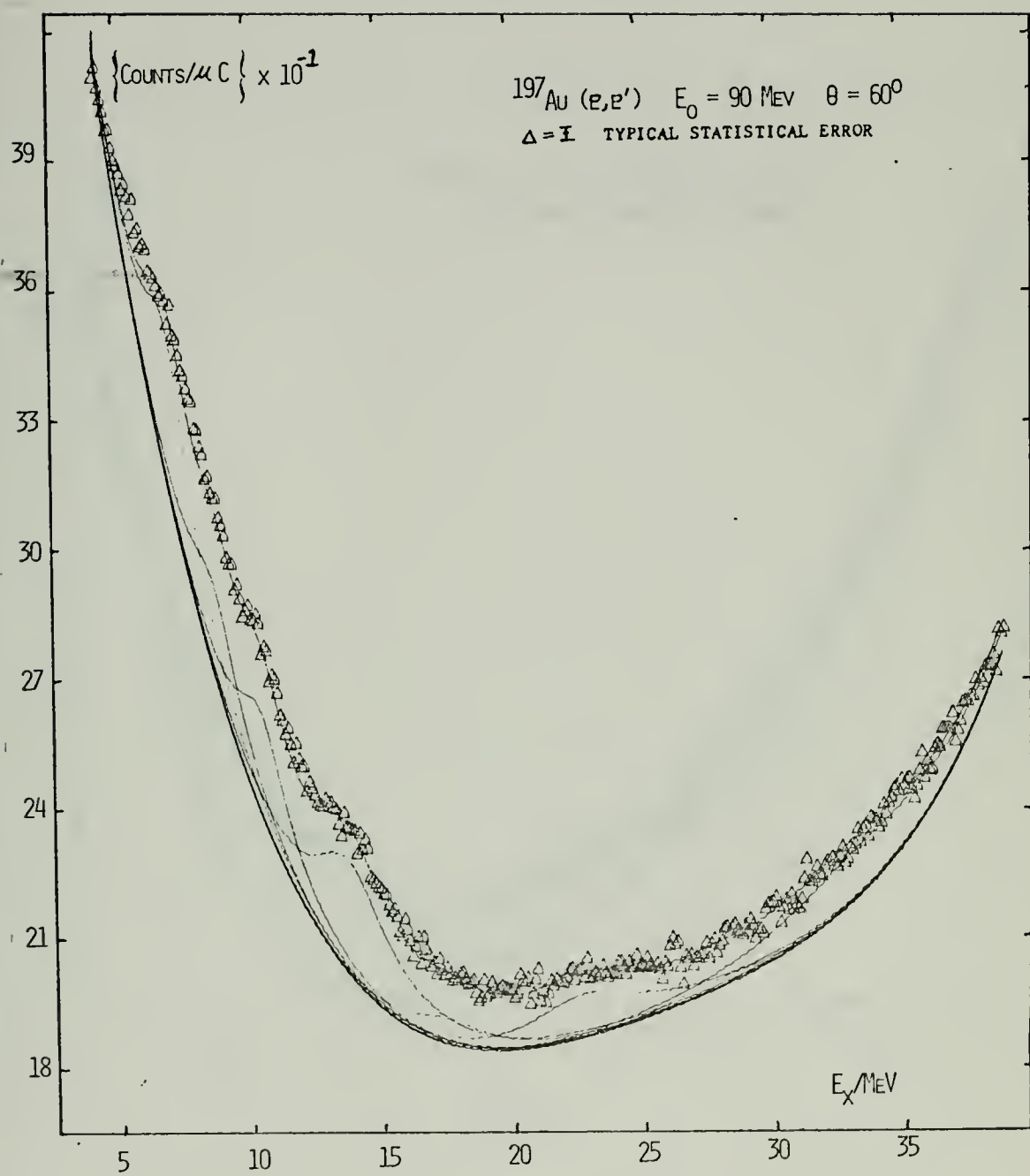


FIGURE 1

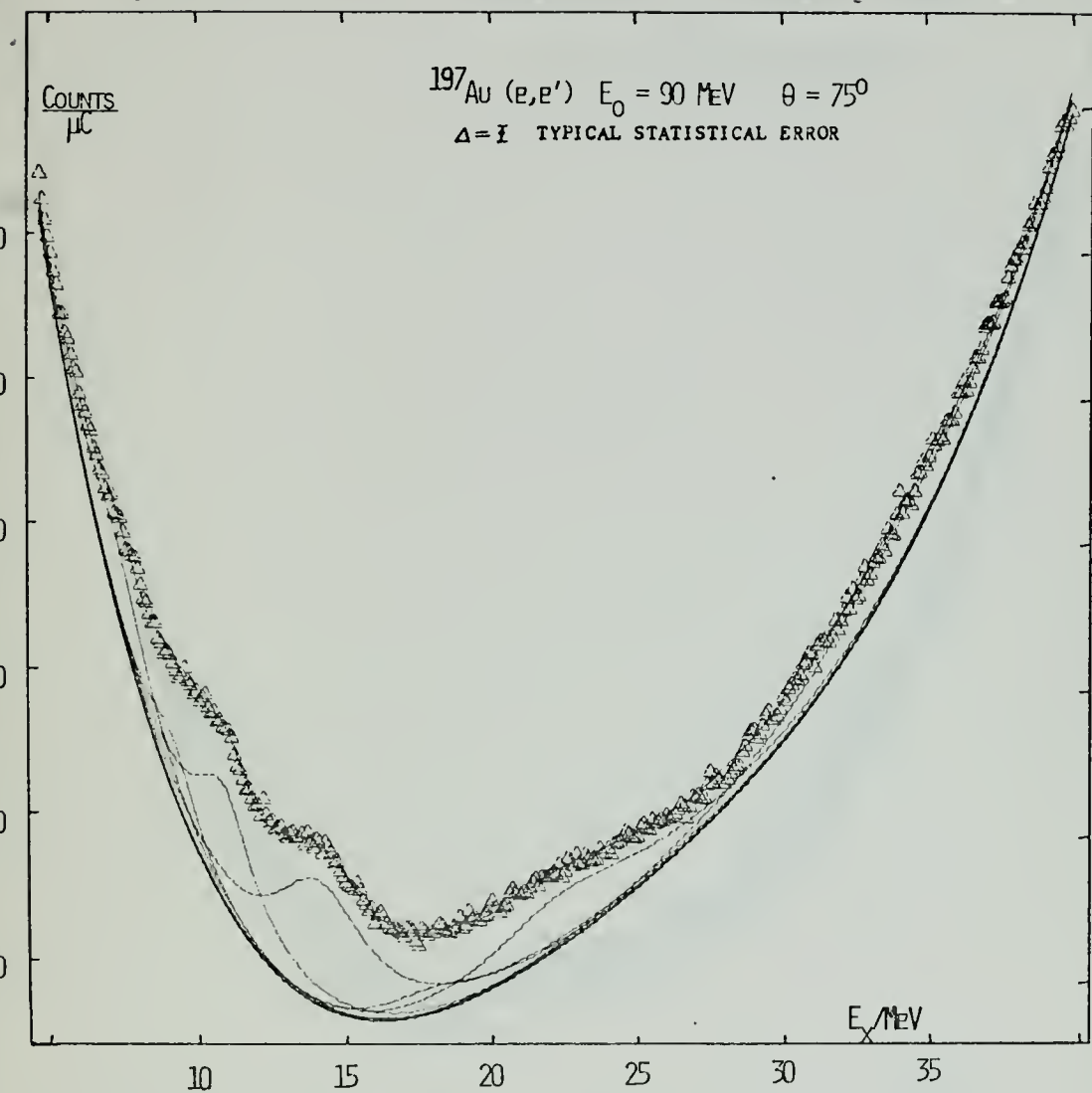


FIGURE 2

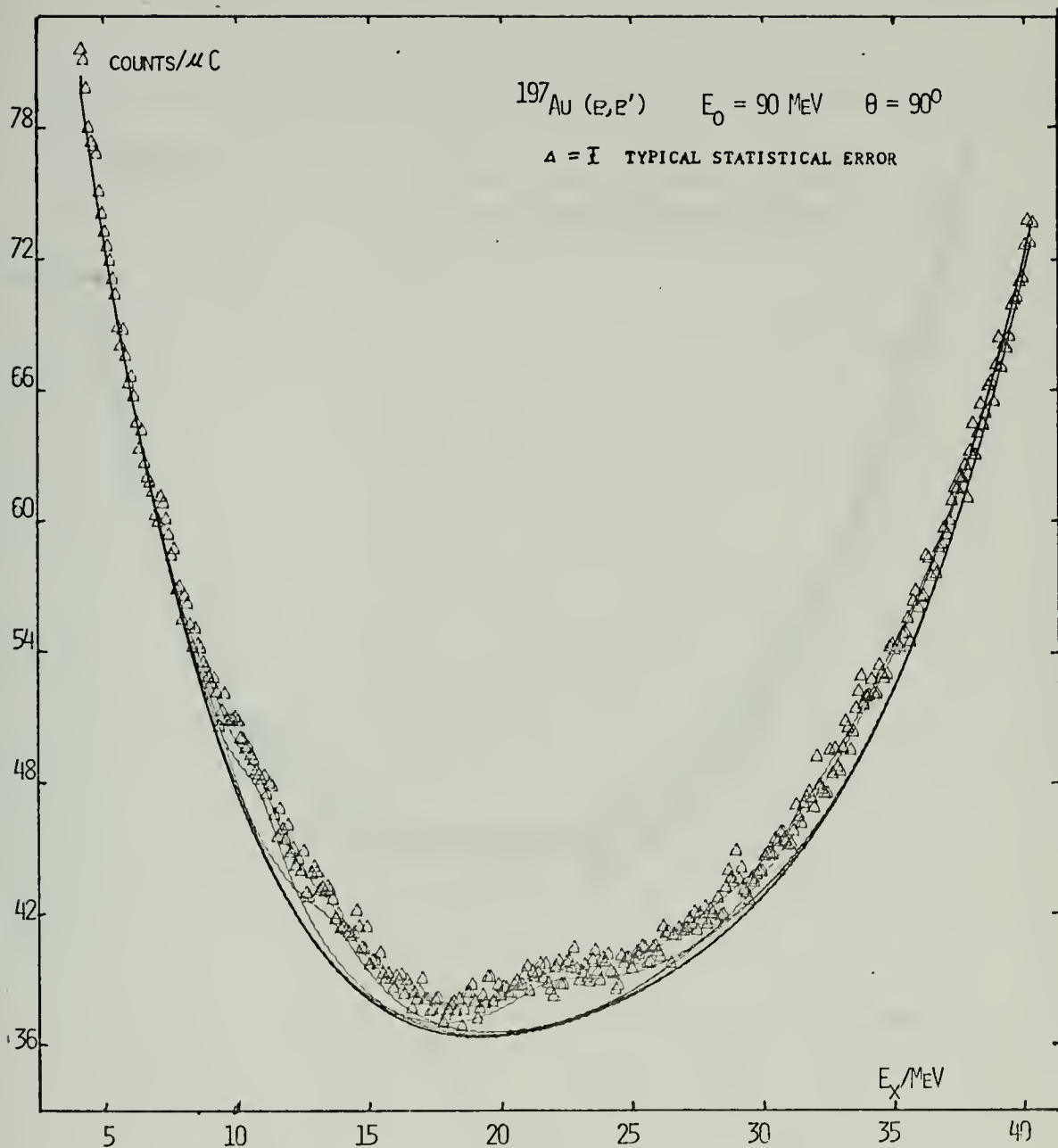


FIGURE 3

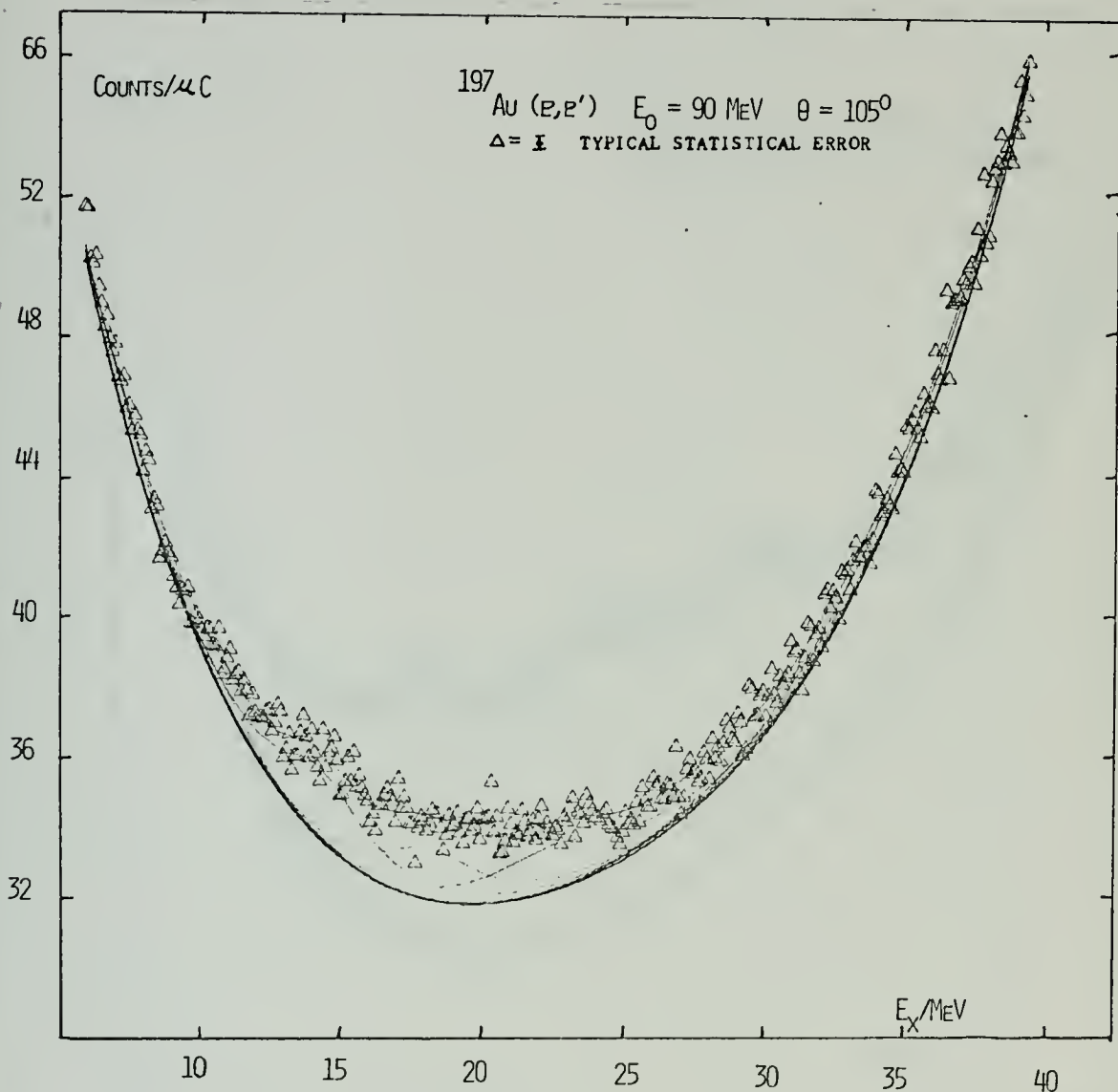


FIGURE 4

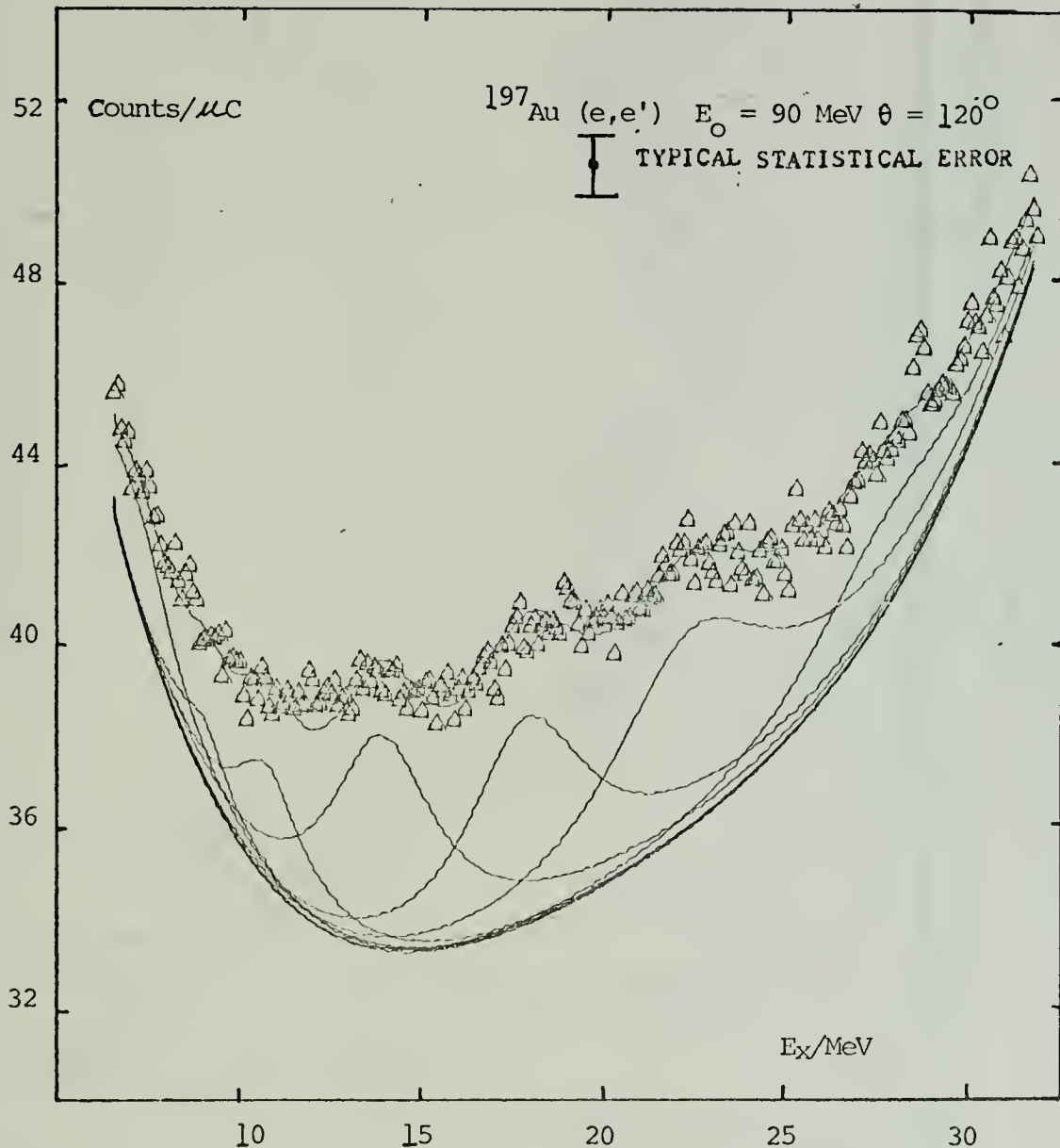


FIGURE 5

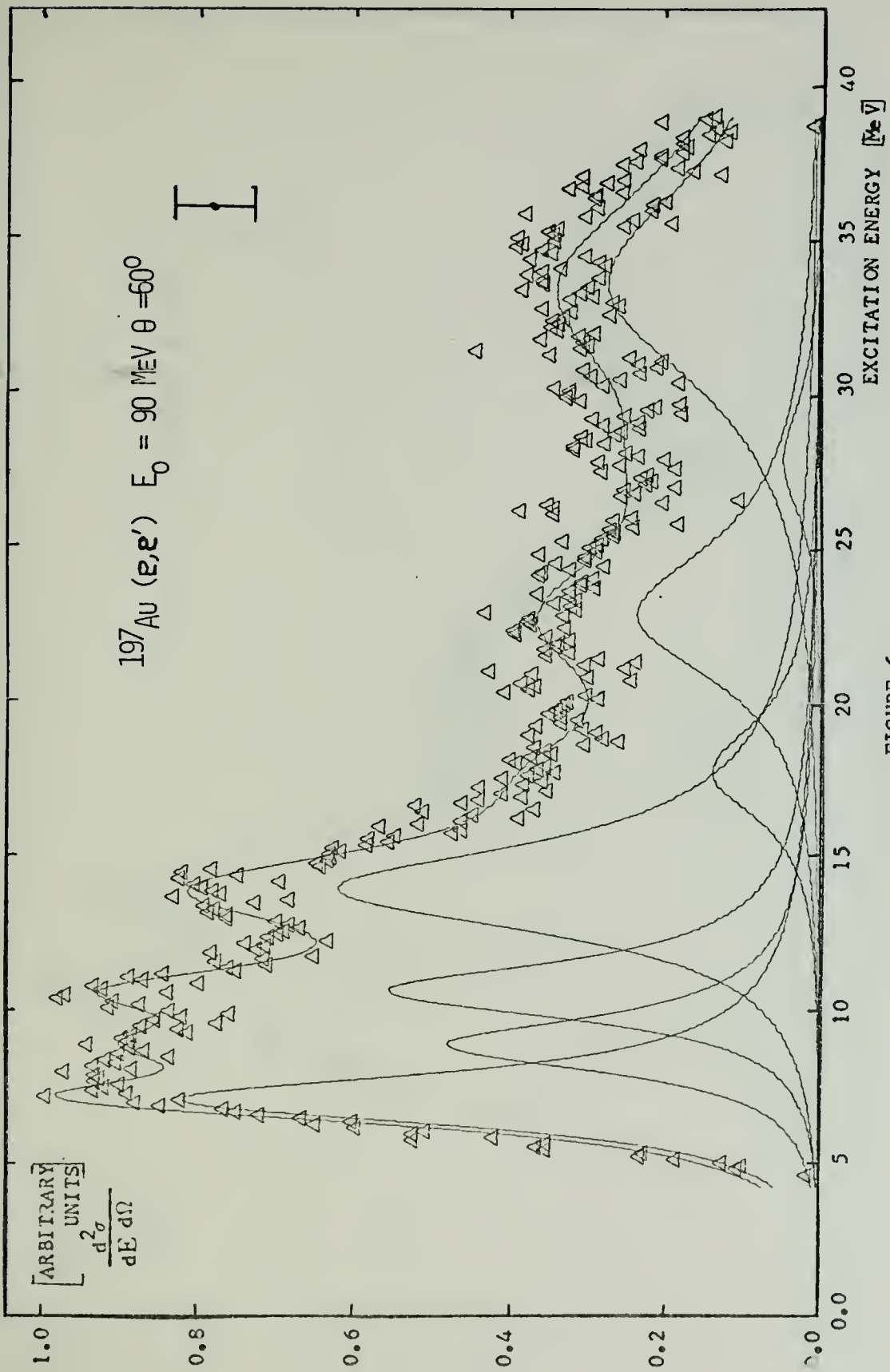
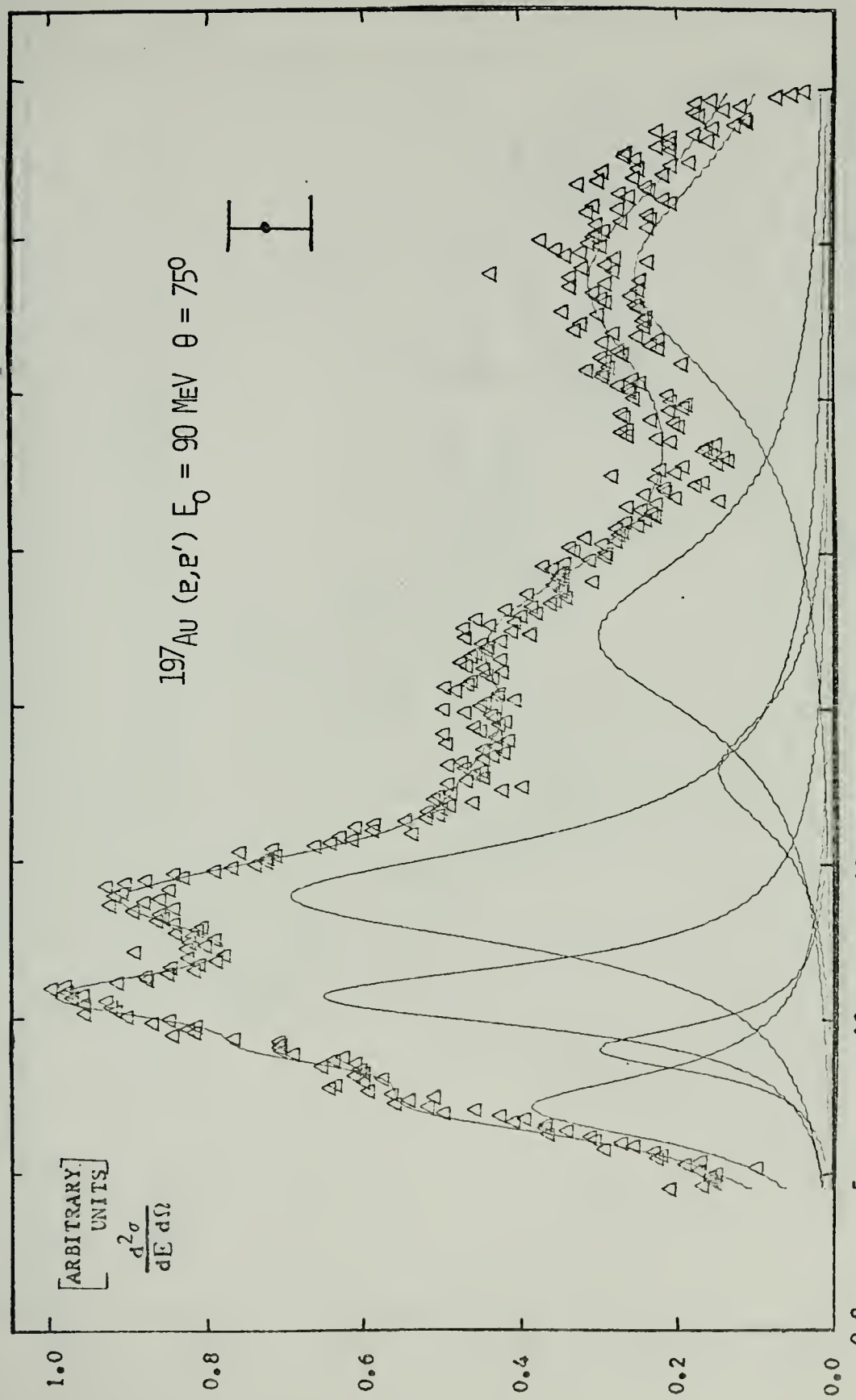


FIGURE 6

197AU (ν, ν') $E_0 = 90$ MeV $\theta = 75^\circ$

FIGURE 7



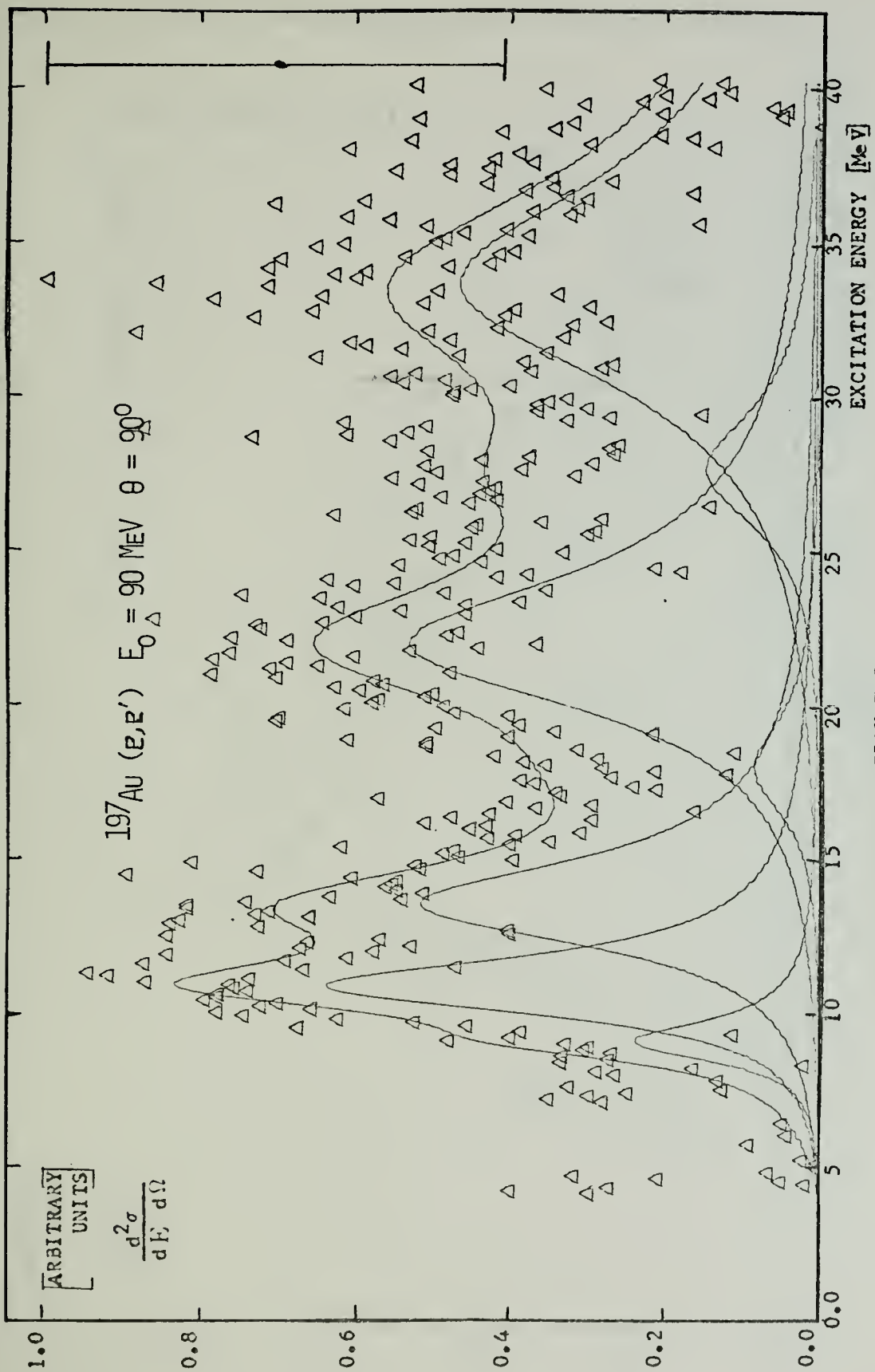


FIGURE 8

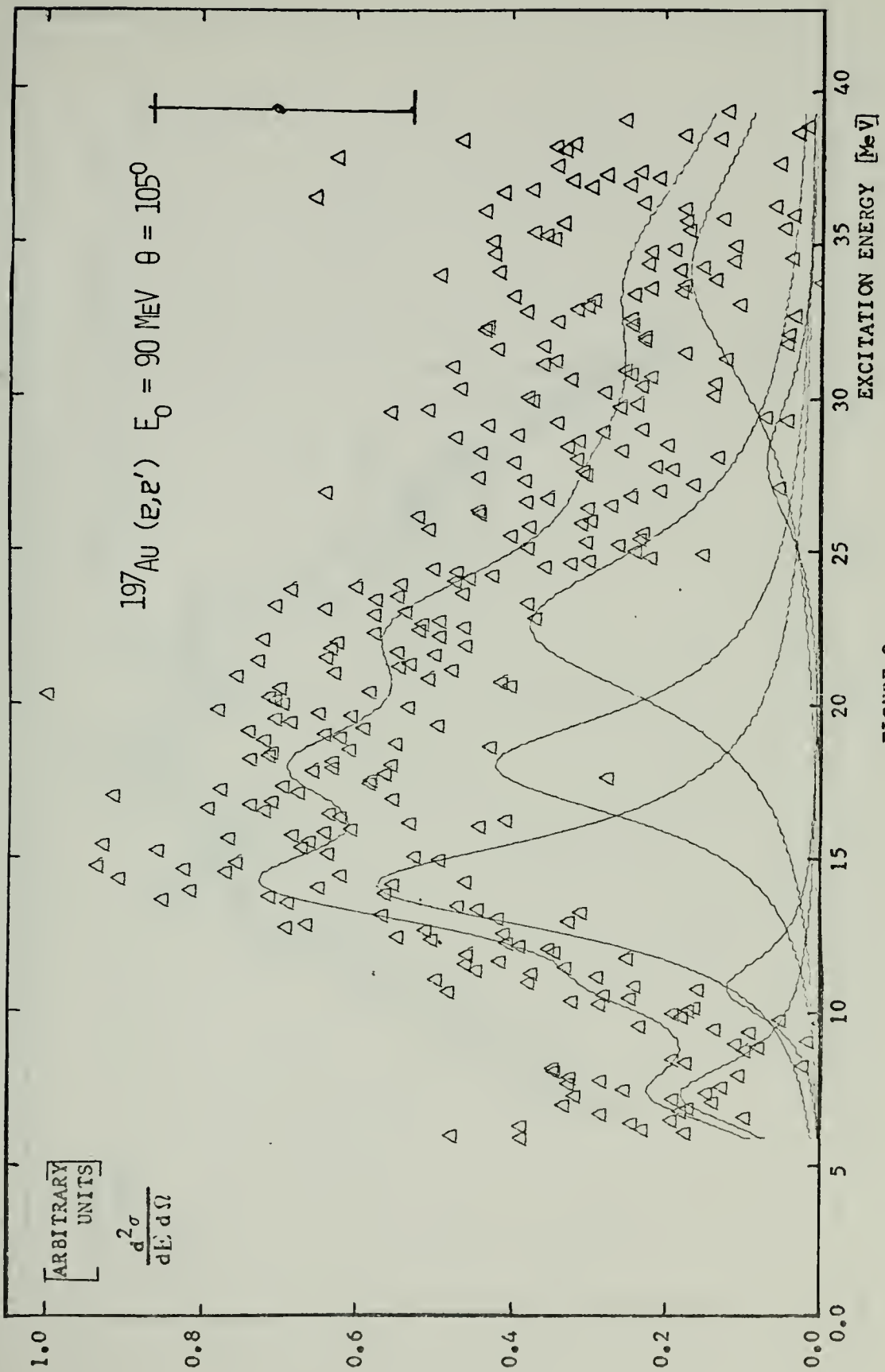


FIGURE 9

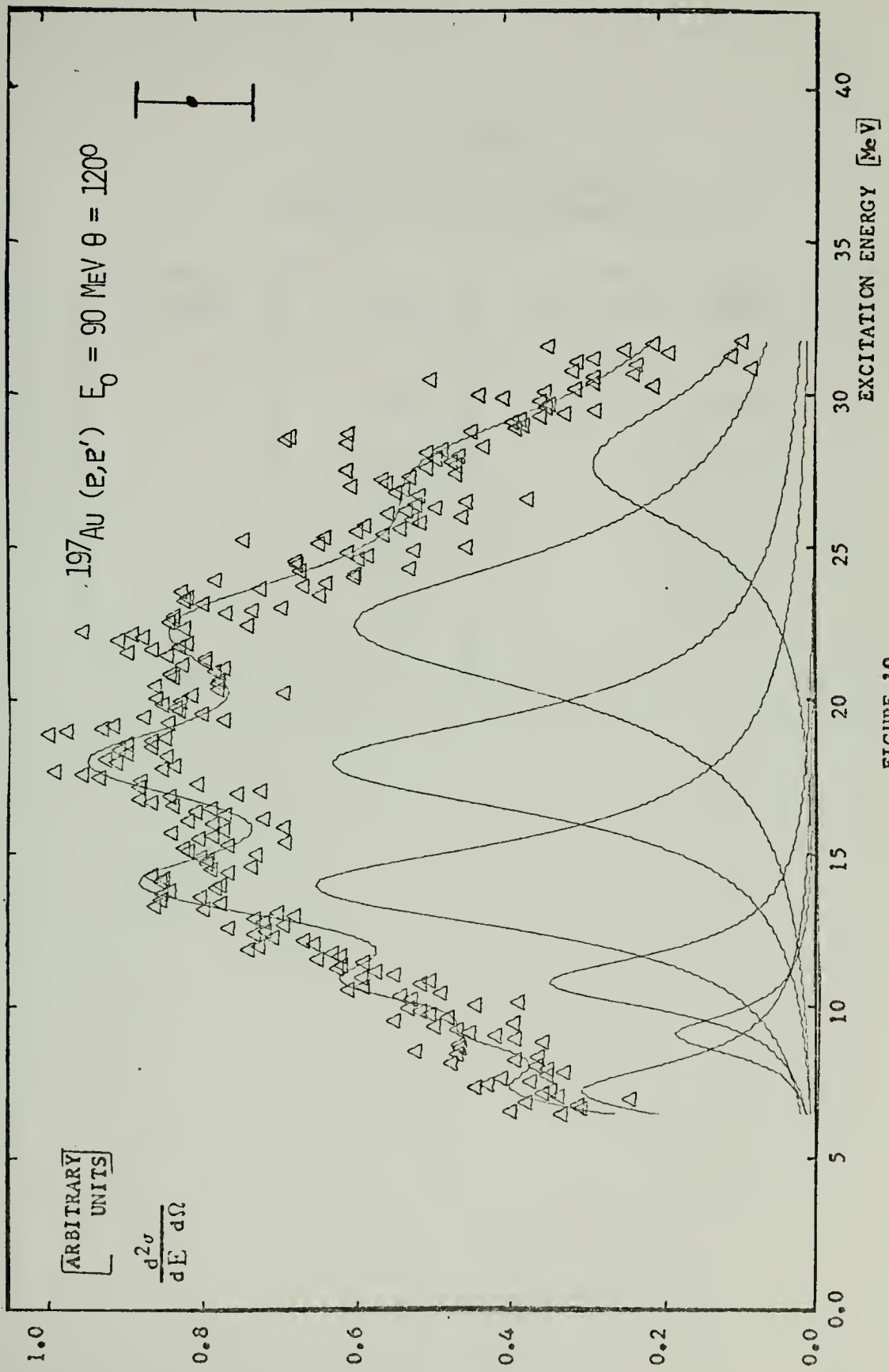


FIGURE 10

TABLE VI
 Scale Factors for Converting
 Arbitrary Units to Experimental Units

Figure	Angle	Scale Factor $\frac{\text{fm}^2}{\text{MeV}\cdot\text{sr}} / \text{Arb. units}$
6	60°	9.9×10^{-4}
7	75°	1.89×10^{-4}
8	90°	2.99×10^{-5}
9	105°	1.53×10^{-5}
10	120°	1.47×10^{-5}

TABLE VII
Area Ratios and Inelastic Form Factors Squared

E_x	Angle	A_i/A_e	Total % Error	$\frac{\sigma}{\sigma_{\text{Mott}}}$
7.3	60	6.37×10^{-3}	21	7.75×10^{-4}
	75	4.00×10^{-3}	25	1.78×10^{-4}
	90	9.7×10^{-4}	--	2.9×10^{-5}
	105	2.70×10^{-3}	85	6.05×10^{-5}
	120	1.01×10^{-2}	50	1.34×10^{-4}
9.2	60	3.19×10^{-3}	60	3.78×10^{-4}
	75	2.20×10^{-3}	60	9.78×10^{-5}
	90	9.73×10^{-4}	85	2.91×10^{-5}
	105	1.5×10^{-4}	--	3.2×10^{-6}
	120	4.34×10^{-3}	75	5.73×10^{-5}
10.8	60	4.47×10^{-3}	25	5.30×10^{-4}
	75	6.53×10^{-3}	20	2.86×10^{-4}
	90	3.58×10^{-3}	30	1.07×10^{-4}
	105	3.9×10^{-3}	--	8.40×10^{-5}
	120	1.07×10^{-2}	35	1.41×10^{-4}

TABLE VII Continued

E_x	Angle	A_i/A_c	Total % Error	$\frac{\sigma}{\sigma_0}$ Mott
14.0	60	7.60×10^{-3}	18	9.02×10^{-4}
	75	1.12×10^{-2}	16	4.98×10^{-4}
	90	4.42×10^{-3}	30	1.32×10^{-4}
	105	8.46×10^{-3}	35	1.84×10^{-4}
	120	3.18×10^{-2}	20	4.2×10^{-4}
18.0	60	1.82×10^{-3}	40	2.16×10^{-4}
	75	2.70×10^{-3}	35	1.20×10^{-4}
	90	1.7×10^{-3}	--	5.10×10^{-5}
	105	6.91×10^{-3}	40	1.50×10^{-4}
	120	3.41×10^{-2}	22	4.50×10^{-4}
22.5	60	4.21×10^{-3}	30	5.00×10^{-4}
	75	7.83×10^{-3}	20	3.47×10^{-4}
	90	7.17×10^{-3}	25	2.14×10^{-4}
	105	8.60×10^{-3}	45	6.02×10^{-4}
33.5	60	7.66×10^{-3}	50	9.09×10^{-4}
	75	9.80×10^{-3}	50	4.35×10^{-4}
	90	9.90×10^{-3}	60	2.48×10^{-4}
	105	1.5×10^{-2}	--	3.2×10^{-4}

B. ERROR ANALYSIS

The procedure outlined in the previous section provides values of the ratios of A_i/A_e but the uncertainties attached to these ratios requires additional considerations. The program NAW computes only statistical errors. There are other errors, both systematic and random which are not strictly statistical. Some of these are the errors resulting from the instrumental effects and are outlined by Bernard and Traverso [Ref. 36].

To obtain a more realistic estimate of the errors in the ratios A_i/A_e , the non-statistical uncertainties are assumed to be those which arise from the uncertainties in locating the resonance positions and determining their respective widths. These arise from two sources: the overall instrumental uncertainty which is estimated to be 0.15 MeV, and the freedom allowed in the resonance peak positions and widths in fitting these spectra. The total uncertainty of the energy in this work is the sum of the fitting possibilities and instrumental errors.

The Breit-Wigner shape is then analysed to see how these variations in energy effect the area under the resonances. The Breit-Wigner shape is given by

$$\frac{d\sigma(E, E_R, \Gamma)}{dE} = \frac{A}{(E - E_R)^2 + (\Gamma/2)^2}; \quad \text{III-1}$$

where E_R is the resonance energy, Γ is the resonance width, A is the strength parameter, and E is the excitation energy. The resonance cross section is given by the integral of the Breit-Wigner form

$$\sigma(E_R, \Gamma) = \frac{A\pi}{\Gamma} + \frac{2A \tan^{-1}(E_R/\Gamma)}{\Gamma} . \quad \text{III-2}$$

The variations in position and width introduce an uncertainty in the resonance cross section,

$$\Delta \sigma(E_R, \Gamma) = \left| \frac{\partial \sigma}{\partial E_R} \right| \Delta E_R + \left| \frac{\partial \sigma}{\partial \Gamma} \right| \Delta \Gamma . \quad \text{III-3}$$

The absolute values of the partial derivatives are assumed since the peak position and width uncertainties may be correlated.

The fractional error in the resonance cross section is

$$\frac{\Delta \sigma}{\sigma} = \frac{\left[\frac{2}{\Gamma^2 + E_R^2} \right] \Delta E_R + \left[\frac{\pi}{\Gamma^2} + \frac{2 \tan^{-1}(E_R/\Gamma)}{\Gamma^2} + \frac{2E_R}{\Gamma^3 + \Gamma E_R^2} \right] \Delta \Gamma}{\frac{\pi}{\Gamma} + \frac{2 \tan^{-1}(E_R/\Gamma)}{\Gamma}} \quad \text{III-4}$$

This uncertainty is then added to the statistical error to provide the total error. Table VIII lists the uncertainties from the two sources.

TABLE VIII
Fractional Error Contributions

E_r	$\frac{\Delta \sigma}{\sigma}$	Statistical Errors				
		60°	75°	90°	105°	120°
7.2	.16	.05	.08	Upper Limit	.67	.32
9.2	.51	.08	.09	.35	Upper Limit	.27
10.8	.16	.07	.05	.34	Upper Limit	.17
14.0	.11	.07	.06	.20	.25	.10
18.0	.13	.27	.21	.10	.25	.08
22.5	.09	.20	.12	.16	.34	
33.5	.27	.25	.21	.30	Upper Limit	

IV. DISCUSSION

A. COLLECTIVITY

Data analysis techniques explained in Chapter III were used to subtract the background and extract the elastic and inelastic spectra of the scattered electrons. A least squares fit was used to evaluate these spectra and resulted in the identification of seven giant resonances at excitation energies of 7.3, 9.2, 10.8, 14.0, 18.0, 22.5, and 33.5 MeV. These resonances have strengths corresponding to an appreciable fraction of the appropriate sum rule as exhibited in Table IX. Additional support to their collective nature is given in Table X where it is seen that the transition strengths are greater than several Weisskopf units. True giant resonances are therefore being observed.

B. MULTIPOLARITY ASSIGNMENTS

7.3 MeV Resonance

The multipolarity assignment of the resonance at 7.3 MeV is uncertain. Buskirk *et. al.* [Ref. 18] and Lone *et. al.* [Ref. 19] have observed this structure in backward angle (e, e') experiments and indicate a transverse excitation. A comparison of the data with calculations using GBROW [Ref. 27] and a code by Drechsel [Ref. 37] is incapable of determining a definite multipolarity assignment. Among possible reasons for this situation are a multipolarity admixture, existence of unknown longitudinal resonances influencing the forward angle data, and experimental difficulties encountered by the high counting rate at forward scattering angles.

9.2 MeV Resonance

The analysis of the 9.2 MeV resonance ($53 \text{ A}^{-1/3}$) favors an EO multipolarity assignment. This resonance exhausts 38% and 18% respectively of the EO and E2 energy-weighted sum rules and its strength corresponds to five Weisskopf units when an E2 assignment is made. However, the angular dependence of the experimental form factors favors EO (Fig. 12). The result would be in agreement with the isoscalar giant monopole resonance predicted at $56 \text{ A}^{-1/3}$ MeV [Ref. 21] and at $58 \text{ A}^{-1/3}$ MeV [Ref. 22]. Resonances exhibiting the characteristics of EO or E2 transitions were also seen at $E_X = 53 \text{ A}^{-1/3}$ MeV in $N = 82$ nuclei [Ref. 23] and in ^{208}Pb [Ref. 24]. An E1 multipolarity assignment is ruled out by comparison with DWBA form factor calculations and furthermore by the fact that no resonance has been seen in γ -absorption measurements [Ref. 25] at this excitation energy.

10.8 MeV Resonance

The resonance at 10.8 MeV ($63 \text{ A}^{-1/3}$) was seen previously in ^{197}Au [Refs. 3 and 18] and in many other nuclei (see e.g. [Ref. 5]). Generally an assignment of E2 was favored in these cases. In this experiment a transition strength of 14 Weisskopf units is obtained assuming an electric quadrupole excitation. Comparison of the experimental form factors to the angular distribution calculated from the DWBA form factors is inconclusive in distinguishing between an EO and E2 modes (Fig. 13). However, the experimental strength corresponds to 113% and 68% of the EO and E2 sum rules, respectively. Together with our results on the 9.2 MeV resonance, the E2 assignment is therefore favored. This resonance is thought to be the isoscalar quadrupole state predicted by the collective vibration model of Bohr and Mottelson [Ref. 38].

14.0 MeV Resonance

The 14 MeV ($81 \text{ \AA}^{-1/3}$) giant dipole resonance was measured with monochromatic γ - experiments [Ref. 25] and has also been seen in other (e,e') experiments [Refs. 3 and 18]. For this experiment, form factor comparisons to DWBA calculations show reasonable agreement at forward angles, but exhibit deviations at backward angles. An attempt was made to further explore the nature of the giant dipole transition by assuming both volume and surface oscillations separately in the DWBA calculations (Fig. 14) [Ref. 23]. Transition strengths of six and eight Weisskopf units and 84% and 104% of the sum rule are obtained for the volume and surface oscillation modes respectively. However, neither model adequately describes the observed data. As suggested by Pitthan [Ref. 39], the discrepancy at backward angles might be explained by an electric spin flip contribution to the E1 resonance [Ref. 40]. Using only the forward angle data to extract the reduced matrix elements, the volume oscillation strength exhausts the sum rule (98%), whereas the surface oscillation exceeds the sum rule. Thus a volume oscillation is favored.

18.0 MeV Resonance

A resonance of undetermined multipolarity is observed at 18.0 MeV ($105 \text{ \AA}^{-1/3}$) excitation energy. Nagao and Torizuka [Ref. 24] have observed E3 strength at the corresponding energy in ^{208}Pb , but the state in ^{197}Au does not conform to this multipolarity. E(0-3) and M (1-2) calculations have been compared to the data (Fig. 15), but no reasonable agreement is found. It appears that the cross-section at this excitation energy contains a mixture of various transitions.

22.5 MeV Resonance

Comparison of the experimental results for the 22.5 MeV ($130\text{A}^{-1/3}$) resonance with DWBA calculations (Fig. 16) gives support to an E2 assignment. At forward angles the data is indistinguishable between the EO and E2 transitions, but the 105° measurement is incompatible with the EO assignment. The Sendai group has reported [Ref. 3] an electric monopole or quadrupole at this excitation energy in ^{197}Au and also at the corresponding energy in ^{208}Pb [Ref. 24]. Other multipolarity assignments are unsuccessful in predicting an angular distribution in agreement with the data. The 22.5 MeV state is thought to be the isovector quadrupole state predicted by the collective vibration model of Bohr and Mottelson [Ref. 38].

33.5 MeV Resonance

A new resonance, previously unreported in ^{197}Au , is observed at 33.5 MeV ($194 \text{ A}^{-1/3}$). This corresponds roughly to the isovector giant monopole resonance predicted by Suzuki [Ref. 22] through calculations based on the collective vibration model of Bohr and Mottelson. Both the EO and E2 assignments exceed their respective energy-weighted sum rule prediction. However, our line shape fit, while very sensitive to any structure in the spectrum, may tend to over-estimate cross-sections for very wide resonances. For this reason, the B-values may be too large. Comparison of the experimental form factors to the DWBA calculations allow both EO and E2 multipolarities to be possible. A similar new resonance was observed in ^{208}Pb at a corresponding energy of 32.5 MeV [Ref. 26] and tentatively given an EO or E2 assignment. It is to be emphasized that consistent fits for all the spectra (^{197}Au) over the entire range from 5 MeV to 40 MeV excitation energy were only possible with the inclusion of this resonance at 33.5 MeV.

TABLE IX

Ratio of Resonance Strengths to Energy Weighted Sum Rules

E_r	Assumed Transition	ΔT	$B(\lambda L)$	$e^2 - f_m 2L$	$E_x B(\lambda L)$	Sum	$E_x B(\lambda L)$ Sum
7.3	M_1	--		.35±.26	--	--	--
7.3	M_2	--		(2.4±.8)x10 ⁻³	--	--	--
9.2	E_0	0		(3.6±1.8)x10 ⁻³	3.4x10 ⁻⁴	9.3x10 ⁻⁴	.36
9.2	E_1	1		9.2±10.0	85	7.0x10 ⁻²	.10
9.2	E_2	0		(1.5±.4)x10 ⁻³	1.4x10 ⁻⁴	7.4x10 ⁻⁴	.19
9.2	E_2	1		(1.5±.9)x10 ⁻³	1.4x10 ⁻⁴	1.10x10 ⁻⁵	.13
10.8	E_0	0		(9.2±1.9)x10 ⁻³	1x10 ⁻⁵	9.3x10 ⁻⁴	1.0
10.8	E_2	0		(4.7±.8)x10 ⁻³	5.1x10 ⁻⁴	7.4x10 ⁻⁴	.68
10.8	E_2	1		(4.7±.8)x10 ⁻³	5.1x10 ⁻⁴	1.1x10 ⁻⁵	.46

* For Monopole Matrix Elements are Given

TABLE IX Continued

E_r	Assumed Transition	ΔT	$B(\lambda L)$	$e^2 \text{- fm}^2 L$	$E_x B(\lambda L)$	Sum	$\frac{E_x B(\lambda L)}{\text{Sum}}$
14.0	$E_1 \left[\rho_{tr} = \rho_0 \right]$	--	(4.9±.7)x10 ¹		6.9x10 ²	7.0x10 ²	.98
14.0	$E_1 \left[\rho_{tr} = \frac{d \rho_0}{dr} \right]$	--	(8.6±1.1)x10 ¹		1.2x10 ³	7.0x10 ²	.17
18.0	M ₂	--	(1.5±.8)x10 ³	--	--	--	--
18.0	E ₀	0	(5.0±1.5)x10 ³		8.9x10 ⁴	9.3x10 ⁴	.46
18.0	E ₂	0	(2.7±1.5)x10 ³		4.8x10 ⁴	7.4x10 ⁴	.65
18.0	E ₂	1	(2.7±1.5)x10 ³		4.8x10 ⁴	1.1x10 ⁵	.44
18.0	E ₃	0	(2.0±1.0)x10 ⁵		3.6x10 ⁶	6.2x10 ⁶	.58
18.0	E ₃	1	(2.0±1.0)x10 ⁵		3.6x10 ⁶	9.2x10 ⁶	.39

TABLE IX Continued

E_r	Assumed Transition	ΔT	$B(\lambda L) e^2 \text{-fm}^2 L$	$E_x B(\lambda L)$	Sum	$\frac{E_x B(\lambda L)}{\text{Sum}}$
22.5	E_0	0	($2\pm.13$) $\times 10^3$	4.3×10^4	9.3×10^4	.46
22.5	E_2	0	($7.1\pm.5$) $\times 10^3$	1.6×10^5	7.4×10^4	2.2
22.5	E_2	1	($7.1\pm.5$) $\times 10^3$	1.6×10^5	1.1×10^5	1.5
22.5	E_3	0	($3.4\pm.8$) $\times 10^5$	7.6×10^6	6.2×10^6	1.2
22.5	E_3	1	($3.4\pm.8$) $\times 10^5$	7.6×10^6	9.2×10^6	.83
55.5	E_0	0	($1.4\pm.7$) $\times 10^4$	8.2×10^5	9.3×10^4	5.0
55.5	E_2	0	(6.3 ± 2.2) $\times 10^3$	2.1×10^5	7.4×10^4	2.8
55.5	E_2	1	(6.3 ± 2.2) $\times 10^4$	2.1×10^5	1.1×10^5	1.9

TABLE X

Transitions Strengths in Weisskopf Units

E_r	Transition	$B(\lambda L) [e^2 \text{-fm}^{2L}]$	$B_{sp}(EL/M_L)/e^2$	$B(\lambda L)/B_{sp}$
7.3	M_1	.35 ± .26	.06	6
7.3	M_2	$(2.4 \pm .8) \times 10^3$	3.1	770
9.2	E_0	$(3.64 \pm 1.80) \times 10^3$	--	--
9.2	E_1	9.2 ± 10.0	6.6	1
9.2	E_2	$(1.49 \pm .92) \times 10^3$	3.4×10^2	4
10.8	E_0	$(9.22 \pm 1.87) \times 10^3$	--	--
10.8	E_2	$(4.68 \pm .80) \times 10^3$	3.4×10^2	14
14.0	$E_1 \left[Q_{tr} = Q_0 \right]$	$(4.9 \pm 7) \times 10^1$	6.6	8
14.0	$E_1 \left[Q_{tr} = \frac{dQ_0}{dR} \right]$	$(8.6 \pm 1.1) \times 10^1$	6.6	13
18.0	M_2	$(1.48 \pm .84) \times 10^3$	3.1	480
18.0	E_0	$(4.96 \pm 24.4) \times 10^3$	--	--
18.0	E_2	$(2.66 \pm 1.51) \times 10^3$	3.4×10^2	8
18.0	E_3	$(1.97 \pm .09) \times 10^6$	1.6×10^4	12

TABLE X Continued

E_r	Transition	$B(\lambda L) [e^2 \text{-fm}^2 L]$	$B_{sp}(EL/ML)c^2$	$B(\lambda L)/B_{sp}$
22.5	E_0	$(1.90 \pm .13) \times 10^3$	--	--
22.5	E_2	$(7.10 \pm .48) \times 10^3$	3.4×10^2	22
22.5	E_5	$(3.39 \pm .78) \times 10^5$	1.63×10^4	21
33.5	E_0	$(1.40 \pm .72) \times 10^4$	--	--
33.5	E_2	$(6.25 \pm 2.15) \times 10^3$	3.4×10^2	19

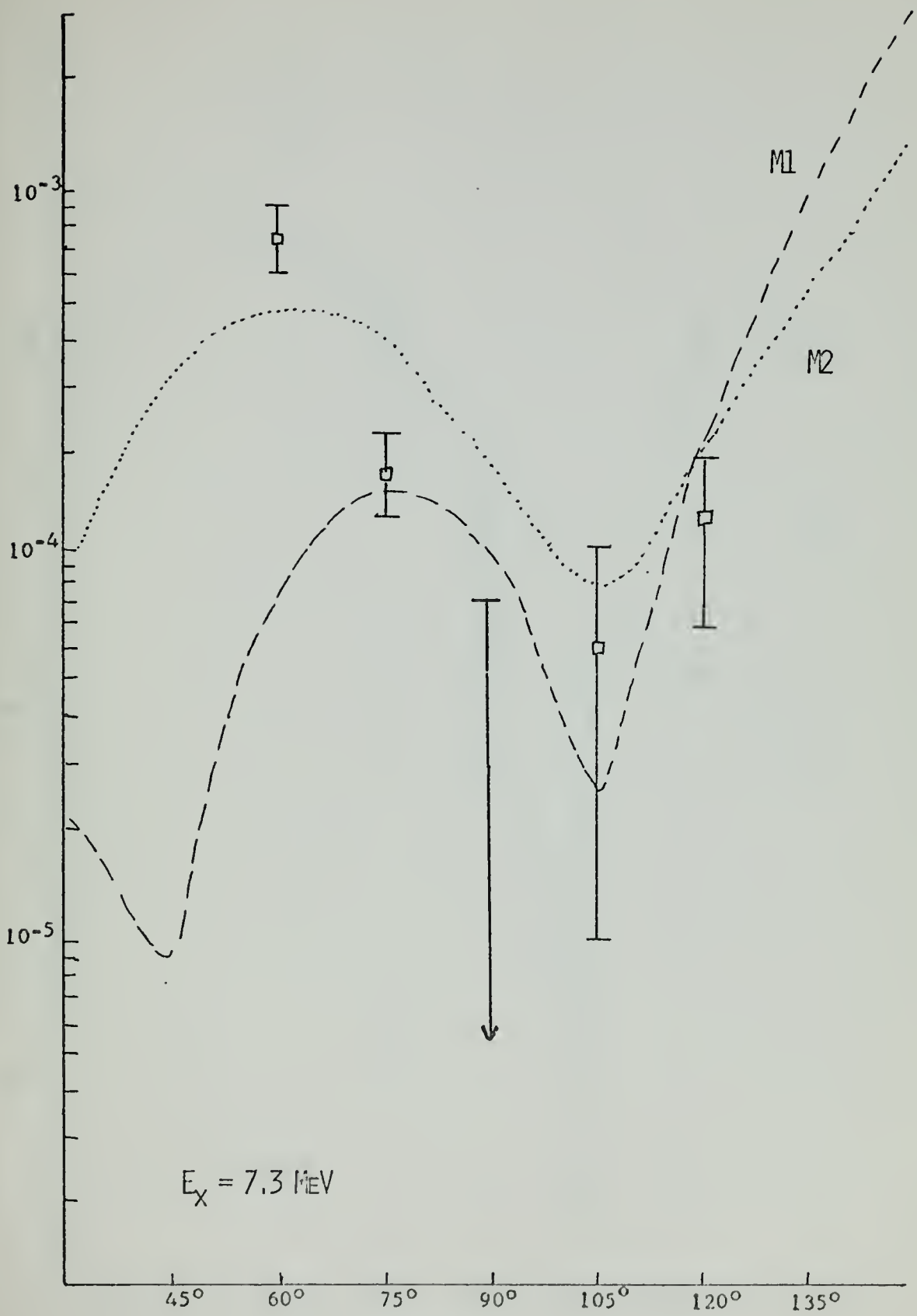


FIGURE 11

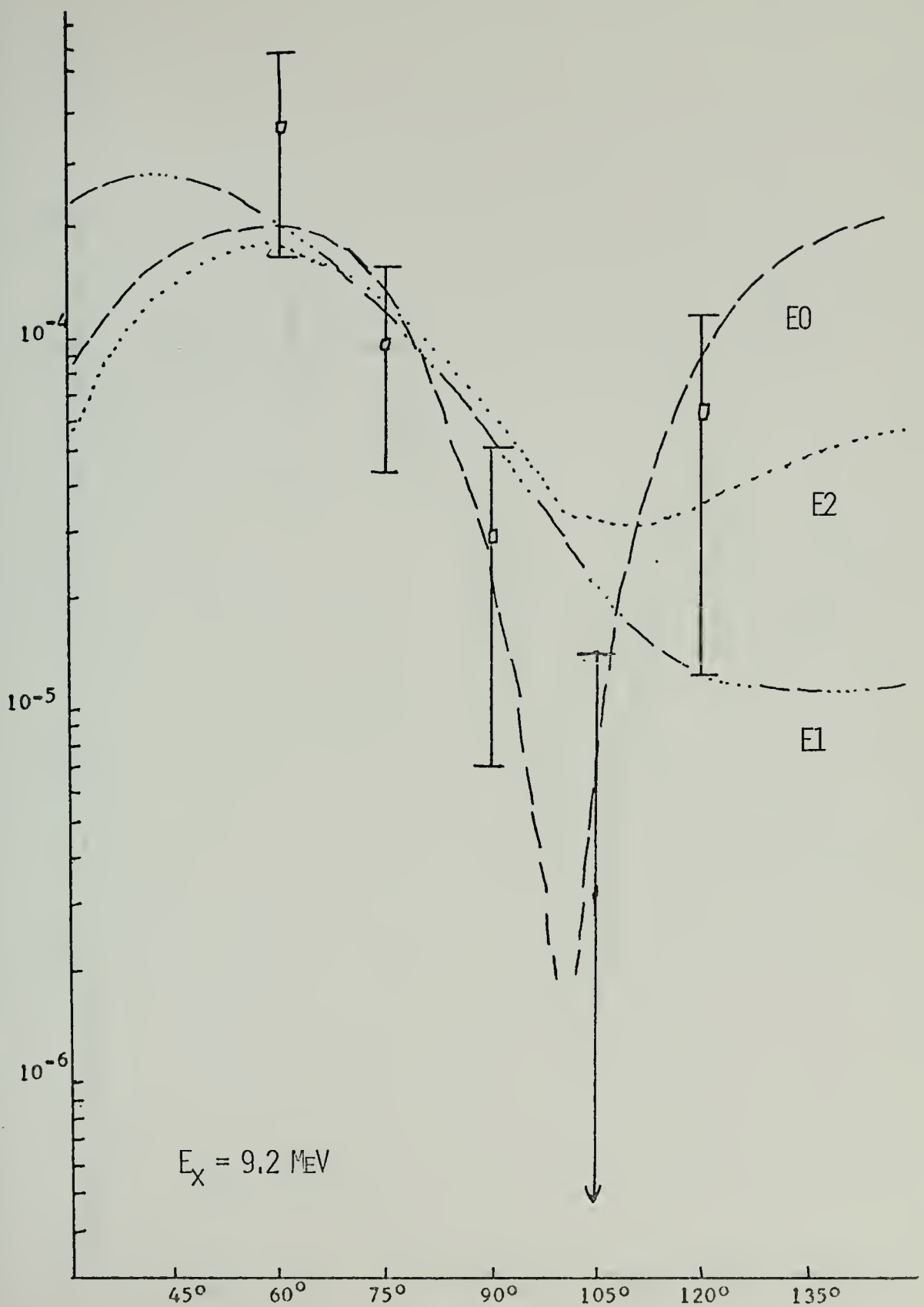


FIGURE 12

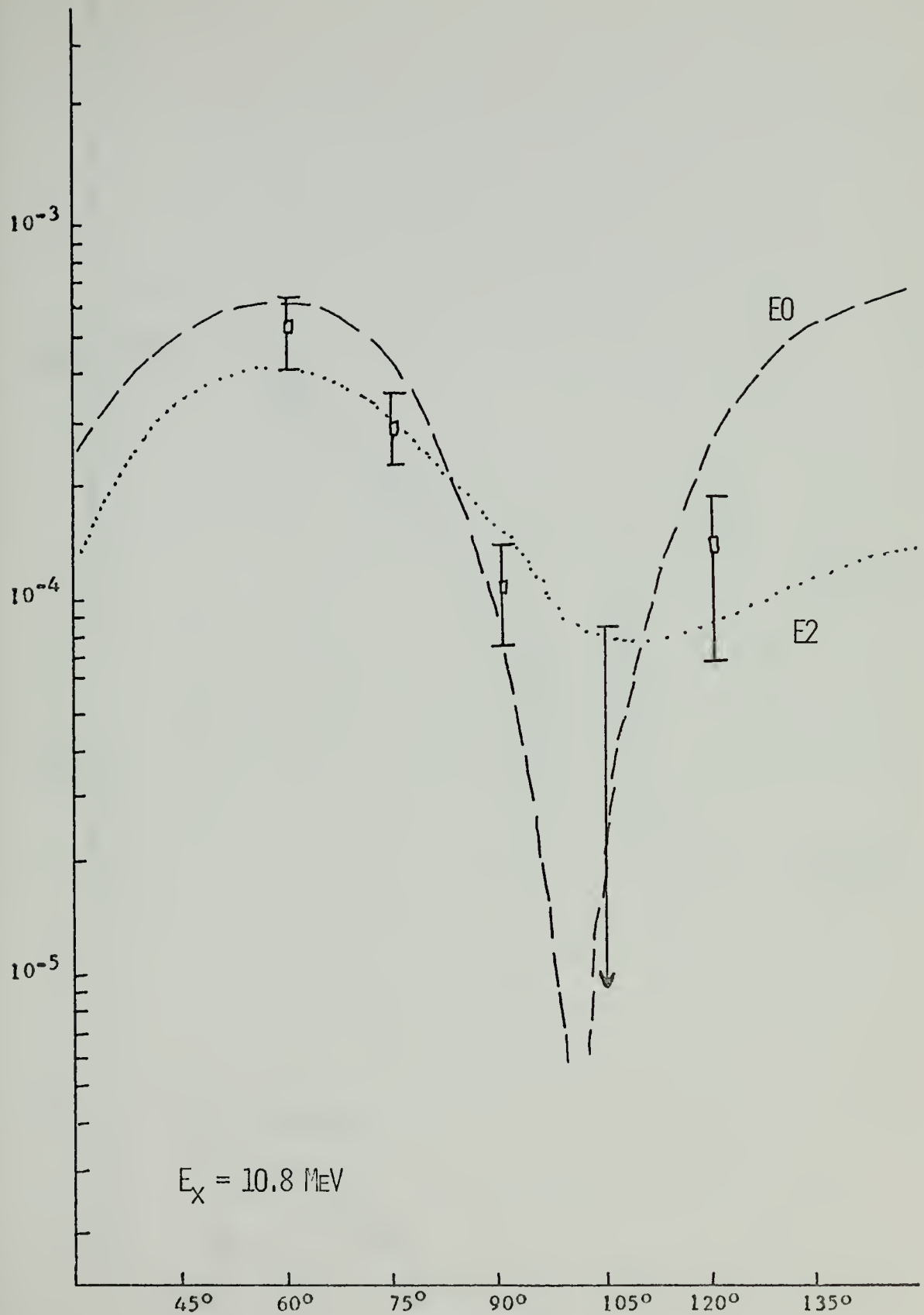


FIGURE 13

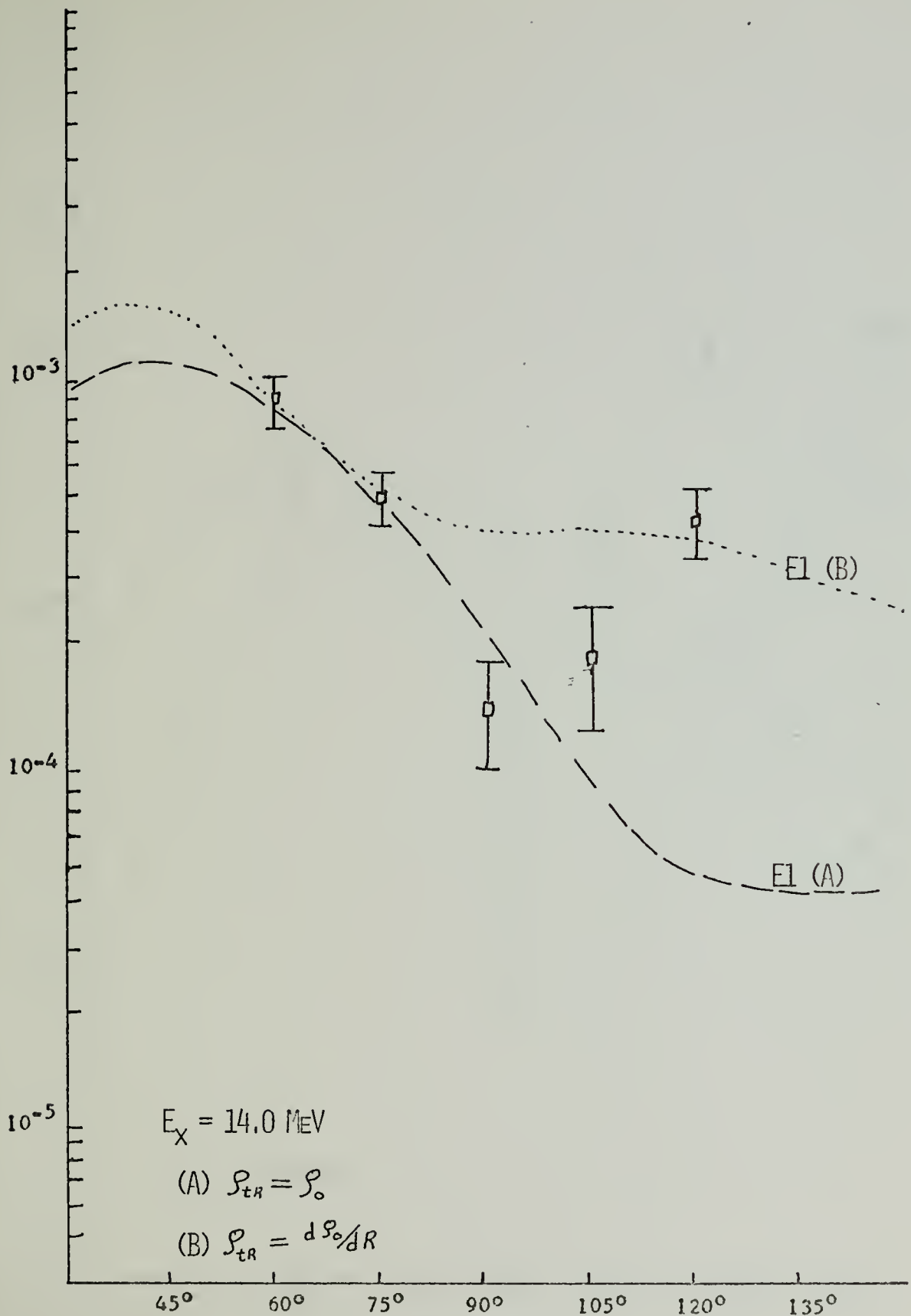


FIGURE 14

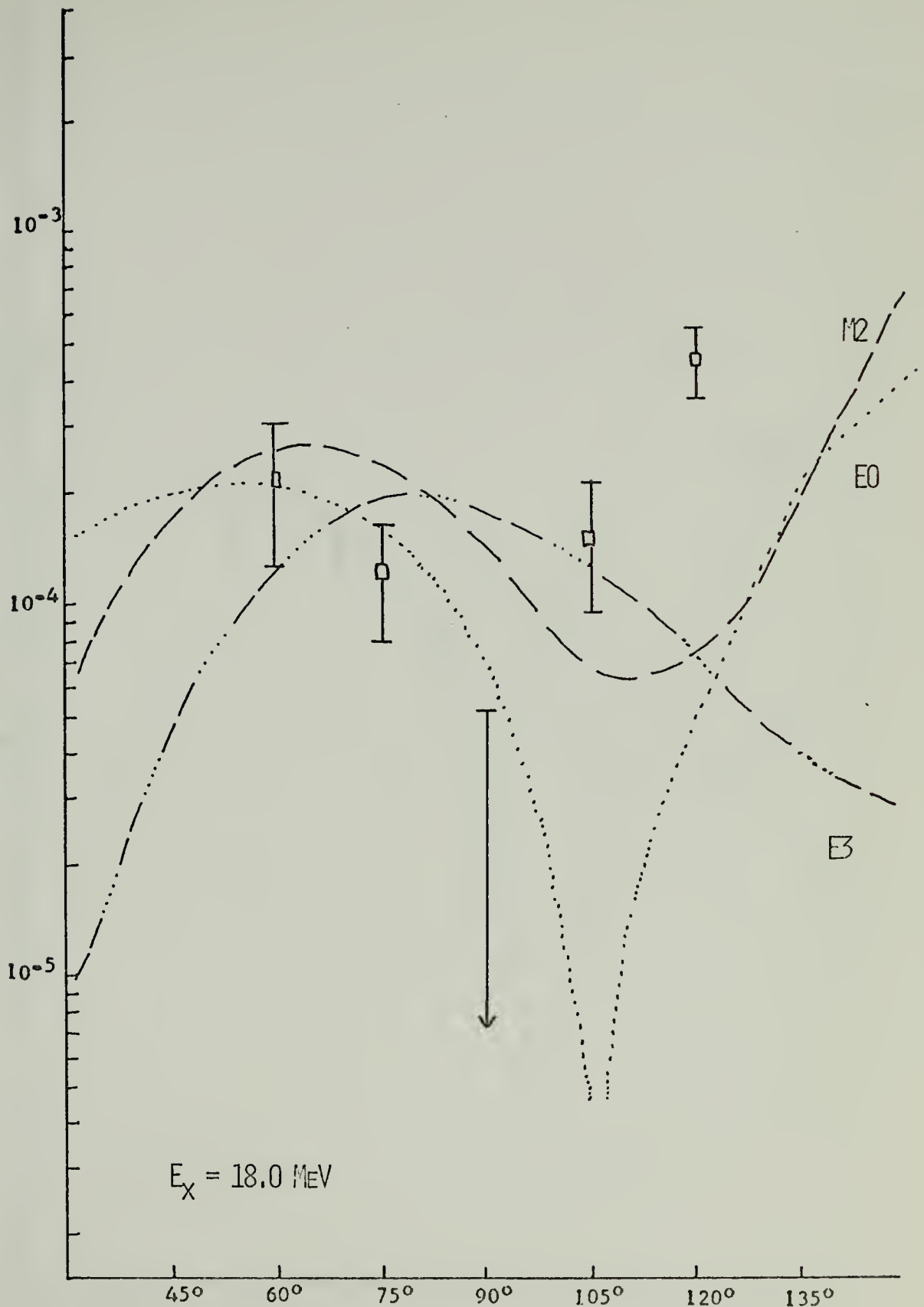


FIGURE 15

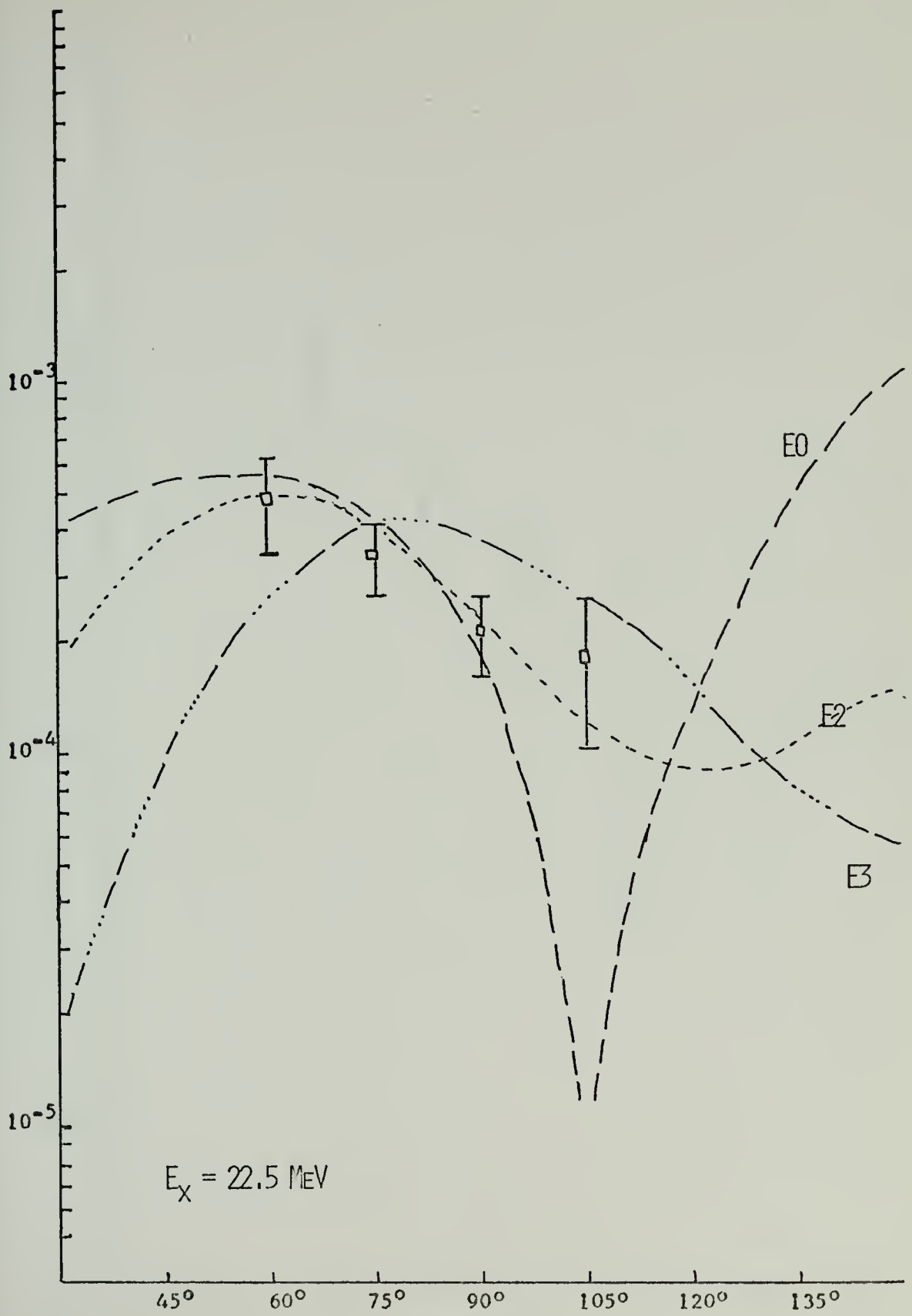


FIGURE 16

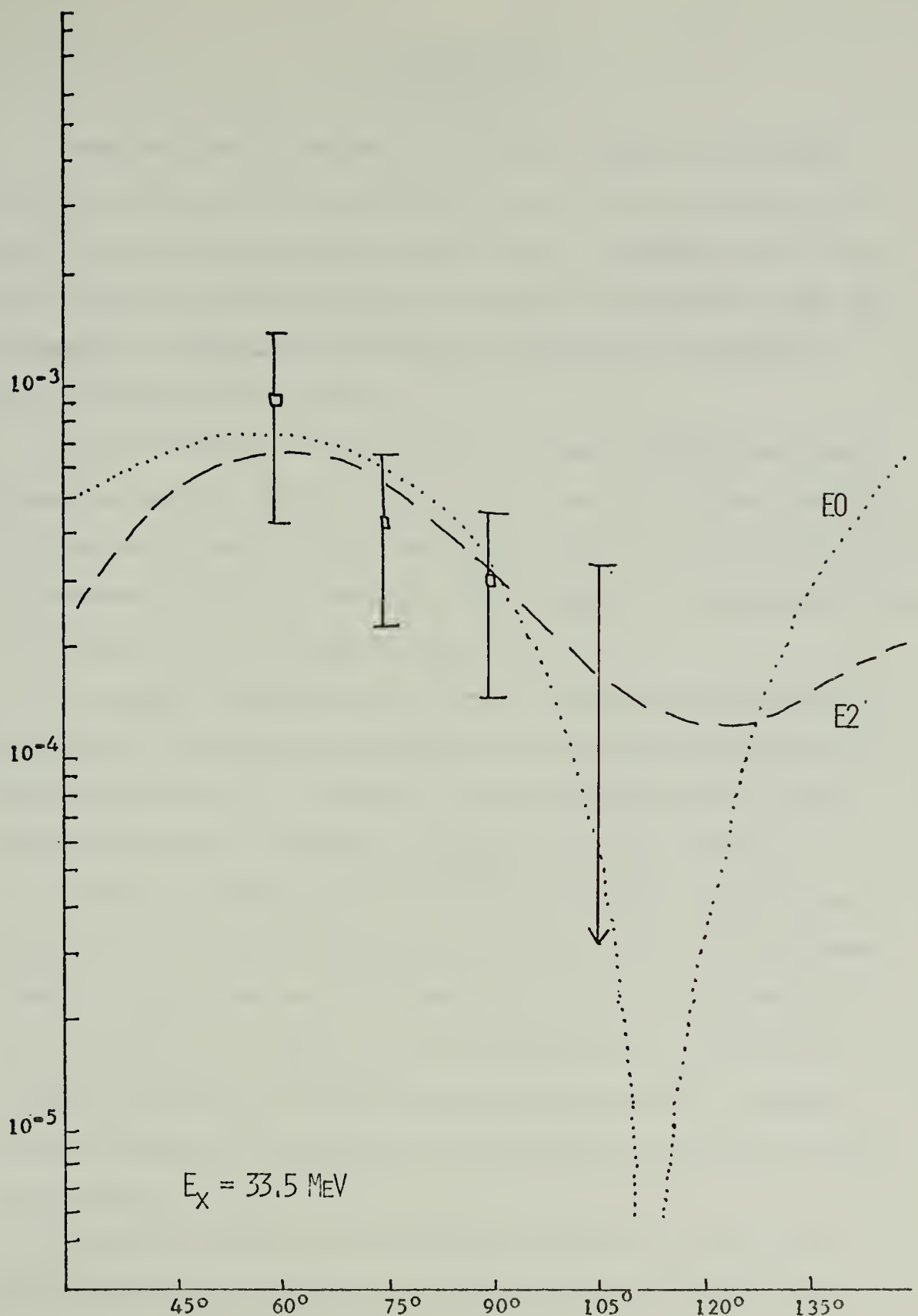


FIGURE 17

V. CONCLUSIONS

Giant multipole resonances in ^{197}Au were studied with inelastic electron scattering. Resonances at 7.3, 9.2, 10.8, 14.0, 18.0, 22.5, and 33.5 MeV excitation energy were observed. Of these, the 9.2, 18.0, 22.5, and 33.5 MeV states have not previously been reported in the open literature. Multipolarity assignments of these states were made as was discussed in section IV-B.

The 14.0 MeV state is identified as the much studied giant dipole resonance, see e.g. [Refs. 3, 5, & 25]. Our analysis suggests that this E1 state may be described by a volume oscillation of the charge distribution. Furthermore, the data is compatible with a suspected transverse spin flip contribution to the E1 cross section.

The angular distributions of the cross-sections for the 10.8 MeV and 22.5 MeV resonances are compatible with previous E2 multipolarity assignments [Ref. 3]. In addition, this investigation adds evidence for the exclusion of a monopole assignment for the 10.8 MeV state.

A state was found at 18 MeV in ^{197}Au . In ^{208}Pb a resonance was seen [Ref. 26] and cross-section analysis of another (e,e') experiment found E3 strength between 16 MeV and 22 MeV [Ref. 24]. The analysis of the experimental results for this energy region in ^{197}Au is not capable of assigning a definite transition multipolarity. The data suggests admixtures of longitudinal and transverse contributions to the cross-section.

The 7.3 MeV transition is known to be magnetic. However, this investigation, like others [Ref. 19], was not able to determine the transition mode.

Theoretical investigation concerning the existence and location of the giant monopole resonance is found in the literature [Refs. 21 and 22]. New resonances, discovered in this experiment at 9.2 MeV and 33.5 MeV, have angular distributions in agreement with monopole assignments. Their excitation energies are comparable to theoretical predictions [Ref. 22] of the location of the isoscalar and isovector monopole states. For the lower state, an E0 transition is favored over an E2 assignment. However, for the 33.5 MeV state, the transition multipolarity is inconclusive. The excitation energies and transition multipolarities are presented in Table XI.

TABLE XI
Multipolarity Assignments

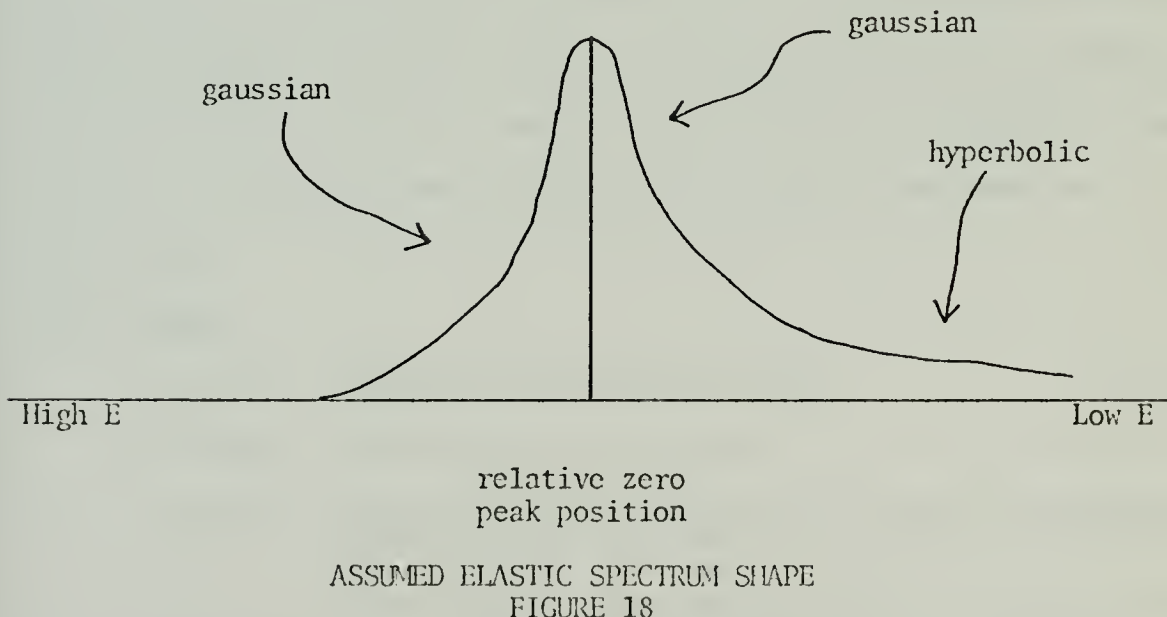
Excitation Energy (MeV)	Transition Multipolarity	Comments
7.3	undetermined	probable magnetic, mixture
9.2	E0	Isoscalar
10.8	E2	Isoscalar
14.0	E1	Isovector, volume oscillation
18.0	undetermined	
22.5	E2	Isovector
33.5	E0 or E2	Isovector

APPENDIX A

PROGRAM NAW, SPECTRUM FITTING CODE

A. GENERAL FEATURES

Naw is a Fortran program developed at Darmstadt [Refs. 41 & 43] which uses analytical expressions to approximate the inelastic and elastic line shapes and radiation tail to best fit the experimental spectra. The elastic line shape is assumed to be two half gaussians of differing half widths matched to a hyperbolic shape approximating the radiation tail. Work done by the experimenters at the Institut Für Technische Kernphysik at Darmstadt have found this parameterization to be an adequate estimate of the shape of the elastic peak (see Figure 18) [Ref. 41].



The elastic radiation tail results from processes occurring during elastic scattering that produce lower energy electrons. The radiation tail is calculated from the theory [Ref. 43] at several designated energies

and these theoretical values are fitted with a polynomial of the fourth degree. The total background, which includes the radiation tail, is then simultaneously fit with a series of Breit-Wigner line shapes representing the nuclear excitation structure to reproduce the experimental spectrum. The positions and widths of the resonances are free parameters to be adjusted by best fit or to be assigned from known values. The areas under these resonances are then calculated from which the ratios A_i/A_e (inelastic peak area divided by the elastic peak area) are determined. The values A_i/A_e are then multiplied by the calculated scattering cross section resulting in the experimental inelastic cross section for each of the resonances.

B. CONTROL CARDS

NAW uses the output from program KIK as the input data. Since NAW's first use at the NPS IBM 360/67 [Ref.1] it has undergone various modifications. The present form is reproduced on the following pages, along with the control information. NAW accepts 200 elastic peak data points, 500 inelastic data points and 25 inelastic resonances per spectrum.

NAW CONTROL

1. TEXT Alphanumeric identifying remarks (20A4)
2. NORM, PN₂, PN₃, PN₄, PN₅, PN₆, PN₇ (7F10.5)
NORM Spectrometer energy normalization factor to change the original energy units (OEU) to MeV: [MeV] = NORM* [OEU]
- PN_i i=2-7, Starting values for the various parameters being used to fit the elastic spectrum with an analytical expression.
- PN₂ Half-width of a gaussian to fit the high energy side of the elastic peak.

PN ₃	Half-width of a gaussian to fit the low energy side of the elastic peak.
PN ₄	Matching point for the low energy gaussian and the hyperbolic segment. PN ₄ is specified in MeV from the position of the zero point and is a negative number.
PN ₅	Dummy.
PN ₆	PN ₆ ≠ 0, Height of a second elastic resonance peak if necessary.
PN ₇	Position of a second elastic resonance peak if necessary, only with PN ₆ ≠ 0.

3. EE, THETA, D, UNT, (4F10.5)

EE	Energy of the elastic peak in MeV. EE is used as a starting value in the elastic fit.
THETA	Electron scattering angle in degrees.
D	Target thickness in g/cm ² .
UNT	Constant background at the high energy end of the elastic resonance spectrum in counts/ μ c.

4. EEL_u, EEL₁, GSSW_u, GSSW₁, DSSW, E_{ref} (6F10.5)

EEL _u	High energy limit for fitting the elastic peak in OEU.
EEL ₁	Low energy limit for fitting the elastic peak in OEU.
GSSW _u	Upper limit for calculating the radiation tail in OEU.
GSSW ₁	Lower limit for calculating the radiation tail in OEU.
DSSW	Energy step to be used in calculating the radiation tail in OEU.
E _{ref}	See card 7, L ₂ . If E _{ref} = 0, E _{ref} is calculated internally.

5. E_u, E₁ (2F10.5)

E _u	High electron energy limit for fitting the inelastic spectrum in excitation energy (MeV).
E ₁	Low electron energy limit for fitting the inelastic spectrum in excitation energy in (MeV).

$$6. \text{ GR}_u^1, \text{GR}_1^1, \text{GR}_u^2, \text{GR}_1^2, \text{GR}_u^3, \text{GR}_1^3 \quad (6F10.5)$$

Regions where it is expected that only background contributes to the spectrum; i.e., between resonances in the inelastic spectrum. There must be at least one set of $\text{GR}_u^1, \text{GR}_1^1$ input, with a maximum of three. It is recommended to set $\text{GR}_u^1 \approx \text{GSSW}$, $\text{GR}_1^1 \approx \text{GSSW}$ for giant resonances, energy in MeV.

$$7. L_i \quad i=1 \text{ to } 22 \quad (22I3)$$

L_i 1 A continuous curve consisting of two gaussians and a segment of a hyperbolic is used for both elastic and inelastic fits.

- 2 The elastic resonance will be fit as if $L_1=1$ and the inelastic resonance will be fit using the Breit-Wigner formula. Each curve will be multiplied by a straight line with an equation $Y=1 + P_i(E_x - E_x^{(i)})$. P_i will be specified on card #10, E_x is the excitation energy, and $E_x^{(i)}$ is the position of the maximum as specified on card #8.
- 3 The elastic resonance will be fit as if $L_1=2$ except that NAW will determine the values P_i and card #10 will be left blank.

L_2 Parameters which choose the analytical expression to fit the background due to the radiative and experimental processes, L_2 is a two digit number, the units give the order of a polynomial e.g. unit=3, $P_1 + P_2 A + P_3 A^2$, the P_i 's are free fitted parameters. The decades choose the function to be multiplied and the argument to be used.

$$1 \leq L_2 < 10 \quad P_1 + P_2 A + P_3 A^2 + \dots + P_{L_2+1} \cdot \text{FSSW}$$

$$10 < L_2 < 20 \quad P_1 + P_2 A + P_3 A^2 + \dots + \text{FSSW}$$

$$20 < L_2 < 30 \quad \left\{ P_1 + P_2 A + P_3 A^2 + \dots + P_{L_2+1} \cdot \text{FSSW} \right\} \exp \left[P_{L_2+2} \left(\frac{E - E_c}{E} \right) \right]$$

$$30 < L_2 < 40 \quad \left\{ P_1 + P_2 A + P_3 A^2 + \dots + \text{FSSW} \right\} \exp \left[P_{L_2+1} \left(\frac{E - E_c}{E} \right) \right]$$

FSSW is the calculated radiative tail, E is the energy of the outgoing electron, E_c , is the energy of the elastic peak. $A - (E - E_{ref})$ for $L_2 < 50$, E_{ref} is read in on card #7. If $50 < L_2 < 90$ the analytical form corresponding to $L_2 = L_2 - 50$ is chosen, but A is replaced by $1/A$.

L_3 The number of resonances with fixed energies. If $L_3 < 0$ then the resonance will be kept fixed relative to $E_x^3(1)$, but $E_x^3(1)$ will be fitted. See card #8.

L_4 The number of resonances with energies to be fitted. Note that $|L_3| + L_4$ must not exceed 25.

L_5	The number of lines widths to be fitted. >0 E.g. $=3$, means that three line widths are free and in fact are $E_x(1)$, $E_x(2)$, and $E_x(3)$. If there are more than three resonances, $E_x(N)$ through $E_x(N)$ will all be fitted with the same line widths.
L_6	For $L_1 \geq 2$ the first L_6 peaks will be fitted with Breit-Wigner forms, the remainders with gaussian shapes. For $L_6=0$, $L_6 = L_3 + L_4$
L_7	Target geometry: $\begin{array}{ll} =0 & \text{Transmission -normal thickness entered on card #3} \\ =1 & \text{Reflection -normal thickness entered on card #3} \\ =2 & \text{Effective thickness entered on card #3} \end{array}$
L_8	Output control: $\begin{array}{ll} =0 & \text{Maximum output} \\ =1 & \text{Minimal output-no tables and no intermediate calculations} \\ =-1 & \text{Limited output-no tables} \end{array}$
L_9	Plotting control: $\begin{array}{ll} =0 & \text{Results are not plotted.} \\ =2 & \text{Results are plotted.} \end{array}$
L_{10}	Repetitions of NAW procedure. $\begin{array}{ll} =0 & \text{No repetitions are performed.} \\ >0 & \text{In this case it is possible to evaluate the data with new parameters. The new parameters will be entered on additional cards placed after the control cards.} \end{array}$
L_{11} - L_{14}	Inelastic spectrum fit iteration control. Only override to the default options need be entered.
L_{11}	Number of iterations where all energies are fixed, default $L_{11}=2$.
L_{12}	Maximum number of iterations; default is $L_{12}=30$.
L_{13}	Minimum number of iterations; default is $L_{13}=5$.
L_{14}	Number of iterations where width are held constant in case $\chi^2_{\text{actual}} > 3 \chi^2_{\text{theory}}$.
L_{15}	$\begin{array}{l} =0 \text{ The radiation tail will be calculated using the Ginsber's method [Ref. 43].} \\ <0 \text{ The radiation tail will be calculated using Schiff's method [Ref. 44].} \end{array}$

$L_{16} - L_{18}$ Radiation tail fit control. Only override options need be entered.

L_{16} Analytical representation of the theoretically calculated radiation tail; default is $L_{16}=1$.

$$=1 \text{ } SSW = P_1 + P_2 A + P_3 A^2 + P_4 A^3 + P_5 A^4$$

$$=2 \text{ } SSW = P_1 + P_2 A + P_3 A^2 + P_4 E + P_5 E^2$$

$$=3 \text{ } SSW = P_1 + P_2 A + P_3 E + P_4 E^2 + P_5 E^3$$

$$=4 \text{ } SSW = P_1 + P_2 E + P_3 E^2 + P_4 E^3 + P_5 E^4$$

$$=5 \text{ } SSW = P_1 + P_2 U + P_3 U^2 + P_4 U^3 + P_5 U^4$$

P_i will be fitted internally by NAW

$$A = 1/(E_{c1} - E)$$

$$U = E - E_b$$

$$E_b = GSSW_1 + (GSSW_u - GSSW_1)/L_{18}$$

☞ the radiation tail parameters P_i and E_b will be specified on card #15.

L_{17} The number of parameters for the radiation tail fit ($3 \leq L_{17} \leq 5$); default is $L_{17} = 4$.

L_{18} See L_{16} ; default is $L_{18} = 2$.

L_{19} >0 Error ellipsoid control values will not be calculated.

L_{20} = 0

L_{21} >0 The calculation of the radiation tail will be modified by the factors entered on card #16.

L_{22} =3 Inelastic spectrum results. Card images will be written on file 7 and may be stored on the data cell for further handling.

8. $E_x(1), E_x(2), \dots, E_x(i)$ (8F10.5)

Resonance excitation energies in MeV; enter those with variable positions first. $i = |L_3| + L_4 < 25$.

9. $V(1), V(2), \dots, V(i)$ (8F10.5)

Resonance line widths, $i = |L_3| + L_4 < 25$
If any $V(i) = 0$, the width of the elastic line will be assumed.

10. P(1), P(2), ..., P(i) (8F10.5)

The P_i factors when $L_1 = 2$ on card #7, $i = |L_3| + L_4 < 25$.

11. Z, A, XRAD, FIRA, C T (4F10.5, 20X, 2F10.5)

Z Atomic number.

A Mass number.

XRAD Radiation length in g/cm².

FIRA Elastic form factor for E_E and THETA of the experiment.

C,T The fermi charge distribution parameters. Since these values are used as the parameters for the trapezoidal charge distribution potential used in the radiation tail calculations in Born Approximation, these values must be entered.

12. XMAS, H (2F10.5)

XMAS Nuclear mas equivalent in MeV.

H Isotope percentage (100% = 1.00).

13. A_i The A_i are the coefficients for the calculations of the elastic form factor using a power series expansion on q^2 :

$$F_{el}^2 = \sum_{i=1}^8 A_i q^{2(i-1)}$$

When $A_1 = 0$ the elastic form factor will be calculated using the Born Approximation.

14. U_i (8F10.5)

U_i may be used to get better starting values for the fit by taking the background parameters from a previous fit. If the $U_i = 0$, the starting values are chosen internally. See card #7.

15. P1, P2, P3, P4, P5, E_b (6F10.5)

This card is read only if $L_{16} < 0$.

P1-P5 Radiation tail parameters, see L_{16} for the expression.

E_b This value is read only when $L_{16} = -5$.

16. XSSW, XM, XB,

(3F10.5)

This card is read only if $L_{21} > 0$.

XSSW Factor Multiplying the area under the elastic peak, A_e

XM Factor multiplying the Møller term.

XB factor multiplying the B

The equation for the radiation tail is now given by

$$SSW = \frac{MAXI}{F2\sigma_{Mott}} + XM(\text{Møller term}) + XB(\text{Brems. term}) \cdot (XSSW) A_e$$

MAXI are form factors as described by Maximon and Isabelle.

The data are assigned to file #4. The elastic and the inelastic data must be followed by one card image having the data energy step width entered beginning in column 72. Repeated evaluations of the same set of data (i.e. $L_{10} = 0$) must have the following set of cards placed after the 14 to 16 control cards as described above; one set for each repetition to be performed.

- 1) $L_1 \dots L_{10}$ see card #7
- 2) E_u, E_l see card #5
- 3) $E_x(1), \dots, E_x(i)$ see card #8
- 4) $V(1), \dots, V(i)$ see card #9
- 5) $P(1), \dots, P(i)$ see card #10

NAW LISTING

```

DIMENSION DUM1(600),LP(25),PR(50),PAR(100),FFF(200),BR(25)
DIMENSION WORD(20),BVAR(25),PVAR(25)
COMMON PAR,LPAR,DUM1,WORD,FFF
COMMON /BVARI1,BVAR2/,BVAR2/PVAR
COMMON /SSWD/ACO(25)
COMMON /SUSSTART/UPAR(10)
CALL ERSETZT(208,1300,-1,1,0,207)
C EINLESEN ZEULASTISCHE LINIE LORENTZKURVE FUER UNELSTISCHEN FIT
C EINGESETZT JAN 72 PITTAN
C UMGESCHRIFTEN FUER TR-440 IM FEBRUAR 1971
C DATA WIEDERHOLEN, ERHLD/4HERHL/
CALL SETIME
PAR(39)=0.0
READ(5,100) WORD(I),I=1,20)
1 DO 99 I=1,600
  DUM1(I)=0.0
  IF(I.LE.100) LPAR(I)=0.
  IF(I.LE.1300) PAR(I)=0.
  IF(I.LE.200) FFF(I)=0.
  IF(I.LE.50) PR(I)=0
  IF(I.GT.25) GO TO 99
  ACO(I)=0.
  PVAR(I)=0.
  BVAR(I)=0.
  BR(I)=0.
  COUNTINUE=10
  UPAR(I)=0.
99 READ(5,1001),PAR(I),I=1,5),(PAR(I),I=13,14),(PAR(I),I=62,63),(PAR(I),I=64,68),(PAR(I),I=6,12),
1 ,PAR(J),J=21,24),(PAR(I),I=15,20),(PAR(I),I=1,2),PAR(64)=1.
1 READ(5,1002),(LPAR(I),I=1,20),LPAR(40),LPAR(38)
1 IF(LLPAR(I),I=1,2)=EQ.3) PAR(64)=2.
1 IF(LLPAR(I),I=1,2)=GE.2) LPAR(I)=1
1 IF(LLPAR(I),I=1,2)=LT.2) LPAR(I)=0
1 IF(LLPAR(I),I=1,2)=EQ.0) LPAR(6)=1M
1 IF(I100=1M+100) (PAR(I),I=101,1M100)
5 READ(5,1005),(PAR(I),I=1,1M),(BVAR(I),I=1,1M)
5 READ(5,1005),(BVAR(I),I=1,1M)
1 IF(NWDH.EQ.1) GOTO 980
1 READ(5,1005),(PAR(I),I=51,58)
1 READ(5,1005),(PAR(59),PAR(61))
C EINLESEN DER KOEFFIZIENTEN FUER FORMFAKTOR(Q**N)

```



```

98 READ(5,1100)(ACO(I),I=1,8)
      READ(5,11002)(LPAR(I),I=1,50)
      IF(LPAR(16)*LT.0) READ(5,1007) (PAR(2*N+89),N=1,5),PAR(81)
      IF(LPAR(40)*GT.0) READ(5,1008) PAR(90),PAR(89),PAR(88),LPAR(39)
1000 FORMAT(20A4)      FORMAT(7F10.5/5F10.5/6F10.5/7F10.5/6F10.5)
1001 FORMAT(22I3)      FORMAT(7F10.5,110)
1002 FORMAT(7F10.5,110)
1003 FORMAT(7F10.5,110)
1004 FORMAT(8F10.5)    OCUBLE PRECISION ABCDE
1005 LPAR(21)=IM        LPAR(25)=0          WRITE(6,1006) (WORD(I),I=1,18)
1006 FORMAT(1H0,18A4)
1007 FORMAT(6F10.5)
1008 FORMAT(3F10.5,13)
1100 FORMAT(8F10.5)
C BERECHNUNG HILFSGRÖSSEN
ILA=0
ECO=PAR(6)*PAR(1)
THETA=PAR(7)*0.0174533
CU2=COS(THETA/2.)
SU2=SIN(THETA/2.)
DEFFF=SPAR(8)
DEFFF(LLPAR(7)*EQ.0) DEFFF=DEFFF/CU2
DEFFF(LLPAR(7)*GT.0) DEFFF=DEFFF/SU2
PAR(41)=DEFFF
PAR(46)=DEFFF*1.4
10 ECO=E00+PAR(46)/2.
PAR(47)=1.*+2.*E00*SU2**2/PAR(59)
ECO=E00*PAR(47)
PAR(47)=1.*EING1080
AUSGABE=DER(EING1110)
9001 FORMAT(3X,2016)
9002 FORMAT(3X,10F12.3)
C DATEIENGABE,AUFWERTUNG ELASTISCH
REWIND 1
REWIND 3
IF(LLPAR(20)*GT.0) CALL ZETK0
1 CALL EGB
IF(LLPAR(20)*GT.0) CALL ZETK0
105 REWIND L
IF(LLPAR(20)*GT.0) CALL ZETK0
1 CALL ELST
      EING0740
      EING0790
      EING0800
      EING0820
      EING0830
      EING0840
      EING0850
      EING0860
      EING0870
      EING0880
      EING0890
      EING0900
      EING0910
      EING0920
      EING0930
      EING0940
      EING0950
      EING0960
      EING0970
      EING0980
      EING0990
      EING1000
      EING1010
      EING1020
      EING1030
      EING1040
      EING1050
      EING1060
      EING1070
      EING1080
      EING1120
      EING1130
      EING1160
      EING1200
      EING1230
      EING1240
      EING1250
      EING1260
      EING1270
      EING1280

```



```

IF(LPAR(20).GT.0) CALL ZETKO
LKD=0
C 8ERECHNE EPS, BREITEN
110 EEO=EE0 PAR(31)*PAR(1)+PAR(46)/2.
PAR(47)=1.+2.*EE0*SU2**2/PAR(59)
EE0=EE0*PAR(47)
PAR(47)=1.+2.*EE0*SU2**2/PAR(59)
EE0=EE0*PAR(47)
PAR(36)=EE0
PAR=(2.^6*PAR(31) /(1000.*PAR(34)))*#2
112 DC120 I=1,IM
PAR(1+150)=PAR(1+100)/PAR(1)*((1.^0+PAR(I+100)/PAR(59))/PAR(47))
PAR(1+125)=SQRT(1.-XBR*PAR(1+150)/PAR(31)*(2.-PAR(I+150)/PAR(31)))
IF(PAR(64).GE.1.) BR(I)=BR(I)/PAR(1)
IF(BR(1).NE.0.) PAR(I+125)=BR(I)
120 CCASTINUE PLOTT WIEDERHOLUNG
C IF(LND.GT.0) REND
DC130 J=1,20
LPR(J)=0
130 PR((LPAR(20)=0.0
IF(LPAR(20).GT.0) CALL ZETKO
CALL LPAR(20).GT.0) CALL ZETKO
IWRITE(6,90000)(PAR(I),I=1,300)
IWRITE(6,90001)(LPAR(I),I=1,50)
IWRITE(6,90002)(BVAR(I),I=1,25)
IWRITE(6,90003)(PVAR(I),I=1,25)
CALL LPAR(20) AUSG
IF(LPAR(20).GT.0) CALL ZETKO
IF(LPAR(9).GT.0) CALL DRUCK
IF(LPAR(20).GT.0) CALL ZETKO
LKD=1
IF((LPAR(10).EQ.0) GO TO 1
C EINLESEN DER WIEDERHOLUNGSDATEN
READ(5,1002,END=1050) (LP(I),I=1,20)
IF(LLP(1).NE.LPAR(4)) LWD=0
READ(5,1001) PAR(13),PAR(14),PR64
IF(PR64.GT.0.) PAR(64)=PR64
NWDH=1
GOT05
980 DC150 I=1,25
IF(LLP(I).EQ.0.AND.I.GT.10) GO TO 140
LPAR(I)=LP(I)
IF(PR(I).NE.0.0) PAR(I+100)=PR(I)
140

```



```

150 IF(PR(1+25).NE..0) BR(1)=PR(1+25)
      COUNTABS(LPAR(3))+LPAR(4)
      LPAR(21)=IM
      IMP=100+IM
      IMB=125+IM
      IWORD(17)=WIED
      WORD(18)=ERHL
      WRITE(16,2070) (WORD(I),I=1,18)
      WRITE(16,1002) (LPAR(I),I=1,12)
      WRITE(16,2075) (PAR(I),I=14)
      WRITE(16,2080) (PAR(I),I=10,IM)
      WRITE(16,2085) (BR(I),I=1,IM)
      FORMAT(1H0,18A4/'10X,13H EINGABEDATEN /')
      FORMAT(1H0,13HNEUEREGUNGSENERGIEN 2F10.4)
      FORMAT(1H0,19HNEUREGUNGSENERGIEN /2(10F10.4/))
      FORMAT(1H0,19HNEUE BREITEN:, /2(10F10.4/))
      LPAR(31)=0
      REWIND 1
      IF(LLPAR(20).GT.0) GO TO 105
      STOP
      END

      IF(LLWD.EQ.0) GO TO 112
      STOP
      END

      1050
      GO TO 112
      STOP
      END

      1000
      FORMAT(6,1000) LZ2,Z3,LZ1,Z4
      F7.3,5H MIN, F7.3,12H SEC, DIFF.
      13,5H MIN
      RETURN
      END

      SUBROUTINE ZETKO
      DIMENSION PAR(300)
      CALL GETIME(IET)
      Z0=FLDAT(IET)*.0000026
      Z1=Z0-PAR(40)
      PAR(40)=Z0
      Z2=PAR(40)/60.0
      LZ2=INT(Z2)
      Z3=ANMOD(PAR(40),60.0)
      Z4=ANMOD(Z1,60.0)
      Z1=Z1/60.0
      LZ1=INT(Z1)
      WRITE(6,1000) LZ2,Z3,LZ1,Z4
      F7.3,5H SEC
      END

      SUBROUTINE INPUT(LB)
      DIMENSION CO(500),HZ(500),FEH(500),PAR(300)
      COMMON PAR
      END

```



```

COMMON/DATA1/HZ,CO,FEH
DO I=1,250
  I1=2*I-1
  I2=2*I
  READ(4,100) (HZ(J),CO(J),FEH(J),J=11,12)
  CO(I1)=CO(I1)-PAR(9)
  CO(I2)=CO(I2)-PAR(9)
  IF(HZ(I1).EQ.0.) GO TO 20
  CONTINUE
  IMAX=2*I
  IF(FEH(IMAX).GT.0.0) LPAR(LB+LB+26)=FEH(IMAX)
  CALL SORT(HZ,CO,FEH,IMAX)
  WRITE(3,1MAX,LB)
  DC 1=1,IMAX
  DC WRITE(3,1) HZ(1),CO(1),FEH(1)
  DC WRITE(3,1) HZ(0),0.0,0.0
  PAR(49)=FLOAT(IFIX(50.*HZ(1))/50.)
  PAR(50)=FLOAT(IFIX(50.*HZ(IMAX-1))/50.)
  RETURN
100  FFORMAT(2(9.4,1X,F15.7,F13.7,2X))
END

SUBROUTINE EGB
DIMENSION PAR(300),LPAR(100)
COMMON PAR,LPAR
PAR(26)=0.0
PAR(27)=0.0
LB=0
CALL INPUT(LB)
LB1=1
CALL INPUT(LB1)
REWIND 3
RETURN
END

SUBROUTINE SORT(HZ,CO,FEH,IMAX)
COMMON HZ(500),CO(500),FEH(500)
LA=1
1  K=IMAX-1
DC 10 L=LA,K
HERZ=HZ(L)
ZN=CO(L)
ZF=FEH(L)
N=L+1
DC 9 I=M,IMAX
IF(HZ(I).NE.0.) GO TO 4
IMAX=IMAX-1

```



```

      3 LL=I,IMAX
      DO 12=LL+1
      HZ(LL)=HZ(L2)
      CO(LL)=CO(L2)
      FEH(LL)=FEH(L2)
      3 LA=L
      GO TO 1
      4 IF(HZ(L)=HZ(I)) 5,9,9
      5 HZ(I)=HERZ
      CO(I)=ZN
      FEH(I)=ZF
      HERZ=CO(L)
      ZF=FEH(L)
      ZX=CONTINUE
      9 CONTINUE
      10 RETURN
      END

```

SUBROUTINE ELST

```

C ELASTISCHER PEAK UND STRAHLUNGSSCHWANZ
C DIMENSION PAR(300),LPAR(100),FREQ(200),ZAEH(200),FEH(200),FF(200),
C DIMMON PAR,LPAR,FREQ,ZAEH,FEH,
C IF(LPAK(20).GT.1) CALL ZETKO
C COMMON/DATA1/XX,YY,ERR
C ZMAX=0.
C LPAR(24)=0
C GAMMA=1000.
C READ(3) IEL,LB
C LPAR(32)=IEL
C DO 9 I=1,IEL
C   IEL=IEL-1+1
C   READ(3) HZ,CO,FEHEL
C   ZAEH(M)=CO
C   FREQ(M)=HZ
C   FEH(M)=FEHEL
C   ZMAX=AMAX1(ZMAX,CO)
C   IF(LPAR(1).EQ.0) GO TO 8
C   IF(HZ.GT.PAR(1).OR.HZ.LT.PAR(12)) GO TO 9
C   LEC=LEO+1
C   XX(LEO)=HZ
C   YY(LEO)=CO
C
      EING2840
      EING2850
      EING2860
      EING2870
      EING2880
      EING2890
      EING2900
      EING2910
      EING2920
      EING2930
      EING2940
      EING2950
      EING2960
      EING2970
      EING2980
      EING2990
      EING3000
      EING3010
      EING3020
      EING3030
      EING3040
      EING3050
      EING3060
      EING3070
      EING3080
      EING3090
      EELST0100
      EELST0110
      EELST0120
      EELST0130
      EELST0140
      EELST0150
      EELST0160
      EELST0170
      EELST0180
      EELST0190
      EELST0200
      EELST0210
      EELST0220
      EELST0230
      EELST0240

```



```

ERR(LEO)=FEHEL
9 CCNTINUE(20)*GT.2) CALL ZETKO
C IF(LPAR(1).GT.0) GO TO 91
C P(1)=ZMAX
P(2)=PAR(2)
P(3)=PAR(3)
P(4)=PAR(4)
P(5)=PAR(6)
P(6)=PAR(62)
P(7)=PAR(63)
NE=5
LPAR(28)=ME
NZEL=5
IF(PAR(62)*NE.0) CALL FIT(NZEL,P,LEO,XX,YY,ERR,O,GAMMA,1)
PAR(31)=PAR(79)

C HALBERTSBREITEN.FLAECHEN BEI ARC4
CALL HALBW(PLPAR(73),PAR(75),PAR(77),PAR(74),PAR(76),HW,DHW,FHW,WH)
PAR(34)=HW*PAR(71)
PAR(33)=PAR(71)
PAR(35)=PAR(71)
PAR(31)=PAR(79)-DHW
PAR(48)=DHW
DESCHW=2.0*PAR(34)*PAR(1)
97 CCNTINUE(20)*GT.1) CALL ZETKO
C AUSDRUCK HALBWERTS BREITEN
C STRAHLUNGS SCHWANZ
NAI=0
NSW=40
IF(LPAR(15)*LT.0) NAI=1
DCUBLE PRECISION U
U=PAR(7)*PAR(31)*PAR(1)
R=PAR(57)
T=PAR(58)
IF(LPAR(49)*EQ.3) R=PAR(55)
IF(LPAR(49)*EQ.3) T=PAR(56)
ATW=PAR(52)
XYZ=PAR(51)
FLAE=PAR(33)*PAR(1)
DES=PAR(34)*2.
XGO=PAR(49)+0.3

```



```

XGCB=(PAR(31)-DES)*50. XGO=FLOAT(IFIX(XGCB))/50.

IF(XGO.GT.0.3)
XGU=PAR(50)-0.3
DIFF=XGO-XGU
DES=PAR(34)*2.*PAR(1)
ABST=0.02 ABST=0.03
IF(DIFF.GT.1.2) ABST=0.04
IF(LPAR(20).GT.i) CALL ZETKO
IF(EIN(GABE-STUETZSTELLEN)
CALL RADTL(U,YY(I),EI,E,R,T,ATW,Z,XRAD,DESCHW,FLAE,PAR(41),NA1,
1 ADISP=E/EI
ADISP=64.EQ.0. YY(I)=YY(I)*ADISP
IF(LPAR(40).EQ.0.) PAR(90)=1.
YY(I)=YY(I)*PAR(90)
ERR(I)=0.01*ABS(YY(I))
NSW1=I-1
IF(LLPAR(39).NE.1) GO TO 31
XX(NSW1+1)=0.
YY(NSW1+1)=0.
ERR(NSW1+1)=0.
WRITE(17,501) (WORD(I),I=1,20)
501 FORMAT(1H1,20A4)
500 FORMAT(2(F9.4,2XX,I,F13.7,2XX),
CONTINUE
C 31 IF(LLPAR(20).GT.1) CALL ZETKO
DO 26 J=91,100
26 PAR(J)=0.0
28 LPAR(24)=1
NPSW=LPAR(17)*EQ.0) NPSW=4
IF(LLPAR(16).EQ.0) LPAR(16)=1
IF(LLPAR(16).EQ.0) LPAR(16)=1
J=J+1
P(4)=0.
P(4)=0.

```



```

P(5)=0. PAR(31)-XX(1)
X1=1./{PAR(31)-XX(NSW1)}
X2=1./{NSW1}
GC TO (50,50,53,53,55) ,J1
C 50 P(3)=(YY(1)/X1-Y2/X2)/ (X1-X2)
P(2)=Y2/X2-P(3)*X2
GO TO 32
P(2)=(YY(1)*XX(NSW1)-Y2*XX(1))/ {XX(NSW1)*X1-XX(1)*X2}
P(3)=YY(1)/XX(1)-(X1/XX(1))*P(2)
IF(J1.EQ.4) GO TO 54
GO TO 32
P(1)=P(2)
P(2)=P(3)
P(3)=0
GO TO 32
IF(LPAR(18).EQ.0) LPAR(18)=2
PAR(L81)=(XG0-XGU)/FLOAT(LPAR(18))+XGU
XK1=XX(1)-PAR(81)
XK2=XX(NSW1)-PAR(81)
P(3)=(YY(1)/XK1-Y2/XK2)/(XK1-XK2)
P(2)=YY(1)/XK1-P(3)*XK1
C 32 CALL FIT(NPSW,P(NSW1),YYERR,O,GAMMA,J)
IF(LPAR(20).GT.1) CALL ZETKO
40 RETURN
END

C SSSWF STRAHALENSCHWANZFIT
SUBROUTINE SSSWF(Y,X)
DIMENSION PAR(300),LPAR(100)
COMMON PAR1,PAR2
J=1ABS(LPAR(16))
IF(J.EQ.5) GO TO 50
A=1/(PAR(31)-X)
Y=PAR(91)+PAR(31)-X
GO TO (10,20,30,40),J
10 Y=Y+PAR(95)*A**2+PAR(97)*A**3+PAR(99)*A**4
RETURN
20 Y=Y+PAR(95)*A**2+PAR(97)*X+PAR(99)*X**2
30 Y=Y+PAR(95)*X+PAR(97)*X**2+PAR(99)*X**3
40 Y=PAR(91)*A+PAR(93)*X+PAR(95)*X**2+PAR(97)*A**2+PAR(99)*X**3
50 A=X-PAR(81)
Y=PAR(91)+PAR(93)*A+PAR(95)*A**2+PAR(97)*A**3+PAR(99)*A**4

```


RETURN
END

C ANPASSUNG NACH DER METHODE DER KLEINSTEN QUADRATEN
C SUBROUTINE FIT(MZ,P,N,X,Y,DY,NR,DELTA,NUM)
C NRW = 0 FALLS DIE MESSFEHLER ABSOLUT SIND
C DIMENSION PAR(300),LPAR(100),DUM(600),WORD(20)
C X(500),DY(500),V1(25),V2(25),U(50,50),
C DP(25),DF(25),DZ(25),DTA(10)
C DIMENSION ZWP(25),PNB(25)
C COMMON PAR,DUM,WORD,
C REAL**8 TEXT,NAME1,NAME2,NAME3
C COMMON/SSWD/ACO(25)
C COMMON/LLING1/DZZ,U
C DATA V1,V2,DP,DF,DZ,ZWP,PNB /175*.0/
C DATA NAME3/.GRD/

MY=5
NRM=0
NORMA=DELT A
M=MZ
JCO6=6
MCO1=5
DC 11 K=1,50
DO 11 L=1,50
DZZ(K,L)=0
DU(K,L)=0
11 DIAGNOSTIK
I1=1
11 IF(M=2)16,17,15
15 WRITE(6,997)
16 FORMAT(40H1 NUR 1 BIS 25 PARAMETER ERLAUBT STATT ,17)
997 RETURN
17 IF(N=500)20,20,18
18 WRITMAT(6,998)N,20,18
998 WRITMAT(42H1 NUR 1 BIS 500 MESSPUNKTE ERLAUBT STATT ,17)
20 RETURN
20 ZSCLL=N - M
24 WRITE(6,999)
999 FCRMAT(19H1 MEHR PARAMETER , 12, 20H) ALS MESSPUNKTE (, 12,
1 RETURN
25 NRM=0

ELST2350
ELST2360
ELST5430
ELST5460
ELST5480
ELST5520
ELST5540
ELST5550
ELST5580
ELST5600
ELST5610
ELST5620
ELST5630
ELST5640
ELST5650
ELST5660
ELST5670
ELST5680
ELST5750
ELST5770
ELST5780
ELST5790
ELST5800
ELST5810
ELST5820
ELST5830
ELST5840
ELST5850
ELST5860
ELST5870
ELST5880
ELST5890
ELST5910
ELST5920
ELST5930


```

26 DO 27 I = 1,N
27 IF(DY(I)) = 28,28,27
28 WRITE(6,1000)1 MESSFEHLER DY(I) IST NULL ODER NEGATIV FUER I = , 14)
1000 FORMAT(49H1
30 RETURN
14 FEH=1.0
15 IF(NORM) = 29,30,30
29 FEH=DY(I)*#2
30 J=0
C BEGINN DER ITERATION ZUR LOESUNG DER NORMAL - GLEICHUNGEN
31 IF(LPAR(8)) = 31,31,32
31 WRITET(6,1002)
1002 FORMAT(1H1,17X,18HZWISCHENERGEBNISSE,ZWANG,1. PARAMETER
1/85HNAEHERUNG USW..... //)
32 3. PARAMETER
32 G=1.0
DATA NAME1/' '.
TEXT=NAME1
32 G=1.0
DATA NAME1/' '.
TEXT=NAME1
C
50 Z = 0.0
DQ 60 K = 1,M
D2(K) = 0.0
DC 60 L = 1,M
60 D2Z(K,L) = 0.0
DQ 70 I = 1,N
CALL THEORY( NUM, X(I), P, F, DF )
H1 = DY(I)**(-2)*FEH
H2 = Y(I)-F
Z = Z + H1*H2*H2
DC 70 K = 1,N
D2(K) = DZ(K) - H1*H2*DF(K)
DC 70 L = 1,N
D2Z(K,L) = D2Z(K,L) + H1*DF(K)*DF(L)
70 Z=Y/FEH
71 IF(NORM) = 72,73,72
72 G=Z/ZSOLL
73 IF(LPAR(8)) = 74,74,78
74 IF(NORM) = 77,77,75
75 WRITET(6,1003)J,TEXT,Z,(P(K),K=1,15)
1003 FORMAT(1X,I3,A6,1PE14.6,3X,7E15.6)
78 GOTO 78
79 WRITE(6,1004)J,TEXT,Z,(P(K),K=1,15)
1004 FORMAT(1X,I3,A6,F14.4,3X,1P7E15.6)
C PRUEFUNG AUF ITERATIONSSTOP
78 IF(J-MY) = 100,80
80 IF(ABS(Z-ZALT)-1.0E-02) 140,140,79

```



```

79 IF (Z-ZALT) 90,102,102
102 DO 103 K=1,M
103 P(K)=ZWP(K)
      GAMMA=0.8*GAMMA
      WRITE(6,104) GAMMA
1040 FORMAT(6,104) GAMMA
      IF(J-M002) 100,130,130
      IF(J-M002) 100,130,130
      100 104  K=1,M
      DO 104 K=1,M
      DP(K)=-DZ(K)
      DC 104  L=1,N
      U(K,L)=D2Z(K,L)
104  CALL LINGL(U,DP,M,1)
105  H1=0.0  K=1,M
106  DC 106  K=1,M
      H1=H1+DP(K)*DP(K)*D2Z(K,K)
      DATA NAME2//".NWT"
      TEXT=NAME2
      GAM1=SQRT(H1)
      IF(GAM1-GAMMA) 113,113,107
      GRADIENTENMETHODE STATT NEWTON
      TEXT=NAME3
107  H1=0.0
      H2=0.0  K=1,M
      DC 109 K=1,M
      H3=DZ(K)
      DZ(K)=H3*D2Z(K,K)
109  H1=H1+H3*DZ(K)
      DO 110 K=1,M
      DC 110 L=1,M
      H2=H2+DZ(K)*D2Z(K,L)
      H3=AM1*N1(H1/H2,GAMMA/SQRT(H1))
      DO 112 K=1,M
      DP(K)=-H3*DZ(K)
112  ZALT=Z
      IF(J.LE.M001) GO TO 114
114  DO 115 K=1,M
      ZWP(K)=P(K)
      P(K)=P(K)+DP(K)
115  J=J+1
      GC 70 50
116  C ALSDRUCK FALLS NOCH KEINE KONVERGENZ NACH 20 ITERATIONEN
      120 ARITMET(6,1005) M002
      1005 FORMAT(6,124H (KEINE KONVERGENZ NACH 13,15H ITERATIONEN)
      140 WRITE(6,1030)(WORD(I),I=1,20)
      1020 FORMAT(1HO,20A4/)

```



```

IF(LPAR(24)) 131,131,132
WRITE(6,1031)
1031 FORMAT(27H FITERGEBNISSE ELAST. PEAK )
1032 WRITE(6,1032)
1032 FCNAT(20H FITERGEBNISSE SSW
1032 IF(ACOT(1)*NE*0.0) WRITE(6,502)
502 FORMAT(1X,SSW MIT PHASEANALYSE WQ BERECHNET. )
1033 IF(NORM) 35,35,40
C
C ERWARTUNGSWERT VON Z IST ZSOLL IST SQRT(N-ZSOLL) FALLS DIE MESSFEHLER DY(I)
C ABSOLUT SIND. STREUUNG (2.0*ZSOLL)
C
35 H1 = SQRT(2.0*ZSOLL)
A012=H1
B012=ZY
WRITE(6,1007) ZSOLL, H1, ZY
1007 FORMAT(9H ZWANG, 9X, 8HSOLLWERT, F8.1, 3H +-, F5.1
1/18X,7HISTWERT,F9.1)
40 WRITE(6,1008)
1008 FORMAT(1H,32X,7HOPTIMAL,13XX,6HFEHLER, '1')
DC 160 K=1,M
DO 150 L=1,M
150 U(K,L)=Q,O
160 CALL LINGL(D2Z, U, M, M)
170 DO 180 K=1,N
180 DP(K) = SQRT(ABS(U(K,K)))
C
KCNTROLLE DURCH BERECHNUNG DES ZWANGES AN DEN EXTREMPUNKTEN
DES FEHLERELLIPOIDS
DO 205 K=1,M
DO 190 L=1,M
U(K,L) = U(K,L)/DP(K)
V1(L) = P(L)-U(K,L)
V2(L) = P(L)+U(K,L)
U(K,L) = U(K,L)/QP(L)
190 J = J+1
H1 = 0.0
DC 195 I = 1,N
CALL THEORY( NUM,X(I),V1(F),DF)
195 H1 = H1+(Y(I)-F)/G
H1 = H1-Z/G
J = J+1
H2 = 0.0
DC 200 I = 1,N
CALL THEORY( NUM,X(I),V2,F,DF)

```



```

200 H2 = H2 + ((Y(I) - F)/DY(I))*2*FEH
205 H2 = (H2 - Z)/G
209 WRITE(6,109)K,P(K),DP(K),H1,H2
1009 FORMAT(1X,I2,10H.KORRELATIONEN ZWISCHEN DEN PARAMETERN
1010 1,FORMAT(6,1010)
1011 1,DC,185,K=1,M
1012 1,WRITE(6,1011)K,(U(K,L),15F8.3,19X,10F8.3)
1013 FORMAT(1X,I2,6H.PA,15F8.3,19X,10F8.3)
C TABELLIERUNG DER ANGEPASSTEN FUNKTION
1014 1,IF(LPAR(8),181,186,181
1015 1,IF(LPAR(9),216,216,182
1016 1,WRITET(6,1015)
1017 1,FORMAT(1H0,154X,13HT A B E L L E // / / 56X,8HORDINATE/
1018 1,114H,NR.
1019 1,BERECHNET DIFFERENZ MESSFEHLER //,
1020 1,IF(LPAR(9).LE.0.OR.LPAR(24).GT.0) GO TO 188
1021 1,WRITE(11)LPAR(24),LPAR(24),
1022 1,LPAR(25)=LPAR(25)+1
1023 1,DC,213,I=1,N
1024 1,CALL THEORY(NUML,X(I),P,F,DF)
1025 1,H1=Y(I)-F
1026 1,H14=H1/DY(I)
1027 1,IF(LPAR(9).EQ.0.OR.LPAR(24).GT.0) GO TO 215
1028 1,UNT=0.0
1029 1,WRITE(1)X(I),Y(I),F,H14,UNT,UNT
1030 1,IF(LPAR(8).NE.0) GO TO 213
1031 1,WRITE(6,1016)I,X(I),Y(I),F,H1,DY(I)
1032 1,FORMAT(15,F19.4,3X,1P2(E27.6,E17.6))
1033 1,CONTINUE
C 216 NO=70
1021 1,IF(LPAR(24).GT.0) NO=90
1022 1,DC,1022,I=1,M
1023 1,NCN=NO+2*I
1024 1,PAR(NON-1)=P(I)
1025 1,PAR(NON)=DP(I)
1026 1,RETURN
1027 1,END
C 216 NO=70
1028 1,IF(LPAR(24).GT.0) NO=90
1029 1,DC,1022,I=1,M
1030 1,NCN=NO+2*I
1031 1,PAR(NON-1)=P(I)
1032 1,PAR(NON)=DP(I)
1033 1,RETURN
C SUBROUTINE THEORY(J,X,P,Y,DA)
C THEORY ELAST DIMENSION P(25),DA(25),PAR(300),LPAR(100)
C COMMON PAR,LPAR
C GO TO (10,20,30,40,50,60) ,J

```



```

10 CALL ARC4( X,P,Y,DA )
RETURN
20 A=1./ (PAR(31)-X)
Y=P(1)+P(2)*A+P(3)*A**2+P(4)*A**3
IF(LLPAR(33).EQ.5) Y=Y+P(5)*A**4
DA(1)=1
DA(2)=A
DA(3)=A**2
DA(4)=A**3
DA(5)=A**4
RETURN
30 A=1./ (PAR(31)-X)
Y=P(1)+P(2)*A+P(3)*A**2+P(4)*X+P(5)*X**2
DA(1)=1.
DA(2)=A
DA(3)=A**2
DA(4)=X
DA(5)=X**2
RETURN
40 A=1./ (PAR(31)-X)
Y=P(1)+P(2)*A+P(3)*X+P(4)*X**2+P(5)*X**3
DA(1)=1.
DA(2)=A
DA(3)=X**2
DA(4)=X**3
DA(5)=X**4
RETURN
50 A=1./ (PAR(31)-X)
Y=P(1)*A+P(2)*X+P(3)*X**2+P(4)*A**2+P(5)*X**3
DA(1)=A
DA(2)=X
DA(3)=X**2
DA(4)=A**2
DA(5)=X**3
RETURN
60 A=X-PAR(81)
Y=P(1)+P(2)*A+P(3)*A**2+P(4)*A**3+P(5)*A**4
DA(1)=1.
DA(2)=A
DA(3)=A**2
DA(4)=A**3
DA(5)=A**4
RETURN
END

```

SUBROUTINE ARC4(X,P,Y,DX)

ELST 9400


```

C      DIMENSION P(25),DY(25)
BT=1.44269505
DEZ=71: ZWEITE EL LINIE MIT HOEHE=P(6), LAGE=P(7)
6      U=(X-P(5))
      V=(X-P(7))
      T=20,10,10
      CONTINUE
      ALPHAI=(U/P(2))**2/BT
      FORMAT(5E15.4)
      Y=P(1)*EXP(-ALPHA)
      DY(1)=Y/P(1)
      DY(2)=2.0*Y*U**2/(BT*P(2)**3)
      DY(3)=0.0
      DY(4)=0.0*U*Y/(BT*P(2)**2)
      DY(5)=2.0*EQ.0) RETURN
      IF(P(6)=P(6))**EXP(-(V/P(2))**2/BT)
      Y6=P(6)/P(6)
      DY(6)=Y6/P(6)
      DY(7)=2.0*V*Y6/(BT*P(2)**2)
      Y=Y+Y6
      DY(2)=DY(2)+2.*V*Y6*(V**2/(BT*P(2)**3))
      RETURN
      10     IF(P(1)*EXP(-P(4)/P(3))**2/BT)
      100    Y=P(1)*EXP(-(U/P(3))**2/BT)
      111    DY(1)=Y/P(1)
      111    DY(2)=0.0
      111    DY(3)=0.0*Y*U/(BT*P(3)**2)
      111    DY(4)=0.0
      111    DY(5)=2.0*Y*U/(BT*P(3)**2)
      111    DY(6)=P(6).EQ.0) RETURN
      111    IF(X*GE.P(7)) GOT 60
      111    Y6=P(6)/P(6)
      111    DY(7)=2.0*V*Y6/(BT*P(3)**2)
      111    DY(3)=DY(3)+2.*V*Y6*(V**2/(BT*P(3)**3))
      111    RETURN
      111    PP=2.0*(P(4)/P(3))**2/BT
      111    K6=0
      112    IF(K6.EQ.1) YP6
      112    C=YP*P(4)**(2.0-PP)
      112    D=YP*P(4)**2*(PP-1.0)
      112    PP=YP*PP
      112    CP3=PPP*PP*(4)*(4.0-PP)/P(3)
      112    DP3=PPP*(P(4)**2/P(3)-3.0*BT*P(3)/2.0)
      112    CP4=PPP*(2.0/PP-5.0+PP)
      112    DF4=PPP*P(4)*(5.0-PP-2.0/PP)

```



```

IF (K6.EQ.1) GOTO 63
Y=C/U+D/U**2
DY(1)=Y/P(1)
DY(2)=0.0
DY(3)=CP3/U+DP3/U**2
DY(4)=CP4/U+DP4/U**2
DY(5)=C/U**2+2.0*D/U**3
IF(P(6).EQ.0)RETURN
IF(X.GE.P(7)) GOTO 60
IF(X.LT.P(7) .AND. X.GE.P(4)) GOTO 61
K6=1
YP6=P(6)*EXP(-P(4)/P(3))*2/BT
GOTO 62
Y6=C/V+D/V**2
DY(6)=Y6/P(6)
Y=Y+Y6
DY(7)=C/V**2+2.0*D/V**3
DY(4)=DY(4)+CP4/V + DP4/V**2
DY(3)=DY(3)+CP3/V + DP3/V**2
RETURN
END

SUBROUTINE HALBW(P2,P3,P4,DP2,DP3,HWB,DHWB,FHW,W)
1
  IF(P2)1,1,2
  HB=0.0
  HWB=0.0
  FHW=0.0
  W=0.0
  RETURN
  PVP=P4/P3
  BT=1.44269505
  YP=EXP(-PVP*2/BT)
  HB=P2+P3
  HWB=(P3-P2)/2.0
  PP=2.0*PVP*2/BT
  C=YP*P4*(2.0-PP)
  D=YP*P4**2*(PP-1.0)
  X=-PVP/SQRT(BT)
  W=ERF(X)
  WO=P2*SQRT(BT*3.14159265)*.5*(1.0+W*P3/P2)
  ZA=2.0
  GRENZ=ZA*HWB+5*DHWB
  W2=C*ALOG(-P4/GRENZ)-D/P4-D/GRENZ
  W=W+W2
  RETURN
END

```



```

SUBROUTINE RADTL(U1,SW,EIMEV,EMMV,R,T,ATW,Z,XRAD,DES,DS,D,NA1,ERR)ELST0410
DIMENSION PAR(300),LPAR(100)ELST0420
DCUBLE PRECISION U1      , DCOS      , WF      , EI      , EF
DCUBLE PRECISION PI      , DSQRT    , XMIN   ; A      ;
DCUBLE PRECISION XA      , XB      , XMAX   ; XMAX;
DCUBLE PRECISION X3      , X1      , X4     , UI      , X2      ;
D=U1=1.0E-10ELST0430
U=U1=1.0E-10ELST0440
X=U1=1.0E-10ELST0450
Y=U1=1.0E-10ELST0460
Z=U1=1.0E-10ELST0470
W=U1=1.0E-10ELST0480
S=U1=1.0E-10ELST0490
T=U1=1.0E-10ELST0500
C=U1=1.0E-10ELST0510
DESMOT=DS=1.0E-10ELST0520
DESMOT=DS=MV/5109ELST0530
CU2=COS(.0174533*SNGL(U)/2.0)
SU2=SIN(.0174533*SNGL(U)/2.0)
U=DCOS(.017453D0*U)
DEF=D/(2.0*XRAD)
REF=(D*Z1)/(ATW)*047829*.5
302 GZ13=ANALOG(.183*0*Z13)
GC=2.0*(SNGL(EI)*SU2)**2
282 CALL FORM(FD,XO,R,T)
CALL DNCTT(DN,CSU2,SU2,Z,EI)
312 CALL DELTAC(DELTA,SDSCHW,EI)
322 SIGMA=DN**2
SES=EMIN
EF=EF-ES
W=EF-DSQRT(EI**2-1.0D0)
PI=DSQRT(EI**2-1.0D0)
PF=DSQRT(PI**2-2.0D0*PI*PF*U+PF**2)
A=DSQRT(PI*PF*U-1.0D0
B=EI*EF-PI*PF*U-1.0D0
DSIGMA=0.0
DF(NA1)=3.03*3.03*3.04
XA=B+W*(W+PF-PI*U)
XB=W*(W-PI+PF*U)+B
XMIN=.5D0*(A-W)**2
XMAX=.5D0*(A+W)**2
IF(SNGL(XA)-SNGL(XB)-15.0*SNGL(W)*(SNGL(EI)+SNGL(EI))/SNGL(EI))>0
303 1(EF)) 5,6,6
5 X2=XB
X3=XA
GC TO 7
6 X2=XB+.10*D0*W*EF/EI
X3=XA-.10*D0*W*EI/EF
7 IF(SNGL(XB)-15.0*SNGL(W)*(SNGL(EI)+SNGL(EI))/SNGL(EI))>0
8 X1=X3
GC TO 10

```



```

9
10 IF(XB-10.*DO*W*EF/EI-SNGL(XA)-15.*0*SNGL(W)*SNGL(EI)) 11,12,12
11 X4=XA TO 2
12 X4=XA+10.*DO*W*EI/EF
13 CCONTINUE
14 CALL WEDDLE(H1,XMIN,X1,ERROR,EI,EF,PI,PF,U,A,B,W,R,T)
15 CALL WEDDLE(H2,X1,X2,ERROR,EI,EF,PI,PF,U,A,B,W,R,T)
16 CALL WEDDLE(H3,X2,X3,ERROR,EI,EF,PI,PF,U,A,B,W,R,T)
17 CALL WEDDLE(H4,X3,X4,ERROR,EI,EF,PI,PF,U,A,B,W,R,T)
18 CALL WEDDLE(H5,X4,XMAX,ERROR,EI,EF,PI,PF,U,A,B,W,R,T)
19 DSIGMA = H1+H2+H3+H4+H5
20 =DSIGMA *#90.2376*(SNGL(FF)/SNGL(P1))*Z**2
21 DSIGMAEV = 5109*ES
22 DSIGMAEV = 2.0*(SNGL(EF)*SU2)**2
23 CALL FORM((FE*XE*RT)/(SNGL(EI)*FE)/(SNGL(EF)*FO))**2 )
24 SCHIFR = (1.0+((SNGL(EI)*FE)/(SNGL(EF)*FO))**2 )
25 SCH=0
26 SCH(NAI.GT.0) CALL SCHIFC(SCH,SU2,EI,EF,W)
27 SCHIFR = BRA
28 DSIGMA=DSIGMA*DSMOT/SIGMA
29 CALL HEINQ(H,REFF,DEF,GG13,EI,EF)
30 HENO = BRA *HEMO
31 SSW=DSIGMA+HEMO
32 SF(NAI.GT.0) SSW=SCHIFR+HEMO
33 SW=SSW*(1.+DEL)
34 FORMAT(5E15.6)
35 RETURN
36 END
37
38 SUBROUTINE CAPR(Z,Y,EI,EF,PI,PF,U,A,B,W,R,T)
39 SUBROUTINE CALCULATION_OF_R(X) FOR ELECTRON SPECTRUM
40 DOUBLE PRECISION A , D , DSQRT , X , EI , EF
41 DOUBLE PRECISION D1 , G1 , D2 , G2 , PI , PF , F .
42 DOUBLE PRECISION Y
43 X = PI**2-PI*PF*U
44 B1=PI**2-PI*PF*U
45 B2=PI**2-PI*PF*U
46 D=2.*D0*X*((EI*EF-1.*DO)*U-PI*PF)*PI*PF
47 D1=DSQRT((PI*X)**2+D+(PF*B)**2)
48 D2=DSQRT((PF*X)**2+D+(PI*B)**2)
49 G1=(2.*D0*EI**2-X)*(B*B1+X*B2)/D2**3
50 G2=(2.*D0*EF**2-X)*(B*B2+X*B1)/D1**3
51 G3=(2.*D0*(EI**2+EF**2)+B-X-2.*DO*(1.*DO+B)*(2.*DO*EI*EF-X)+B*W**2)/(B
52 -X)
53 F=((1.*DO/D2)-(1.*DO/D1))*G3-G2-61-(2.*DO/A)
54 Z=SNGL(F)/SNGL(X)**2

```



```

XX=SNGL(X)
CALL FORM(FOR,XX,R,T)
Z=Z*FOR**2
RETURN
END

```

```

C      SUBROUTINE FORM(F,X,R,T)
C      WAHLWEISE TRAPEZ-ODER EXAKTER FCRMFAKTOR IN POTENZEN VON Q**2
C      EINIGE FUEGT AUGUST 72 PITTHAN, WALCHER
C      EICMMON/SSWD/ACO(25)
C      IF(ACO(1).EQ.0.) GOTO 5
C      QC=X**2./386.1**2
C      F=0.
C      DC 4 I=1 12
C      F=F+ACO(I)*QQ**((I-1))
C      RETURN
C      TRAPEZFORMFAKTOR:
C      5   Q=(R+5.0*T/8.0)**SQRT((2.0*X)/(R+5.0*T/8.0))
C      ETA=(R-5.0*T/8.0)/(R+5.0*T/8.0)
C      QN=ETA*Q
C      F=12.0*(QN*SIN(QN)-Q*SIN(Q))+2.0*COS(QN)-2.0*COS(Q))/((Q**4-QN**4))
C      WRITE(6,10)
C      10  FORMAT(2F20.10)
C      RETURN
C      END

SUBROUTINE DMOTT(X,CU2,SU2,Z,EI)
DCUBLE PRECISION PI,W,PF,A,EI,B
DCUBLE PRECISION U,U,U,U
ANGL=CU2**2/(SU2**4)
X=ANGL*(Z/(2.0*EI))**2*79411.0
RETURN
END

SUBROUTINE SCHIFF(X,SU2,EI,EF,W)
DCUBLE PRECISION PI,W,PF,A,EI,B
DCUBLE PRECISION U,U,U,U
X1=(1.0+(EF/EI)**2)*(DLOG((2.0*EI*SU2)-0.5)/
X=0.2323*X1/(W*.5109)
RETURN
END

CSCHIFF SUBROUTINE SCHIFF(X,EI,EF,W)
DCUBLE PRECISION PI,W,PF,A,EI,B
DCUBLE PRECISION U,U,U,U
X1=DLOG((2.0*EI*SU2)-0.5)
RETURN
END

CSUBD SUBROUTINE SCHWINGER CORRECTION
SUBROUTINE DELTA(X,SU2,DESCHN,EI)
DCUBLE PRECISION PI,W,PF,A,EI,B
DCUBLE PRECISION U,U,U,U
RI=DLOG((2.0*EI*SU2)-0.5)

```



```

A1= DESCHW/.5109
R2=DLOG(EI/A1)-1.0833
X=.009236*(R1*R2+.2361)
RETURN
END

```

```

SUBROUTINE WEDDLE(V,A,B,ERRCOR,EIN,EF,PI,PF,UCL,A01,B01,W01,R01,T01) ELST2110
C WEDDLE EVALUATION OF QUADRATURES USING WEDDLE-S RULE
C DIMENSION C(7),F(200)
C DOUBLE PRECISION U01 , W01 , EI PF , EI A01 , EF B01 , A , B
100 FORMAT(29H**INTEGRAL NOT CONVERGENT**, //)
101 FORMAT(8E14.6)
102 FORMAT(//17H INTEGRAL FROM,E14.6,4H TO,E14.6,10H GIVES W=,E14.6,1H),//)
103 FORMAT(21H E14.6,24H {PREVIOUS VALUE - _W=,E14.6,1H},//)
1 IF(B-A)2,3,2
2 WRITE(6,103)
3 V=0
GO TO 1
4 DC 10 I=1,7,2
5 DC(1)=1.0
6 DC(2)=5.0
7 DC(4)=6.0
8 DC(6)=5.0
9 DY=(B-A)/192.0
10 SUN=0.0
L=0
DC 20 I=1,193,32
L=L+1
Y=A+DY*FLOAT(I-1)
CALL CAPR(Z01,Y,EI,EF,PI,PF,U01,A01,B01,W01,R01,T01)
11 F(I)=Z01
12 SUM=SUM+F(I)*C(L)
13 V=.3*SUM*DY*32.0
DC 50 N=1,5
V=Y
14 K=2**((6-N)
15 M=K/2
16 K1=M+1
17 K2=193-M
18 DC 30 J=K1,K2,
19 Y=A+DY*FLOAT(J-1)
CALL CAPR(Z01,Y,EI,EF,PI,PF,U01,A01,B01,W01,R01,T01)
20 F(J)=Z01
K3=3*K
J1=193-K3
30

```



```

SUM=0.0
DC 40 J=J+K3
L=0
DC 40 I=J, J2, M
L=L+1
L=SUM+F(I)*C(L)
40 V=Y*SUM*DY*FLDAT(M)
IF(ABS((V-W)/V)-ERROR) 1,1,50
50 CONTINUE (6,100)
1 RETURN
1 END

SUBROUTINE HEIMOL(X,REFF,DEFF,GZ13,EI,EF)
CHEMO
DIMENSION HEITLER-MOELLER
PAR(LPAR(300),LPAR(100))
CCMMON PAR(LPAR
DCDOUBLE PRECISION U , W , PF , EI , A , EF , B
DCDOUBLE PRECISION PI
B=EI-EF
B=EOE=EF
19.0*GZ13)
1X1=BEOE*DEFF/W
1F(LPAR(40).EQ.0) PAR(88)=1.
1X1=X1*PAR(88)
X21=6*2.8319*REFF
X22=1.0/EF
1W**2-(2.0*EI**+1.0)/(EF *W * (EI **2+1.0)**2
1X2=X21*X22
1F(LPAR(40).EQ.0) PAR(89)=1.
X2=X2*PAR(89)
X=X1+X2/.5109
RETURN
END

SUBROUTINE UNST
UNELASTISCH
DIMENSION PAR(300),LPAR(100),FREQ(200),ZAEH(200),FEH(200),
WORD(20),XX(500),ERR(500),P(50)
IHO(25)
DIMENSION DUMMY(50)
DIMENSION PVAR(25),BVAR(25)
CCMMON PAR(LPAR
CCMMON/BVAR1/BVAR
CCMMON/BVAR2/PVAR
CCMMON/DATA1/XX,YY*ERR
CCMMON/USTART/UPAR(10)


```



```

IF(LPAR(20).GT.1) CALL ZETKO
IM=LPAR(21)
IAN=15
ISS=0
LFE=IABS(LPAR(3))
LVE=LPAR(4)
LBV=LPAR(5)
GAMMA=1000.
UNAH=0.
FNAH=0.
DO 2 I=1,25
  IF(I.LE.LFE) PVAR(I)=BVAR(LVE+I)
  IF(I.GT.LFE .AND. I.LE.IM) PVAR(I)=BVAR(I-LFE)
2  IHQ(I)=0

C EINLESEN UND HOEHEN-NAEHERUNGSWERTE
LEO=0
5  READ(3,IUN,LB
  IF(LB.GT.0) GO TO 20
  DCAD(10,I=1,IUN
10  READ(3,DMY1,DMY2,DMY3
  GC TO 5
20  DO 30 I=1,IUN
    READ(3,HZ,CO,FEHEL
    IF(PAR(IAN).EQ.0.OR.IAN.GT.20) GO TO 15
    IF(HZ-PAR(IAN)) 12,12,15
    IF(HZ-PAR(IAN+1)) 14,13,13
    CALL SSWF(FSSW,HZ)
    FNAH=FNAH+CO/FSSW
    IF(LPAR(2).GT.20) UNAH=UNAH+CO-FSSW
    ISS=ISS+1
    GO TO 15
14  IAN=IAN+2
15  CONTINUE
    IF(HZ.GT.PAR(13).OR.HZ.LT.PAR(14)) GO TO 30
    LEO=LEO+1
    XXX(LEO)=HZ
    DISP=1
    DISP=PAR(64)*GE*1.0  DISP=PAR(31)/XX(LEO)
    IF(YY(LEO)=CO*DISP
    ERR(LEO)=FEHEL*DISP
    DO 29 J=1,IM
    IF(HZ.LE.(PAR(31)-PAR(J+150)).AND.IHO(J).LE.0) IHO(J)=LEO
29  CONTINUE
30

```



```

C NAEHERUNGSSUNTERGRUND, HOEHENVERHAELTNISSE
DO 40 I=1,IM
  IZ = IH(1)
  CALL SSKF(FSSW,XX(IZ))
  PAR(I+175) = (YY(IZ)-FNAH*FSSW)/FLOAT(ISS)/PAR(35)
  IF(PAR(1+175).GT.20) PAR(I+175) = (YY(IZ)-UNAH/FLOAT(ISS)-FSSW)/PAR(35)
  IF(PAR(1+175).LE.0.0) PAR(I+175) = 0.01*PAR(176)
  IF(PAR(1+175).GT.1) PAR(I+175) = (YY(IZ)-FSSW)/PAR(35)
40 CCNTINUE
  NAEHERUNGSPARAMETER FUER FIT
  NPJ=INT(FLOAT(LPAR(2))/10.)
  NPA=LPAR(2)-10*Npj
  LPAR2=LPAR(2)*GT.50) LPAR2=LPAR2-50
  NST=NPA+1
  IF(LPAR2.GT.10) NST=NPA+2
  IF(LPAR2.GT.30) NST=NPA+1
  DC(4)=I,NST
  P(I)=UPAR(I)
  LBEZ=5.*(PAR(13)+PAR(14))
  PAR(45)=0.1*FLOAT(LBEZ)
  IF(LPAR2.GT.30 .AND. LPAR2.LT.20) GO TO 45
  IF(LPAR2.GT.30 .AND. LPAR2.LT.40) GO TO 45
  IF(UPAR(NPA+1).EQ.0.) P(NPA+1)=FNAH/FLOAT(ISS)
  GO TO 46
45 CCNTINUE
  P(I)=UNAH/FLOAT(ISS)
46 LPAR(22)=NST
  IF(CUPAR(I).EQ.0.) GOTO 44
  DO 43 I=1,IM
    IZ = IH(1)
    CALL UNTF(XX(IZ),P,DUMMY,UNT,FSSW)
    PAR(I+175) = (YY(IZ)-UNT)/PAR(35)
43 CCNTINUE
44 ENERGIEESTIMATE VARIABEL
  IF(LFE.EQ.0) LFE=1
  DO 50 I=1,LFE
    NP=NST+i
    NE=175+LVE+i
    P(NP)=PAR(NE)
54   LFE=1ABS(LPAR(3))
    IF(LVE.EQ.0) LVE=1
    DC(5)=NST+LFE+2*I-1
    NP=NST+LFE+2*I-1
    P(NP)=PAR(I+175)
    P(NP+1)=PAR(I+150)
55
49
50
54
48
55

```



```

56    LVE=LPAR(4)
      BREITEN EQ.0) GO TO 61
      DC 60 I=1,LBV
      NP=NST+LFE+2*LVE+1
      60 P(NP)=PAR(1+125)
      M=NST+LFE+2*LVE+LBV
      LPAR(29)=M
      LPAR(24)=1

C     NUM=LPAR(1)+1
      IF(LPAR(20)*GT.1) CALL ZETKO
      CALL FIT(N,P,LEO,XX,Y,ERR,-1,GAMMA,NUM,680)
      IF(LPAR(20)*GT.1) CALL ZETKO

C     IF(LPAR(31)*LE.0) GO TO 75
      DC 70 J=1,IM
      FEH(J)=PAR(31)-PAR(J+150)
      NP1=(NST+LFE)*2+200+1
      NP=NP1+4*j-2
      IF(J.GT.LVE) ZAEH(J)=PAR(31)-PAR(NP)
      IF(J.GT.LVE.AND.LPAR(3).GT.0) ZAEH(J)=FEH(J)
      IF(J.GT.LVE.AND.LPAR(3).LT.0) ZAEH(J)=FEH(J)-PAR(NP1+2)+PAR(151)

70    WRITE(1)(FEH(J),J=1,IM)
      WRITE(1)(ZAEH(J),J=1,IM)
      WRF(LPAR(20)*GT.1) CALL ZETKO
      CONTINUE
      75 CONTINUE
      80 RETURN
      END

      SUBROUTINE UNTF(X,P,DY,UNT,FSSW)
      DIMENSION P(50),DY(50)
      COMMON PAR(300),LPAR(100)
      IF(PAR(24).NE.0) PAR(45)=PAR(24)
      A=X-PAR(45)
      LPAR2=LPAR(2)
      IF(LLPAR2.GT.50) LPAR2=LPAR2-50
      IF(LLPAR(2).GT.50) A=1./(-A)
      CALL SSWF(FSSW,X)
      NPJ=INT(FLQAT(LPAR(2))/10.)
      NPA=LPAR(2)-NPJ*10

C     UNT=.0
      DC 5 I=1,NPA
      UNT=UNT+P(I)*A**(I-1)
      5 DY(I)=A**(I-1)
      GO TO (10,20,10,20), NPJ

```



```

1C UNT=UNT+FSSW*P((NPA+1)
DY(NPA+1)=FSSW
IF(LPAR2.LE.10) RETURN
GOTO 30
20 UNT=UNT+FSSW
IF(LPAR2.LE.20) RETURN
30 DY(NPA+2)=-UNT*((PAR(31)-X)/X
RETURN
END

```

```

SUBROUTINE FITUN(MZ,P,N,X,Y,DY,NRM,DELTA,NUM,*)
NRM = 0
DIMENSION PAR(300),LPAR(100),DUM(600),WORD(20)
DIMENSION X(500),Y(500),DY(500),V1(50),V2(50)
1 P(50),DP(50),DF(50),DZ(50),D2Z(50,50),U(50,50)
1 DIMENSION JOTA(25)
DIMENSION ZNP(50),PNB(50)
CCMNON PAR,LPAR,DUM,WORD
CCMNON/NZP/ LEO,LX,LV2
CCMNON/XKURV/YKURV(10)
CCMNON/LING1/D2Z1,U
REAL*8 TEXT;NAME1,NAME2,NAME3
DATA TEXT / * . GRD* /
DATA NAME3 / * . GRD* /
DATA GAM1=0
NORM=NRM
GAMMA=DELTA
LEC=N
LEV2=0
M=MZ
MY=5
J006=6
NC02=30
LFIT=1
LFIT1=LPAR(3)
NKURV=LFIT+LFIT1
KC01=LPAR(22)+1
LPAR(31)=0
NC01=2
DC5 K=1,50
DC5 L=1,50
D2Z(K,L)=0
5 DIAGNOSTIK
C D1=1
1 IF(NUM=4) LZ=N-LPAR(6)
11

```

UNST0030
UNST0050
UNST0090
UNST100
UNST0110
UNST0120
UNST0150
UNST0160
UNST0170
UNST0180
UNST0190
UNST0200
UNST0210
UNST0220
UNST0230
UNST0240
UNST0250
UNST0260
UNST0270
UNST0280
UNST0290
UNST0300
UNST0310
UNST0320
UNST0340
UNST0360
UNST0370
UNST0380


```

IF(LPAR(11)*GT.0) M001=LPAR(11)
IF(LPAR(12)*GT.0) M002=LPAR(12)
IF(LPAR(13)*GT.0) MY=LPAR(13)
IF(LPAR(14)*GT.0) J006=LPAR(14)
DO TAU(8)=1,LFIT1
  DUCTA(I)=LFIT+2*I+LPAR(22)
END
IF(W-50) 16,16,15
15  WRITE(6,997)N
16  FORMAT(40H1 NUR 1 BIS 50 PARAMETER ERLAUBT STATT ,17)
997 RETURN
17 IF(NE-500) 20,20,18
18  WRITE(6,998)N
19  FORMAT(42H1 NUR 1 BIS 500 MESSPUNKTE ERLAUBT STATT ,17)
998 RETURN
20  ZSCLL=N - W
21  IF(ZSOLL .LT. 24,25,26
24  WRITE(6,999)M,N
25  FORMAT(19H1 MEHR PARAMETER (, 12, 20H) ALS MESSPUNKTE (, 12,
999 1H) )
1  RETURN
25  NORM=0
26  DO 27 I = 1,N
27  COUNTUE
28  GOTO 14
29  WRITE(6,1000)I
1000 FORMAT(49H1 MESSFEHLER DY(I) IST NULL ODER NEGATIV FUER I = , 14)
14  RETURN
15  FEH=1.0
16  IF(NORM) 29,30,30
29  FEH=DY(I)**2
30  J=0
C   BEGINN DER ITERATION ZUR LOESUNG DER NORMAL - GLEICHUNGEN
C   IF(LPAR(8) ) 31,31,32
31  WRITE(6,1002)17X,18HZWISCHENERGEBNISSE,ZWANG
1002 1  /85HNAEHERUNG USW.....//,1. PARAMETER
2  3. PARAMETER
32  G=1.0
      DATA NAME1/' /'
      TEXT=NAME1
C   50  Z = 0.0
      DC 60      K = 1,M
      DZ(K) = 0.0
      DC 60      L = 1,M

```



```

60 D2Z(K,L) = 0.0
DG70 I = 1'NUM,X(I),P,F,DF)
CALL THEORU
H1 = DY(I)**(-2)*FEH
H2 = Y(I)-F
Z = Z + H1*H2*H2
DO 70 DZ(K) = DZ(K)-H1*H2*DF(K)
DO 70 D2Z(K,L) = D2Z(K,L) + H1*DF(K)*DF(L)
70 ZY=Z/FEH
71 IF(NORM) 72,73,72
72 G=Z/ZSOLL
73 IF(LPAR(8)) 74,74,78
74 IF(INORM) 77,77,75
75 WRITE(6,1003) J, TEXT', Z, (P(K), K=1,M)
1003 FORMAT(1X,13,A6,1PE14.6,3X,7E15.6)
77 WRITE(6,1004) J, TEXT', ZY, (P(K), K=1,M)
1004 FORMAT(1X,13,A6,1PE14.4,3X,1P7E15.6/(27X,7E15.6))
C 78 IF(J-MY) 100, 80,
8C IF(Z-ZALT) 101,101
101 IF(NDUR) 140,102,102
102 DO 103 K=1,N
103 P(K)=ZKP(K)
GAMMA=0.8*GAMM1
WRITE(6,1040) GAMMA
1040 FORMAT(13X,10H,GAMMA, = F13.6)
9C IF(J-MOOZ) 100,130
C 100 DURCHFUEHRUNG DER ITERATION
DO 104 DF(K) = -DZ(K)
DO 104 K=L=1,M
104 DZ(K,L) = D2Z(K,L)
CALL LINL(U,D,P,M,1,DETERM)
1IF(LLPAR(120)*GT*2,1CALL,ZETKO
105 H1=0.0
DO 106 K=1,M
106 H1=H1+DP(K)*DP(K)*NWT/
DATA NAME2/,NAME2/
TEXT=SQRT(H1)
GAM1=GAM1-GAMMA
113,113,107
C 107 GRAIDENTEN METHODE STATT NEWTON
TEXT=NAME3

```



```

H1 = 0.0
H2 = 0.0 K = 1, M
DC 109 DZ(K) = H3/DZZ(K,K)
D2(K) = H3*DZZ(K,K)
H1 = H1 + H3*DZ(K)
DC 110 K = 1, M
L = 1, N
DC 110 DZ(K) = H2 + DZ(H1)*DZZ(K,L)*DZ(H1)
H2 = AMIN1(H1/H2, GAMMA/SQRT(H1))
DC 112 K = 1, N
DP(K) = - H3*DZ(K)
112 ZALT = Z
113 IF(J.LE.NQ001) GO TO 114
114 DC 120 K = 1, M
ZWP(K)=P(K)
120 P(K)=P(K)+DP(K)
121 DC 123 K=K001,M
IF(I1-25) 116,116,115
116 NDUR=0
DC 118 KY=11,25
IF(K-JOTA(KY)) 118,117,118
117 NDUR=1
GO TO 119
118 CONTINUE
119 IF(K-{LPAR(22)+LFIT +2*LPAR(4)}) 125,125,126
120 IF(Z-ZSOLL*FEH*3.0) 128,128,127
121 P(K)=ZWP(K)
119 P(K)=ZWP(K)
NDUR=1
DC TO 123
128 IF(ABS(DP(K))-0.15*ZWP(K) ) 125,125,129
129 P(K)=ZWP(K)+0.10*DP(K)*ZWP(K)/ABS(DP(K))
130 WRITE(6,1042) K
1042 FORMAT(14X,17HBREITE(PARAMETER 12,22H) UM 10 PROZ. GEAEND.
125 FOPEN(P(K))
126 WRITE(6,1041) K,P(K)
127 FFORMAT(10X)15,20H. PARAMETER NEGATIV( E15.6,3H )
128 FOPEN(P(K))
129 CONTINUE
130 J=J+1
131 GO TO 50
130 WRITE(6,1005) M000Z
1005 FORMAT(24H (KEINE KONVERGENZ NACH 13, 15H ITERATIONEN) )
130 WRITE(6,1030) WORD(I),I=1,18
1030 FORMAT(1H18A4//)
132 WRITE(6,1032)

```



```

1032 FORMAT(23H,FILTERGEBNISSE SPEKTRUM )
1133 IF(NORM)35,35,40
C   C   ERWARTUNGSWERT VON Z IST ZSOLL = N - M FALLS DIE MESSFEHLER DY(I)
C   C   ABSOLUT SIND. STREUUNG IST SQRT (2*ZSOLL)
C   35 H1 = SQRT(2.0*ZSOLL)
C
C   A012=H1
C   B012=ZY
C   PAR(42)=ZSOLL
C   PAR(43)=A012
C   PAR(44)=B012
C   IF(LPAR(20)*67*2)=CALL ZETKO
C   WRITE(6,1007)ZSOLL,ZY,ZY
C   1007 FORMAT(18X,7HISTWERT,F9.1)
C   40 WRITE(6,1008)
C   1008 FORMAT(1H,32X,7HOPTIONAL,3X,6HFEHLER,(SOLLWERT IST 1),//)
C
C   DO 160 K=1,N
C   150 U(K,K)=0.0
C   160 CALL LINGL(D2Z,2,U,M,DETERM)
C   170 IF(DETERM)170,210,CALL ZETKO
C   170 DO 180 K=1,M
C   180 DP(K)=SQRT(ABS(U(K,K)))
C
C   DETERM=1.0/DETERM
C   KONTROLLE DURCH BERECHNUNG DES ZWANGES AN DEN EXTREMPUNKTEN
C   DES FEHLERFELDIPSOIDS
C   DO 205 K=1,M
C   H1=0.0
C   H2=0.0
C   IF(LPAR(19)*GT.0) GO TO 205
C   190 IF(DP(K)*EQ.0.)DP(K)=1. E-15
C   U(K,L)=U(K,L)/DP(K)
C   V1(K,L)=P(L)-U(K,L)
C   V2(L)=P(L)+U(K,L)
C   191 IF(DP(L)*EQ.0.)DP(L)=1. E-15
C   192 U(K,L)=U(K,L)/DP(L)
C   DO 195 I=1,N
C   CALL THEORU( NUM,X(I);V1,F,DF)
C   195 H1=H1+((Y(I)-F)/DY(I))**2*FEH
C   196 H1=(H1-Z)/G
C   200 I=1,N
C   CALL THEORU( NUM,X(I),V2,F,DF)

```



```

200 H2 = H2 + ((Y(I) - F)/DY(I))**2*FEH
205 WRITE(6,1009)K,D(K),H1,H2
1009 FCRRMAT(IX,12,10H,PARAMETER,I5X,IP15.6,5H      +-,E15.6,11X,0P2F20.5
1     IF(LPAR(19).GT.0) GO TO 333
1     WRITET(6,1010)
1010 FCRRMAT(40H,KORRELATIONEN ZWISCHEN DEN PARAMETERN
1     //12X,31H1,PA2,PA3.PA.....)
1     DC185 WRITET(6,1011)K,(U(K,L),15F8.3,3(/9X,15F8.3))
1011 FCRRMAT(1X,12,6H,PA1,10H,DETERM
1     WRITET(6,1014)DETERM=1PE11.3///)
1014 FCRRMAT(1H0,11X,8HDETERM=1PE11.3///)
C     TABELLIERUNG DER ANGEPASSTEN FUNKTION
333 LPAR(19)=0 CALLT(KO
181 IF(LPAR(8)) 181,186,181
182 IF(LPAR(9)) 216,216,182
186 WRITET(6,1015)
1015 1    WRITET(1H0,54X,13HT,A,B,E,L,E, //,29X,14HZAELRLATE,
1     17H NR,FREQUENZ,7X,8HGEMESSEN,8X,9HBERECHNET,8X,
2    7H-Y-UNT,8X,7HUNT,9X,7HSSW,8X,9HDIFERENZ,7X,6HFEHLER//)UNST2710
2    IF(LPAR(64)) GE1000 WRITE(6,1019)
1019 FCRRMAT(1X,1,ZAELRLATE,AUF DISPERSSION KORRIGIERT.)
1018 2   IF(LPAR(9)) 2006,187
1020 2   IF(LPAR(1)) LPAR(24),M,N,2S0LL,A012,B012
1021 2   LPAR(25)=LPAR(25)+1
1022 2   LPAR(31)=1
1023 2   LPAR(38)=1
1024 2   NE=1 GO TO 188
2006 2   WRITE(7,2001) WORD(1),I=1,20
2007 2   WRITE(7,2002) PAR(31),PAR(7),PAR(59),PAR(1)
2008 2   WRITE(7,2003) (PAR(2*I+89),I=1,5),PAR(81),LPAR(16)
2009 2   WRITE(7,2004) (P(I),I=1,4),PAR(45),PAR(24),LPAR(2)
2010 2   FCRRMAT(20A4)
2001 2   FCRRMAT(4E12.4)
2002 2   FCRRMAT(6E12.4,13)
2003 2   FCRRMAT(6E12.4,13)
2004 2   LY2=1
2188 2   DO 213 I = 1,N
2189 2   LX=I THEORU (NUM ,X(I),P,F,DF)
2190 2   H1=Y(I)-F
2191 2   H14=H1/DY(I)
2192 2   CALL UNTFX(I),P,DY,UNT,FSSW
197   H7=Y(I)-UNT,FSSW
2193 2   H21=Y(I)-FSSW
2194 2   H22=UNT-FSSW

```



```

H13=F-UNT
189 IF(LLPAR(9)) 215,215,189
     WRITE(1)X(I),H7,H13,H14,UNT,(YKURV(K),K=1,NKURV),FSSW
215 1IF(LLPAR(8)) 213,214,213
214 1IF(LLPAR(6)I,X(I),Y(I),F17,H7,UNT,FSSW,H1,DY(I)
1016 1016 FORMAT(15,F12.4,2X,1P(2(E17.6,E15.6),E15.6,E17.6,E15.6))
1IF(LLPAR(38).NE.2) GO TO 213
H31=F-FSSW
UNST3250
2005 FORMAT(15.6(1PE12.4),1X(I),Y(I),DY(I),F,UNT,FSSW
213 CONTINUE
C
216 DO 1022 I=1,M
   PAR(2*I+199)=P(I)
1022 PAR(2*I+200)=DP(I)
      RETURN
1022 IIF(LLPAR(20).GT.2) CALL ZETKO
C
210 1012 IF(SICH DAS LINEARE GLEICHUNGSSYSTEM NICHT AUFLOESEN LAESST
      WRITE(6,1012)
1012 FORMAT(42H0 NORMAL-GLEICHUNGEN SIND NICHT AUFLOESBAR //)
      DC220 K=1,N
220 1013 WRITE(6,1013)(U(K,L), L = 1,M)
1013 FFORMAT(1X,1P7E15.7)
245 RETURN1
END
C
SUBROUTINE LINGL(A,B,N,M,DETERM)
AUFLÖSUNG LINEARER GLEICHUNGSSYSTEME BIS ZUR ORDNUNG 25
DIMENSION A(50,N),B(50,M)
60 IF(N)15,16
16 IF(M)15,17
17 DETERM=1.0
DET=0.
ANAX=ABS(A(1,1))
LP=1
DC2,I=2,N
1 ANAX=ABS(A(I,1))-AMAX
1 LP=I
2 CONTINUE
C
DO 11 J=1,N
1P=LP
T=A(I,P,J)
53 1F(T,3,15,3)
53 1F(J-N)4,8,8
4 A(I,P,J)=A(J,J)
JP1=J+1

```



```

L P = J P 1 N
A MAX = 0.0
D C 7 K = J P 1 N
H = A ( I P , K ) / T
A ( I P , K ) = H
A ( J , K ) = H
D O 7 I = J P 1 N
A ( I , K ) = A ( I , K ) - A ( I , J ) * H
I F ( K - J P 1 ) 5 , 5 7
I F ( ABS ( A ( I , K ) ) - A MAX ) 7 , 7 , 6
5 A MAX = ABS ( A ( I , K ) )
L P = I
C O N T I N U E
C
8 D C 1 1 K = 1 , M
H = B ( I P , K ) / T
B ( I P , K ) = B ( J , K )
B ( J , K ) = H
I F ( J - N ) 9 , 1 1 , 1 1
9 D O 1 0 I = J P 1 N
B ( I , K ) = B ( I , K ) - A ( I , J ) * H
1 0 B ( I , K ) = B ( I , K ) - A ( I , J ) * H
1 1 C C N T I N U E
C
I F ( N - 1 ) 1 5 , 1 5 , 1 2
1 2 D C 1 3 I = 2 , N
I P = N - 1 + 1
L P = I P + 1
D C 1 3 J = 1 , M
D C 1 3 K = L P 1 N
1 3 B ( I P , J ) = B ( I P , J ) - A ( I P , K ) * B ( K , J )
C
1 5 R E T U R N
E N D
C
SUBROUTINE THEORU ( X , Y , P , Y , D A )
D I M E N S I O N P ( 5 0 ) , D A ( 5 0 )
2 0 C A L L A R C 5 ( X , P , Y , D A )
R E T U R N
E N D
C
S U B R O U T I N E A R C 4 U ( X , P , Y , D Y , I )
D I M E N S I O N P ( 2 5 ) , D Y ( 2 5 ) , P Y A R ( 2 5 )
C C M M D N P A R ( 3 0 0 ) , L P A R ( 1 0 0 )
C C M M D N / B V A R 2 / P V A R
B T = 1 . 4 4 2 6 9 5 0 5
I F ( P ( 2 5 ) - 1 . 0 ) 5 , 6 , 5
5 P ( 6 ) = 1 . 0
6 P = X - P ( 5 ) / P ( 6 )

```



```

IF(PAR(64).GE.1.. AND. I.LE.LPAR(6)) GOTO 110
10 CCNTINUE
100 ALPHAF=(U/P(2))**2/BT
101 FORMAT(5E15.4)
11 Y=P(1)*EXP(-ALPHA)
DY(1)=Y/P(1)
DY(2)=2.0*Y*U**2/(BT*p(2)**3)
DY(3)=0.0
DY(4)=0.0
DY(5)=2.0*U*Y/(BT*p(2)**2)/P(6)
DY(6)=U*DY(5)
RETURN
12 Y=P(1)**EXP(-(P(4)/P(3))**2/BT)
DY(2)=Y/P(1)
DY(5)=0.0*Y*U/(BT*p(3)**2/BT)
DY(4)=0.0
DY(3)=DY(5)*U/P(3)*P(6)
DY(6)=U*DY(5)
RETURN
13 PP=2.0*(P(4)/P(3))**2/BT
C=Y*P*(4)*(2.0-PP)
D=Y*P*(4)**2*(PP-1.0)
PPP=Y*P*P*(4)*(4.0-PP)/P(3)
CF3=PPP*(P(4)**2/P(3)-3.0*BTP(3)/2.0)
CP4=PPP*(2.0/PP-5.0*PP)
DF4=PPP*(4)*(5.0-PP-2.0/PP)
Y=C/U+D/U**2
DY(1)=Y/P(1)
DY(2)=0.0
DY(3)=CP3/U+DP3/U**2
DY(4)=CP4/U+DP4/U**2
DY(5)=C/U**2+2.0*D/U**3/P(6)
RETURN
14 BREIT-WIGNER-KURVE MIT FESTEM P-FAKTOR (DISS PIT 72) AB 110
MIT GEFITTEM P-FAKTOR AB 120
C1=U/P(2)
C2=1.0+C1**2
CTE(PAR(64).GT.1.) GOTO 120
Y=Y*(1.0+PVAR(1)*X-P(5))
DY(2)=2.*P(1)*C1**2/P(2)/C2**2

```



```

UNST6180
UNST6200
UNST6210
UNST6220
UNST6230
UNST6240
UNST6250
UNST6260
UNST6270
UNST6280
UNST6290
UNST6300
UNST6310
UNST6320
UNST6330
UNST6340
UNST6350
UNST6360
UNST6380
UNST6390
UNST6420
UNST6430
UNST6460
UNST6900
UNST6910
UNST6920
UNST6930
UNST6940
UNST6950
UNST6960
UNST6970
UNST6980
UNST6990
UNST7000
UNST7010
UNST7020
UNST7030
UNST7040
UNST7050
UNST7060
UNST7070
UNST7080
UNST7090

DY(4)=2.*P(1)*C1**2/P(3)/C2**2
DY(5)=2.*DY(2)*C1/P(6)
DY(6)=DY(5)*U
RETURN
IF(FLCR=P(1)/C2) GOTO 130
Y=P(1)*(1+P(4)*U)/C2
DY(1)=Y/P(1)
DY(2)=2.*FLCR*(1+P(4)*U)*C1**2/P(2)/C2
DY(3)=DY(2)*P(2)/P(3)
DY(4)=FLCR*U
DY(5)=(-FLCR*P(4)+2.*DY(2)*C1)/P(6)
DY(6)=DY(5)*U
RETURN
CONTINUE
END

120
130

SUBROUTINE ARC5(X,P,Y,DY)
DIMENSION P(50),DY(50),PAR(300),LPAR(100),DUM(600)
DIMENSION PW(25),DYM(25)
COMMON PAR,LPAR,DUM
COMMON /BVARI/BVAR
COMMON /NZP/LEO,LX,LV2
COMMON /XKURV/YKURV(10)
COMMON GRUND
CALL UNTF(X,P,DY,UNT,FSSW)
C
30
MZH=LPAR(29)
LFFIT=IABS(LPAR(3))
LFFIT=LPAR(4)
L=LFFIT
ME=LFFIT+LPAR(4)
M=LFFIT+LPAR(4)
KZ=M+LPAR(4)+L
PW(2)=PAR(73)
PW(3)=PAR(75)
PW(4)=PAR(77)
PW(25)=1.0
DPY=0.0
NP=LFFIT+LPAR(22)+2
DEPS=P(NP)-PAR(151)
OC 120 I=1,M
K=150+L PAR(4)+1
INS=I+LPAR(22)
KE=I+LPAR(4)+LFFIT+INS

```



```

KC=2*I-LPAR(4) +LPAR(22)-1
KD=N+LPAR(K) -LFIT+INS
EPS=PAR(3) 35,36,36
IF(LPAR(K)+DEPS 35,36,36
EP*(1)=PAR(1NS)*PAR(71)
33 PW(15)=PAR(79)-EPS
36 PW(6)=PAR(K-25)
38 PW(LPAR(15))=55,55,40
40 IF(X(6)=P(K8))=45,45,55
45 P(6)=P(LFIT1+L) 45,45,55
55 P(I-LFIT)=P(KC)*PAR(71)
60 P(5)=PAR(79)-P(KC+1)
65 P(6)=P(KZ) 75,75,65
70 P(6)=P(KD) 70,70,80
75 KW=I-LFIT+125
PW(6)=PAR(KW)

C
80 CALL ARC4U(X,PW,YK,DYWM,I) YKURV(I)=YK
Y=I*LE.10 AND. LV2-EQ.I
IF(I-1-LFIT) 84,84,85
IF(INS)=DYW(1)*PAR(71)
84 DPY=DPY-DYW(5)
GC TO 90
95 DY(KC)=DYW(1)*PAR(71)
DPY=DPY+DYW(2)
DY(KC+1)=-DYW(5)
90 IF(LPAR(15))=120,120,95
95 IF(I-LFIT)=100,100,130
100 DY(KZ)=DY(KZ)+DYW(6)
105 GC TO 120
110 IF(I-L+LFIT)=115,105,105
115 DY(KB)=CYW(6)
120 GC TO 120
130 IF(I-LFIT-L)=135,140,140
135 GC TO 120
140 DY(KZ)=DY(KZ)+DYW(6)
120 CONTINUE
150 LJ=LFIT+LPAR(22)+2

```


160
 DY(LJT)=DY(LJT)+DPY
 CCNTINUE
 RETURN
 END

SUBROUTINE AUSG
 DIMENSION FIF(25),DEPS(25),BR(25),DBR(25),PIP(25),DPIP(25)
 DIMENSION PAR(300),LPAR(100),DUM,WORD(20)
 COMMON PAR,DUM,WORD(25)
 COMMON/BVAR/BVAR(25)
 COMMON/SSWD/ACO(25)
 DATA A001/4H
 C
 1000 FORMAT(1H,10H ERGEBNISSE /
 1001 FORMAT(1H,34HELASTISCH /
 1002 FORMAT(1H,20HENERGIERELASTISCH PEAK /
 1003 FORMAT(1H,15H PRIMAER ENERGIEE /
 1004 FORMAT(1H,15H HALbwERTS BREITE /
 1005 FORMAT(1H,12H KEY = F8.0 AECHER,
 1006 FORMAT(1H,24X,7H HF LAEKHOEHE /
 1007 FORMAT(1H,9H PEAKHOEHE INTEGRA
 1008 FORMAT(1H,43H UNTEREST /
 1009 FORMAT(1H,12H UNTELAST /
 1010 FORMAT(1H,17H SSW=1PE12.4,3H,
 1011 E11.4,6H*U**4,
 1012 FORMAT(1H,10H UNTERGRUNDSPARE
 1013 FORMAT(1H,13H(EPSI /
 1014 FORMAT(1H,14H(EPSI /
 C
 1000 FORMAT(1H,12H MIT X= E=F6.2,4H MHz)
 1001 FORMAT(1H,7(1PE12.2))
 1002 FORMAT(1H,22H UNTELAS
 1003 LIBERECHNET, VARIABEL, F FEST, FB ENER
 1004 EPSI LIBERECHNET, VORGEGESENES
 1005 1), FEST, BREITE /
 1006 BREITENVERHAELTNIS, BREITE UNABHAENGIG, G
 1007 BREITE /
 1008 VARIERT, FEST, BREITENVERHAELTNIS -- /
 1009 BREITE
 1010 VARIERT, FEST, BREITENVERHAELTNIS,
 1011 HOEHENVERHAELTNIS, F/F FLAECHEN
 1012 17X, 4HEPSI /
 1013 4HEPSI 17X, 4HEPSI /
 1014 17X, 4HEPSI 17X, 4HEPSI /
 C
 NST=LPAR(22)
 LF=LIPAR(4)
 LF1=LIPAR(4)
 LBV=LIPAR(5)
 LY=LIPAR(21)
 LFWB=PAR(48)

AUSG0020
 AUSG0050
 AUSG0060
 AUSG0080
 AUSG0090
 AUSG0100
 AUSG0110
 AUSG0120
 AUSG0130
 AUSG0140
 AUSG0150
 AUSG0160
 AUSG0170
 AUSG0180
 AUSG0190
 AUSG0200
 AUSG0210
 AUSG0230
 AUSG0250
 AUSG0260
 AUSG0390
 AUSG0430
 AUSG0440
 AUSG0450
 AUSG0460
 AUSG0470
 AUSG0480
 AUSG0490
 AUSG0500
 AUSG0510
 AUSG0520
 AUSG0530
 AUSG0540
 AUSG0550
 AUSG0560
 AUSG0570
 AUSG0580
 AUSG0590
 AUSG0600


```

AUSG0610
AUSG0620
AUSG0630
AUSG0640
AUSG0650
AUSG0660
AUSG0670
AUSG0680
AUSG0690
AUSG0700
AUSG0710
AUSG0720
AUSG0730
AUSG0740
AUSG0750
AUSG0760
AUSG0770
AUSG0780
AUSG0790
AUSG0800
AUSG0810
AUSG0820
AUSG0830
AUSG0840
AUSG0850
AUSG0860
AUSG0870
AUSG0880
AUSG0890
AUSG0900
AUSG0910
AUSG0920
AUSG0930
AUSG0940
AUSG0950
AUSG0960
AUSG0970
AUSG0980
AUSG1000
AUSG1010
AUSG1110
AUSG1120
AUSG1130
AUSG1140
AUSG1150

WRITE (6,1000) (WORD(1),I=1,18), (PAR(I), I=42,44)
DATA ARC3/4HARC3 /
DATA ARC4/4HARC4 /
DATA EFT/4H F
DATA EVA/4H V
DATA EFB/4H FB
DATA BUG/4H U
DATA BG/E/4H G
DATA BF/T/4H F
A001=ARC3
12T=PAR(151)
WRITE (6,1015) PAR(1),PAR(9)
WRITE (6,1016) IZT,(PAR(I),I=52,59)
WRITE (6,1017) (PAR(I),I=11,14)
WRITE (6,1018) (PAR(I),I=15,20)
F8.4,2H - F8.4,
1017 1 FORMAT(1HUNELAST,13HEINGABEWERTE // 12H EICHFAKTOR
1015 1 FORMAT(1HUNTERGRUND OBERHALB ELAST. PEAK F10.5, 5X
1016 1 FORMAT(2HUNTERGRUND 14:5H,ATW F7.2*6H,XRAD F7.3*3H,R F7.3,
1018 1 3H G F7.3*3H C F8.4*3H T F8.4*12H,MASSEN(MEV) ,3(F11.4,2H -F8.4))
IF(LPAR(1,1)*GT.0) A001=ARC4
KEE=PAR(31)
EEE=NEV=EE#PAR(1)
EOO=PAR(36)/PAR(1)
HW=MEV=HW/EE
HWPRO=PAR(33)
FLN=PAR(FL*PAR(1))
FLN=PAR(6,1002) EE,EENEV
FLN=PAR(6,1003) EO,EOMEV
FLN=PAR(6,1004) HW,HMMEV,HWPRO
FLN=PAR(6,1006) PAR(35)
IF(LPAR(1,1)*GT.0) WRITE(16)
JCL=ABS(LPAR(1,1)*GT.0)
KRITE(6,1009)(PAR(2*I+89),I=1,5)
KRITE(6,1010)(PAR(2*I+89),I=1,5)
KRITE(6,1011)(PAR(2*I+199),I=1,NST)
KRITE(6,1013)(PAR(2*I+199),I=1,NST)
1035 1 IF(PAR(64)*GE 1.0) WRITE(6,1035)
IF(CRMEV/2.,*FE*FUER BREITWIGNER- FORM, BERECHNETAUS PI*BRRB*HWNEV*ZAU
1 /FLMEV/2., BREITEN ABSOLUT IN MEV ),
```


C

```

140 I=1,IM
DBR(I)=PAR(I+125)
DBR(LBV*EQ*0) GO TO 100
MB=2*(NST+LF)+4*LF1+2*I-1
MB=PAR(MB+200)
MB=PAR(MB+201)
GO TO 110
IF(2*(NST+LF)+4*I-3+200
MP=MP+2
MEPS(I)=PAR(ME)
MEPS(PAR(ME)*EQ*0) GO TO 119
DEPS(I)=PAR(ME+1)/PAR(ME)
GC=2*NST+2*(I-LF1)+199
EPSS(I)=PAR(I+150)
DEPS(LPAR(3)*LT*0) EPS(I)=EPS(I)+DHWB*(BR(I)-1.0)
NP1=LPAR(3)*LT*03 EPS(I)=EPS(I)+PAR(NP1)-PAR(151)
IF(TO 120 EPS(I)=0
DEPS(I)=PAR(MP)
PIF(PAR(MP)*EQ*0) GOTO 125
DPIP(I)=PAR(MP+1)/PAR(MP)
GO TO 126
DPIP(I)=0
119 DPOINT(I)=EPS(I)*PAR(1)*PAR(47)
120 EPSS(I)=EPS(I)*PAR(1)*PAR(47)
125 DPOINT(I)=EPS(I)*PAR(1)*PAR(47)
130 ILA=0
EPSS(I)=EPS(I+1)*PAR(1)*PAR(47)
131 ILA=ILA+1
IF(I=ILA*LE*3) GO TO 131
IF(I=PIR(I)*BR(I))**#2+DBR(I)**#2
DFIF(I)=SQR(DPIP(I))
DEP=EPS(I)*DEPS(I)
DFF=CFF(I)*FIF(I)
DP=DP*PIP(I)
DBB=DBR(I)*BR(I)
ZN=PIFT(I)*PAR(35)
TXE=ELEFT
IF(I*LE*LF1) TXE=EVA
IF(I*GT*LF1) AND.LPAR(3).LT.0 TXE=EFB
IF(LBV.GT.0) TXB=BUN

```



```

C      IF(LBV.GT.0 .AND. I.GE.LBV) TXB=BGE
      PAR(64)=BREIT-WIGNER-FORM
      IF(PAR(64).GE.1 .AND. I.LE.LPAR(6)) GOTO 136
      GOTO 138
136   CCNTINUE=ZM*3.1416*BR(I)*HWMEV/FLMEV/2.
      FIF(I+125)=PAR(I+125)*PAR(I)*PAR(34)
      PAR(PIP(I),NE.O)=OFF=DFF*FIF(I)/(PIP(I)*BR(I))
      DBB=DDBB*PAR(I)*PAR(34)
      BR(I)=BR(I)*PAR(1)*PAR(34)
      IF(I.EQ.LPAR(6)+1) WRITE(6,1036)
      IF(CRMAT(I).EQ.'X')//FOLGENDE LINIE SIND GAUSSKURVEN::'
      1036 IF(BVAR(I).NE.O.O) WRITE(6,1037)
      1037 IF(FORMAT(IH2).NE.O.O) FOLGENDE LINIE WURDE MIT DER GERADEN 1+X**,F10.3, 'AUSG1720
      1037 FORMAT(IH2,IERT)
      1MULTPLIZIERT)

140   WRITE(6,1014) PAR(I+100),EPS(I),DEP,TXE,TXB,PAR(I+125),BR(I),
      1DBBB,ZM,PIP(I),DPP,FIF(I),DFF,DFIF(I)
      CALL RESULT(EPS,DEPS,FIF,DFIF,BR)
      RETURN
      END

SUBROUTINE RESULT(EPS,DEPS,FIF,DFIF,BR)
DIMENSION DI(25),DEPS(25);FIF(25),DFIF(25),BR(25)
DIMENSION PAR(300),LPAR(100),DUMMY(600),WORD(20)
DIMENSION FKCR(25),FORF(25)
COMMON PAR,LPAR,DUMMY,WORD
COMMON /SSWD/ACO(25)
C1F(PAR(61),EQ.O) PAR(61)=1.
C1ZET=PAR(51)
ZW=PAR(52)
XO=PAR(53)
FIRAF=PAR(54)
FIF(FIRAF.EQ.0) FIRAF=1.
DEFF=PAR(41)
DEE=PAR(34)*PAR(1)
DIY=LPAR(21)
DC(I)=BR(I)
DC(I)=2,I=1,IM
2 DC(6,I=1,IM
DC(PAR(64),EQ.O.) DI(I)=DI(I)*DEE
6 CONTINUE
1020 FORMAT(F10.5)
1102 FORMAT(F10.4)
1103 FORMAT(10I3)
1104 FORMAT(10F6.3)
1105 FORMAT(10F5.3)
      AUSG1670
      AUSG1590
      AUSG1720
      AUSG1730
      AUSG1740
      AUSG1750
      AUSG1780
      AUSG1790
      AUSG1830
      AUSG1840
      AUSG1880
      AUSG1940
      AUSG1950
      AUSG1960
      AUSG2020
      AUSG2030
      AUSG2050
      AUSG2100
      AUSG2110
      AUSG2120
      AUSG2130
      AUSG2140
      AUSG2150
      AUSG2160
      AUSG2170
      AUSG2180

```


LIST OF REFERENCES

1. Warshawsky, A.S. and Webber, M.W., Jr., Naval Postgraduate School Thesis (1973).
2. Lewis, M.B. Phys. Rev. C 7, 2041 (1973).
3. Torizuka, Y. et. al., private communication.
4. Moalem, A., Benenson, W. and Crawley, G.M., Phys. Rev. Lett 31, 482 (1973).
5. Walcher, T., Invited talk presented at the International Conference of Nuclear Physics, Munich (1973).
6. Hofstadter, R., Rev. Mod. Phys. 28, 214 (1956).
7. Isabelle, D.B. and Bishop, G. R., Nuc. Phys. 45, 209 (1963).
8. Tuan, S.T., Wright, L. E. and Onley, D.S., Nucl. Instru. and Meth. 60, 70 (1968); Duke University program as compiled by ITK Darmstadt.
9. Überall, H., Electron Scattering From Complex Nuclei, Academic Press, New York (1971).
10. Wilkinson, D.H., Physica (Utrecht) 22, 1039 (1956).
11. Brown, G.E. and Bolsterli, M., Phys. Rev. Lett. 3, 472 (1959).
12. Yamaguchi, A., Terasawa, T., Nakahara, K. and Torizuka, Y., Phys. Rev. C 3, 1750 (1970).
13. Carlos, P., Beil, H., Bergere, R., Lepretre, A. and Veyssiére, A., Nuc. Phys. A172, 437 (1971).
14. Pitthan, R. and Walcher, T., Phys. Lett. 56B, 563 (1971).
15. Lewis, M.B. and Bertrand, F.E., Nuc. Phys. A196, 337 (1972).
16. Fukuda, S. and Torizuka, Y., Phys. Rev. Lett. 29, 1109 (1972).
17. Danos, M. and Steinwedel, H., Z. Naturforsch. 6, 217 (1951).
18. Buskirk, F.R., Gräf, H.D., Pitthan, R., Theissen, H., Titze, O. and Walcher, Th., Proceedings, Vol. I, International Conference of Photonuclear Reactions and Applications, Lawrence Livermore Laboratory, California (1973).

19. Lone, M.A., Fagg, L.W., Bendel, W.L., Jones, E.C.Jr., Maruyama, X.K. and Lindgren, R.A., Bull. Am. Phys. Soc. 19, 111 (1974).
20. Bowman, C.D., Baglan, R.J., Beiman, B.L. and Phillips, T.W., Phys. Rev. Lett. 25, 1302 (1970).
21. Walecka, J.D., Phys. Rev. 126, 653 (1962).
22. Suzuki, T., Nuc. Phys. A217, 182 (1973).
23. Pitthan, R., Z. Physik 260, 283 (1973).
24. Nagao, M. and Torizuka, Y., Phys. Rev. Lett. 30, 1068 (1973).
25. Veyssiére, A., Beil, H., Bergere, R., Carlos, P. and Lepretre, A., Nuc. Phys. A159, 561 (1970).
26. Buskirk, F.R., Dally, E.B., Dyer, J.N., Ferlic, K., Maruyama, X.K., Waddell, R. and Pitthan, R.; Contribution to the International Conference on Nuclear Structure and Spectroscopy, Amsterdam (1974).
27. Ziegler, J.F., The Calculation of Inelastic Electron Scattering by Nuclei (1967): Available from the Clearinghouse for Federal Scientific and Technical Information, National Bureau of Standards, U.S. Department of Commerce, Springfield, Va. 22151 under publication number Yale 2726E-49.
28. Skorka, S.J., Hertel, J. and Retz-Schmidt, T.W., Nuc. Data A Vol. 2, 347 (1966).
29. Nathan, O. and Nilsson, S.G., in Alpha, Beta, and Gamma-ray Spectroscopy, edited by K. Siegbahn, North-Holland Publishing Company, Amsterdam (1966).
30. Ferrel, R.A., Phys. Rev. 107, 1631 (1957).
31. Warburton, E.K. and Wenner, G., in The Role of Isospin in Electromagnetic Transitions, edited by D.H. Wilkinson, North-Holland Publishing Company, Amsterdam (1969).
32. Moniz, E.J., Phys. Rev. 184, 1154 (1969).
33. Kawaii, M. and Kikuchi, K., Nuclear Matter and Nuclear Reactions, North-Holland Publishing Company, Amsterdam (1968).
34. Moniz, E.J., Sick, I., Whitney, R.R., Ficenec, J.R., Kephart, R.D. and Trower, W.P., Phys. Rev. Lett. 26, 445 (1971).
35. Fischer, C.R. and Rawitscher, G.A., Phys. Rev. 135, B377(1964).
36. Berard, R.W. and Traverso, T.J., Naval Postgraduate School Thesis (1973).

37. Drechsel, D., Nuc. Phys. A113, 656 (1968).
38. Bohr, A. and Mottelson, B.R., in Nuclear Structure Vol. II, edited by W. Benjamin, New York (to be published).
39. Pitthan, R., Dissertation, Institut für Kernphysik der TH Darmstadt (1972): unpublished.
40. Lewis, F.H. and Walecka, J.D., Phys. Rev. 133, B849 (1964).
41. Titze, O., Technical Report, Institut für Technische Kernphysik der TH Darmstadt (1967); Unpublished.
42. Pitthan, R., Technical Report, Institut für Kernphysik der TH Darmstadt, (1973); Unpublished.
43. Ginsberg, E.S. and Pratt, R.H., Phys. Rev. 134, B773 (1964).
44. Schiff, L.I., Phys. Rev. 87, 759 (1952).

INITIAL DISTRIBUTION LIST

	No. Copies
1. Library Code 0212 Naval Postgraduate School Monterey, California 93940	2
2. Defense Documentation Center Cameron Station Alexandria, Virginia 22314	2
3. Lt. Ronald D. Waddell, UNS Class 41 (3-74) Naval Destroyer School Newport, Rhode Island 02840	2
4. Ens Kenneth P. Ferlic, USN Naval Nuclear Power School Mare Island, California 94592	2
5. Professor F. R. Buskirk, Code 61BS Department of Physics Naval Postgraduate School Monterey, California 93940	5
6. Professor X.K. Maruyama, Code 61Mp Department of Physics Naval Postgraduate School Monterey, California 93940	5
7. Professor W.R. Pitthan, Code 61Pt Department of Physics Naval Postgraduate School Monterey, California 93940	5
8. Professor J.N. Dyer Code 61Dy Department of Physics Naval Postgraduate School Monterey, California 93940	2
9. Professor E. B. Dally Code 61DA Department of Physics Naval Postgraduate School Monterey, California 93940	2
10. Code 61 Department of Physics and Chemistry Naval Postgraduate School Monterey, California 93940	1

153475

Thesis

F259 Ferlic
c.1 Electroexcitation of
giant resonances between
5 MeV and 40 MeV excita-
tion energy in ^{197}Au .

153475

Thesis

F259 Ferlic
c.1 Electroexcitation of
giant resonances between
5 MeV and 40 MeV excita-
tion energy in ^{197}Au .

thesF259
Electroexcitation of giant resonances be



3 2768 002 06549 2
DUDLEY KNOX LIBRARY